

# The Role of TGF- $\beta$ Signaling in Development and Maintenance of the Ocular Vasculature



Dissertation

Zur Erlangung des Doktorgrades der Naturwissenschaften (Dr. rer. nat.) der  
Fakultät der Biologie und Vorklinischen Medizin der Universität Regensburg

Durchgeführt am Lehrstuhl für Embryologie und Humananatomie der  
Universität Regensburg

vorgelegt von

**Anja Schlecht**

aus Roding

2016



# The Role of TGF- $\beta$ Signaling in Development and Maintenance of the Ocular Vasculature



Dissertation

Zur Erlangung des Doktorgrades der Naturwissenschaften (Dr. rer. nat.) der  
Fakultät der Biologie und Vorklinischen Medizin der Universität Regensburg

Durchgeführt am Lehrstuhl für Embryologie und Humananatomie der  
Universität Regensburg

vorgelegt von

**Anja Schlecht**

aus Roding

2016

Das Promotionsgesuch wurde eingereicht am: 21.10.2016.

Die Arbeit wurde angeleitet von: Prof. Dr. Ernst R. Tamm

Unterschrift:

Manuscripts included in this thesis:

Schlecht A, Leimbeck SV, Tamm ER, Braunger BM. **Tamoxifen-containing eyedrops successfully trigger Cre-mediated recombination in the entire eye.** Adv Exp Med Biol 2016, 854:495-500.

Braunger BM, Leimbeck SV, Schlecht A, Volz C, Jägle H, Tamm ER. **Deletion of ocular transforming growth factor  $\beta$  signaling mimics essential characteristics of diabetic retinopathy.** Am J Pathol. 2015, 185(6):1749-68.

Schlecht A, Leimbeck SV, Jägle H, Feuchtinger A, Tamm ER, Braunger BM. **Ablation of endothelial TGF- $\beta$  signaling causes choroidal neovascularization.** Submitted to Journal of Clinical Investigation.

Authors' contribution is noted in each figure legend.

---

Anja Schlecht

# Table of content

## Chapter 1

<b>1 General Introduction .....</b>	<b>2</b>
1.1 TGF- $\beta$ signaling .....	2
1.2 Cre loxP system .....	3
1.3 The ocular vasculature .....	5
1.3.1 Development of the retinal vasculature .....	6
1.3.2 Blood retinal barrier .....	7
1.4 Pathologies of the ocular vasculature .....	9
1.4.1 Diabetic retinopathy .....	9
1.4.2 Age-related macular degeneration .....	11
1.5 Aim of the study .....	13

## Chapter 2

<b>2 Tamoxifen-Containing Eye Drops Successfully Trigger Cre-Mediated Recombination in the Entire Eye .....</b>	<b>16</b>
2.1 Abstract.....	16
2.2 Introduction .....	17

<b>2.3 Material and Methods .....</b>	<b>18</b>
2.3.1 Mice .....	18
2.3.2 Tamoxifen Treatment .....	18
2.3.3 PCR Analysis .....	18
2.3.4 $\beta$ -galactosidase Staining .....	19
<b>2.4 Results - Localization of Cre-mediated Recombination in Ocular Tissues .....</b>	<b>20</b>
<b>2.5 Discussion .....</b>	<b>22</b>

## Chapter 3

### **3 Deletion of ocular TGF- $\beta$ signaling mimics essential characteristics of diabetic retinopathy..... 24**

<b>3.1 Abstract.....</b>	<b>24</b>
<b>3.2 Introduction .....</b>	<b>25</b>
<b>3.3 Materials and Methods .....</b>	<b>27</b>
3.3.1 Mice .....	27
3.3.2 Western blot analysis .....	27
3.3.3 Microscopy and morphometry .....	28
3.3.4 LacZ staining .....	29
3.3.5 Immunohistochemistry .....	29

3.3.6 Dextran perfusion and retinal whole mounts .....	31
3.3.7 Apoptosis .....	31
3.3.8 Trypsin digest .....	31
3.3.9 Electroretinography .....	32
3.3.10 Fundus imaging and angiography .....	32
3.3.11 RNA analysis .....	32
3.3.12 Statistical analysis .....	34
<b>3.4 Results .....</b>	<b>35</b>
3.4.1 Conditional deletion of T $\beta$ RII in the eye following local tamoxifen treatment .....	35
3.4.2 Conditional deletion of TGF- $\beta$ signaling results in leaky retinal capillaries that form microaneurysms .....	37
3.4.3 Lack of pericyte differentiation upon absence of retinal TGF- $\beta$ signaling .....	39
3.4.4 Hemorrhages and vessel loss in TGF- $\beta$ -deficient retinae .....	45
3.4.5 Lack of ocular TGF- $\beta$ signaling leads to hyaloid vasculature persistence .....	47
3.4.6 Absence of TGF- $\beta$ signaling induces microglia reactivity in the retina .....	49
3.4.7 Continuous lack of retinal TGF- $\beta$ signaling leads to proliferative retinopathy .....	51
<b>3.5 Discussion .....</b>	<b>56</b>
3.5.1 TGF- $\beta$ signaling determines pericyte differentiation during development of the retinal vasculature .....	57
3.5.2 Lack of retinal TGF- $\beta$ signaling leads to vascular leakage .....	58

3.5.3 Lack of retinal TGF- $\beta$ signaling induces the formation of capillary microaneurysms .....	59
3.5.4 Lack of retinal TGF- $\beta$ signaling induces capillary closure and reactive microglia....	60
3.5.5 Phenotypic changes in retinae progress to proliferative retinopathy .....	61
3.5.6 Conclusion .....	62

## Chapter 4

<b>4 Ablation of endothelial TGF-<math>\beta</math> signaling causes choroidal neovascularization.....</b>	<b>64</b>
4.1 Abstract.....	64
4.2 Introduction .....	65
4.3 Material and Methods.....	67
4.3.1 Mice .....	67
4.3.2 Induction of Cre recombinase .....	67
4.3.3 <i>mT/mG</i> reporter mice .....	68
4.3.4 <i>Tgfb2</i> deletion PCR .....	69
4.3.5 Morphology and microscopy .....	69
4.3.6 Immunohistochemistry .....	69
4.3.7 Dextran Perfusion .....	71

4.3.8 Electroretinography (ERG).....	71
4.3.9 Fundus Imaging and Angiography .....	72
4.3.10 RNA Analysis .....	72
4.3.11 Deep tissue imaging by 3D light-sheet fluorescence microscopy .....	74
4.3.12 Statistical Analysis .....	74
<b>4.4 Results .....</b>	<b>75</b>
4.4.1 Deletion of ocular TGF- $\beta$ signaling in mouse pups leads to choroidal neovascularization .....	75
4.4.2 TGF- $\beta$ signaling is required to prevent choroidal neovascularization in late-induced <i>Tgfr2</i> <sup><math>\Delta</math>eye</sup> mice .....	80
4.4.3 Expression of angiogenic factors and immune modulating cytokines in <i>Tgfr2</i> <sup><math>\Delta</math>eye</sup> mice.....	85
4.4.4 Formation of basal lamina deposits in <i>Tgfr2</i> <sup><math>\Delta</math>eye</sup> mice .....	88
4.4.5 Cell-specific conditional deletion of <i>Tgfr2</i> in RPE and vascular endothelium .....	91
<b>4.5 Discussion .....</b>	<b>96</b>
4.5.1 TGF- $\beta$ functions at the retinal/choroidal interface to prevent CNV .....	96
4.5.2 TGF- $\beta$ and VEGF as part of a homeostatic system to maintain integrity of the choriocapillaris .....	97
4.5.3 Potential neuroprotective effects of TGF- $\beta$ .....	98
4.5.4 The formation of BlamD-like material is not required for CNV .....	99

4.5.5 Neovascularization is associated with macrophage accumulation.....	100
4.5.6 TGF- $\beta$ signaling and endothelial proliferation .....	100
4.5.7 TGF- $\beta$ signaling in human patients with AMD .....	102
4.5.8 Conclusion .....	102
<b>4.6 Supplementary Data.....</b>	<b>103</b>
<b>5 General discussion .....</b>	<b>105</b>
5.1 Tamoxifen eye drops: A new delivery method without side effects? .....	106
5.2 TGF- $\beta$ signaling is required for pericyte differentiation .....	108
5.3 Early-induced deletion of ocular TGF- $\beta$ signaling leads to formation of multiple microaneurysms.....	109
5.4 Early-induced deletion of ocular TGF- $\beta$ signaling results in non-perfused capillaries and activation of the ocular immune system .....	110
5.5 Early-induced deletion of ocular TGF- $\beta$ signaling causes vitreal neovascularization, impaired retinal function and retinal detachment .....	111
5.6 Early-induced deletion of ocular TGF- $\beta$ signaling leads to an AMD-like phenotype .....	111
5.7 Late-induced deletion of ocular TGF- $\beta$ signaling results in CNV and a alterations of the Bruch's membrane .....	113
5.8 Deletion of endothelial TGF- $\beta$ signaling leads to development of CNV and changes in the Bruch's membrane .....	114

**6 Summary..... 116**

**7 Table of Figures ..... 118**

**8 List of Tables..... 120**

**9 References..... 121**

**10 Abbreviations ..... 154**

**11 Acknowledgments - Danksagung ..... 157**

**12 Curriculum vitae..... 159**

## Chapter 1

### General Introduction

## 1 General Introduction

Visual impairment and blindness can be caused by various diseases and may affect people of every age and social class. The leading causes of blindness worldwide are, for example, cataract, glaucoma, age-related macular degeneration and diabetic retinopathy (Thylefors et al. 1995). Every disease has its own possible risk factors. Among them are environmental factors, aging, smoking and genetic predispositions. Dysregulation of signaling pathways which are critical for development and homeostasis of the ocular environment may also cause malfunctions which can then lead to blindness.

### 1.1 TGF- $\beta$ signaling

During development and adulthood, TGF- $\beta$  signaling modulates essential processes e.g. cell growth and differentiation, tissue maintenance and apoptosis (Massagué 2012, Heldin et al. 1997). However, TGF- $\beta$  has diverse functions which are discussed controversially, as the effects of TGF- $\beta$  depend on the affected cell type and the cellular environment (Massagué 2012). To date, three different isoforms of the cytokine TGF- $\beta$  are known in mammals (TGF- $\beta$ 1-3) (Massagué 1992, Kingsley 1994). These ligands have the ability to bind TGF- $\beta$  receptor type II (*Tgfb $\beta$ 2*, T $\beta$ RII) which is essential for TGF- $\beta$  signaling. TGF- $\beta$  receptor type I recognizes this process, joins the complex and is phosphorylated by receptor type II (Wrana et al. 1992, Wrana et al. 1994). TGF- $\beta$  receptor type II as well as type I are transmembrane serine/threonine kinases. Phosphorylation correlates with their kinase activity (Massagué et al. 1994, Wrana et al. 1994). Upon complex formation, the activated type I receptor phosphorylates the receptor-regulated (R-) Smads, Smad2 and 3, which form a complex with the co-mediator Smad, Smad4. This complex translocates into the nucleus to regulate the expression of target genes (Figure 1) (Visser and Themmen 1998, Massagué 1998).

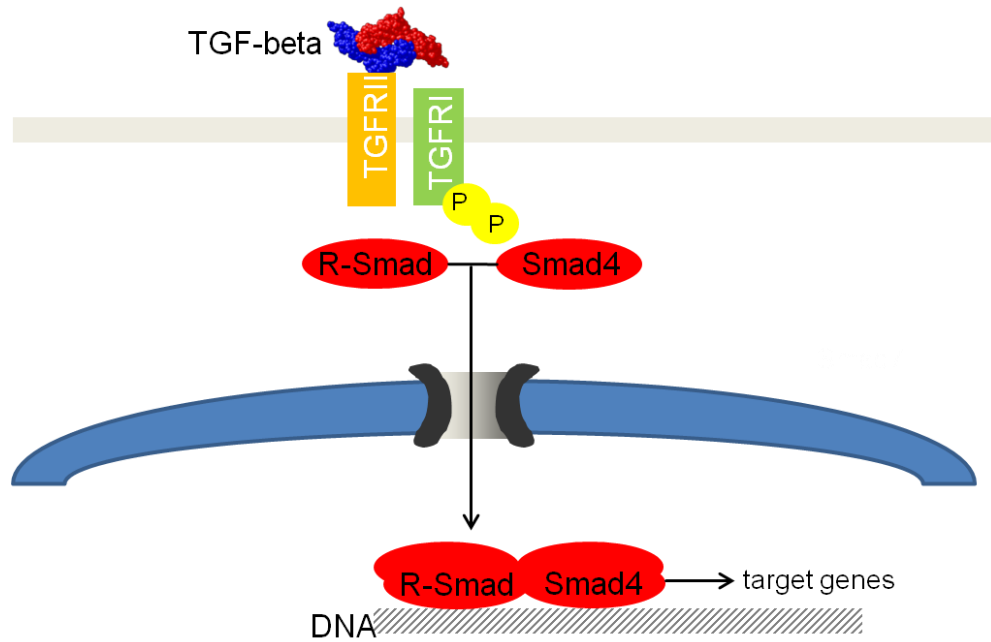


**Figure 1: TGF- $\beta$  signaling pathway.** Binding of TGF- $\beta$  to Tgfr2 leads to recruitment and phosphorylation of Tgfr1 which phosphorylates and thereby activates the R-Smads. The R-Smads form a complex with the Co-Smad Smad4. This complex translocates into the nucleus and regulates the expression of target genes.

## 1.2 Cre loxP system

To understand the function of a specific gene *in vivo*, a common experimental approach is to analyze its function by generating animal models that harbor an inactivation or mutation of the gene (Rajewsky et al. 1996). However, when working with genes that have important functions during cell development or maintenance, researchers are frequently confronted with the problem of embryonic lethality (Branda and Dymecki 2004, Maddison and Clarke 2005). The establishment of the Cre loxP system in mouse models greatly enhanced the opportunities in this context. When using a Cre that is expressed in mice carrying a loxP targeted gene, the gene modification can be restricted to certain cell types or developmental stages depending on the use of specific promoters.

In general, two specific components, both derived from the bacteriophage P1, are necessary to achieve recombination using this system, namely a Cre recombinase and loxP sites: Cre stands for causes recombination and denotes a 38 kDa protein that recognizes and recombines loxP flanked DNA sequences. LoxP is an abbreviation for locus of crossover (x) in P1 bacteriophage

and describes a 34 bp asymmetric DNA sequence (Kuhn and Torres 2002, Sternberg and Hamilton 1981).

Tamoxifen inducible Cre recombinases are known as a special variant of the Cre loxP system (Figure 2). These allow recombination of the target gene at any desired time point. A tamoxifen-inducible Cre recombinase is characterized by its fusion with a mutated form of an estrogen receptor binding domain (ER<sup>TM</sup>). This mutation prevents the binding of endogenous 17 $\beta$ -estradiol but makes the ER<sup>TM</sup> domain susceptible to tamoxifen. Furthermore, this fusion leads to a sequestration of the Cre in the cytoplasm by interaction with Hsp90, thus preventing the Cre's access to the nucleus and therefore recombination. The binding of tamoxifen causes a disruption of this complex. Thus, the Cre is able to translocate into the nucleus to initiate recombination (Hayashi and McMahon 2002).

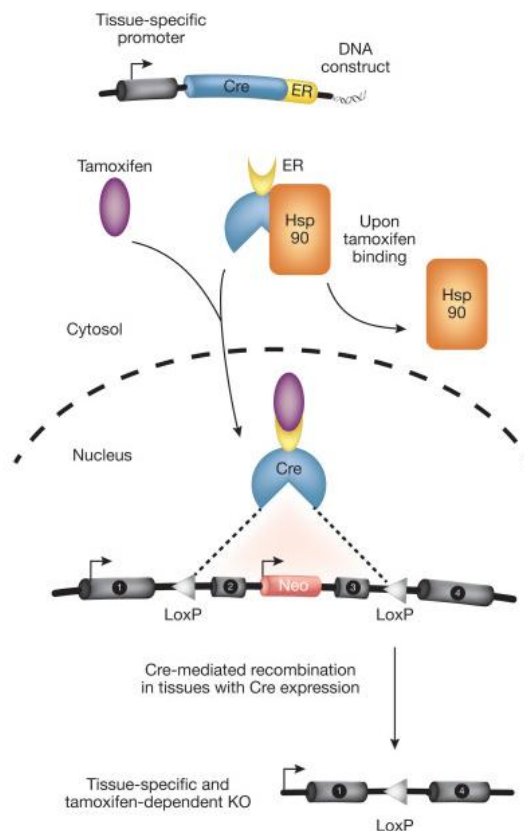


**Figure 2: Tamoxifen-inducible Cre-loxP system.** The Cre recombinase is fused to a modified estrogen receptor (ER) and controlled by a specific promoter. In the inactivated state, heat shock protein 90 (Hsp90) binds to the ER, retaining it in the cytosol. Upon tamoxifen treatment, tamoxifen binds the ER, the Hsp90 protein is released, and the Cre-ER fusion protein can translocate in the nucleus to initiate recombination. Slightly modified from (Gunschmann et al. 2014).

### 1.3 The ocular vasculature

The oxygenation of the retina during initial development is ensured by two different and independent circulatory systems: the choroidal vessels and the hyaloid system. The mature and fully developed retina has the highest oxygen consumption per unit weight of any human tissue and thus needs a perfect system for oxygen supply (Saint-Geniez and D'amore 2004). Therefore, during ocular development and maturation, the embryonic, hyaloid vascular system is replaced by the mature retinal vasculature which consists of three vascular plexus, namely the superior, intermediate and deep plexus (Stahl et al. 2010).

The inner wall of capillaries consists of a single layer of endothelial cells (ECs). These cells are densely coated with either several layers of vascular smooth muscle cells (in larger arteries) or a single layer of non-overlapping pericytes (in smaller arteries and arterioles) (Saint-Geniez and D'amore 2004). Together, the endothelial cells and the pericytes form the vascular basement membrane (Figure 3) (Mandarino et al. 1993). In general, pericytes have long cytoplasmatic processes which they use for contacting neighbouring endothelial cells and therefore can integrate signals along the vessel length (Bergers and Song 2005). Furthermore, they show various characteristics correlating with muscle-cell activity and have the ability to produce vasoconstriction and vasodilation to regulate capillary blood flow (Rucker et al. 2000).

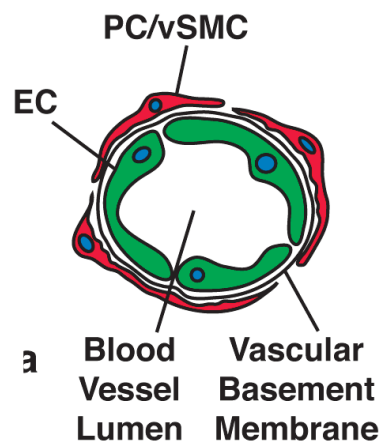


**Figure 3: Composition of capillaries.** Endothelial cells (EC, green) form the inner wall of capillaries, surrounded by the basement membrane in which pericytes (PC, red) or,vascular smooth muscle cells are embedded. Drawing taken from (Bergers and Song 2005)

### 1.3.1 Development of the retinal vasculature

There are two mechanisms responsible for the formation of new blood vessels, namely vasculogenesis and angiogenesis. The term vasculogenesis stands for the de novo formation of blood vessels which begins with the formation of clusters consisting of primitive vascular cells or hemangioblasts (Doetschman et al. 1987). These clusters form tube-like structures that fuse to form a vascular network (Vokes 2004). Angiogenesis, however, refers to the formation of vessels by the sprouting of capillaries from already existing vessels (Risau et al. 1988). In the human retina, both processes occur during vascularization, whereas in mice, retinal vascularization appears to be mediated only via angiogenesis (Hughes et al. 2000, Jiang et al. 1995, Fruttiger 2007, Ashton 1970).

During early stages of retinal development, oxygen supply is provided by the hyaloid vasculature. The hyaloid artery enters the optic cup through the optic nerve and forms an arterial network in the vitreous (Fruttiger 2007, Anand-Apte and Hollyfield 2010). In the more developed retina, the hyaloid vascular system regresses and is replaced by the retinal vasculature. This phenomenon occurs in humans around mid-gestation, in mice regression starts around birth and is finished at approx. P7 (Fruttiger 2007, Lang and Bishop 1993). The regression of the hyaloid arteries starts with an atrophy of the capillaries a process that is mediated via macrophage activity and WNT signaling (Fruttiger 2007, Diez-Roux and Lang 1997, Lobov et al. 2005). Herein, the occlusion of the capillaries by macrophages seems to be a critical step to induce their atrophy. (Anand-Apte and Hollyfield 2010).

Simultaneously with the regression of the hyaloid system, the development of the retinal vasculature starts. Endothelial cells migrate from the optic nerve head over the inner surface of the retina toward the periphery of the retina and form the superficial plexus (Figure 4A). This migration is guided by a gradient of angiogenic factors, e.g. VEGF (vascular endothelial growth factor), expressed from a preexisting astrocytic template (Figure 4E) (Dorrell et al. 2002, Hughes et al. 2000, Ling et al. 1989). The endothelial cells follow the VEGF gradient of the astrocytic network (Stone et al. 1995). Endothelial cells at the vascular front possess filopodia and are called “tip cells” (Figure 4D). Astrocytes guide these tip cells to the remaining avascular areas (Siemerink et al. 2013).

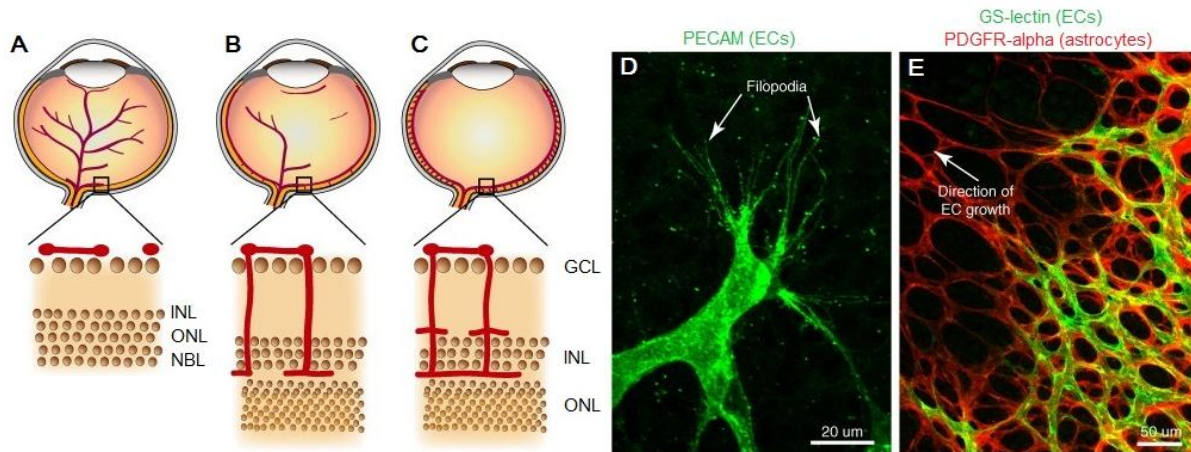


**Figure 4: Development of the retinal vasculature in the mouse.** **A.** Growth of the retinal vasculature starts at the optic nerve head and extends to the periphery to build the superficial plexus. **B.** Secondary branches grow into the retina and reach the outer plexiform layer to develop the deep vascular plexus. **C.** From the deep plexus, vessels extend to the inner plexiform layer, where the intermediate plexus is located. **D.** Endothelial cell at the vascular front shows long filopodia (arrows). **E.** Astrocytes (red) guide endothelial cells (green) to form the superficial plexus. INL, inner nuclear layer; ONL, outer nuclear layer; GCL, ganglion cell layer; NBL, neuroblast layer. Pictures taken from (Ye et al. 2010), slightly modified.

In mice, the vessels of the superficial plexus reach the periphery of the retina on postnatal day 9 (P9). Subsequently, the vessels from the already existing plexus are growing toward the outer plexiform layer to form the deep vascular plexus (Figure 4B). Just a few days later, the intermediate plexus begins to develop from vertical sprouting of the deep plexus upwards to the inner plexiform layer (Figure 4C) (Stahl et al. 2010). Studies assume that the intermediate and deep vascular plexus are built independently of astrocyte guidance (Fruttiger 2007). There are some differences in the development of the retinal vasculature between humans and mice: In mice the development of the retinal vasculature is completed at P21 and in humans already at birth. Also, the chronology of plexus formation in humans is different compared to mice: After the development of the superficial plexus, the intermediate plexus is formed, and finally the deep vascular plexus (Gariano 2003).

### 1.3.2 Blood retinal barrier

The blood retinal barrier (BRB) plays an essential role in the microenvironment of the retina and retinal neurons, as it regulates ion, protein and water in- and outflow of the retina (Cunha-Vaz et al. 2011). This barrier allows the neural retina to develop and maintain specific substrate and ion

concentrations which are substantial for proper neuronal function (Cunha-Vaz et al. 2011). Furthermore, it regulates infiltration of immune competent cells, toxins and various other factors that could have negative effects on the neurons e.g. impede with their function (Cunha-Vaz 2009, Phillips et al. 2007). The blood supply for the retina is secured by two vascular systems, one at the level of the retinal vasculature, and the other at the interface of the choroid and RPE retinal pigment epithelial. Both systems have a BRB which is consequently, subdivided into two major components: the inner blood retinal barrier (iBRB) which comprises the endothelium of the retinal vessels and an interaction with glial cells and perivascular cells like pericytes, and the outer blood retinal barrier (oBRB) which is formed by the retinal pigment epithelium (RPE) (Phillips et al. 2007, Cunha-Vaz 1976, Chen et al. 2008, Klaassen et al. 2013).

The iBRB is formed by tight junctions between the neighboring endothelial cells of the retinal vessels. These junctions make the endothelial cells impermeable to any molecules that are larger than approximately 30 kDa. Small molecules, like glucose and ascorbate, are transported via facilitated diffusion (Chen et al. 2008). The continuous endothelial layer at the inside of the vessel's basal lamina, comprises the main structure of the inner blood retinal barrier. However, at the outside, the basal lamina is covered by pericytes, which together with endothelial cells form the basal lamina, processes of astrocytes and Müller glia cells (Bergers and Song 2005). It is of interest to note that the pericytes do not form a continuous layer (Jordan and Ruiz-Moreno 2013). However, morphological studies could show that pericytes may act as suppressors of endothelial cell growth and contact between these two cell types is necessary for the activation of latent TGF $\beta$ -1 (Antonelli-Orlidge et al. 1989) Activation of TGF $\beta$ -1 inhibits proliferation and migration of endothelial cells (Orlidge 1987). Furthermore, TGF $\beta$ -1 is an important player during vessel formation, as it induces differentiation of mesenchymal stem cells and neuro crest cells into pericytes (Chen and Lechleider 2004, Ding et al. 2004, Bergers and Song 2005)

Astrocytes, pericytes and Müller glia cells influence the activity of retinal endothelial cells and the iBRB by transmitting regulatory signals to ECs (Chen et al. 2008, Bergers and Song 2005). In humans, a loss of pericytes, a phenomenon called “pericyte-dropout” in patients suffering from diabetic retinopathy, results in a weakening of the vascular walls and can result in the development of microaneurysms (Wilkinson-Berka et al. 2004, Hammes et al. 2002). However, in mice, lacking >50% of pericytes, retinal microaneurysms are not a prominent finding (Enge 2002, Hammes et al. 2002, Hammes 2005). In general, a breakdown of the inner blood retinal barrier is associated with diseases like diabetic retinopathy (Cunha-Vaz 2009, Cunha-Vaz 1976, Chen et al. 2008)

The outer blood retinal barrier is formed by tight junctions (zonulae occludentes) between the neighboring cells of the retinal pigment epithelium (Peyman and Bok 1972, Strauss 2005). The RPE consists of a single layer of pigmented cells and disconnects the neural retina from the underlying fenestrated endothelium of the choriocapillaris and therefore plays an essential role in extracting nutrients from the blood and making them accessible to the photoreceptors. Furthermore, the RPE eliminates debris and maintains retinal adhesion. The relationship between the retinal pigment epithelium and the photoreceptor layer is essential for maintaining visual function (Cunha-Vaz 2009, Strauss 2005). Alterations in the tightness of the outer blood retinal barrier may result in diseases like age-related macular degeneration (AMD) (Cunha-Vaz 1976, Cunha-Vaz 2009).

### 1.4 Pathologies of the ocular vasculature

#### 1.4.1 Diabetic retinopathy

Diabetic retinopathy (DR) is the leading cause of blindness in the developed world (Cai and McGinnis 2016). This disease can be divided into two stages: nonproliferative DR and proliferative DR (Engerman 1989). An early sign of nonproliferative diabetic retinopathy is the appearance of multiple microaneurysms (Speiser et al. 1968). These microaneurysms are presumed to be the result of loss of pericytes, a phenomenon that is called “pericyte dropout” (Wilkinson-Berka et al. 2004, Hammes et al. 2002). The loss of pericytes initiates the death of ECs and therefore leads to a weakening of the vascular walls. When microaneurysms rupture, microhemorrhages (Figure 5) can be observed throughout the retina (Wilkinson-Berka et al. 2004, Bandello et al. 2014). Further symptoms for nonproliferative diabetic retinopathy are a thickening of the basement membrane, development of hard exudates, cotton wool spots (Figure 5) and occlusion of retinal vessels (Cai and McGinnis 2016, 2016, Bandello et al., Cai and Boulton 2002, Engerman 1989). When diabetic retinopathy changes toward a proliferative phenotype, neovascularizations can be observed. Neovascularizations towards the vitreous can in the following lead to vitreous contraction, hemorrhage and tractional retinal detachment (Cai and McGinnis 2016, Cheung et al. 2010, Antonetti et al. 2012).

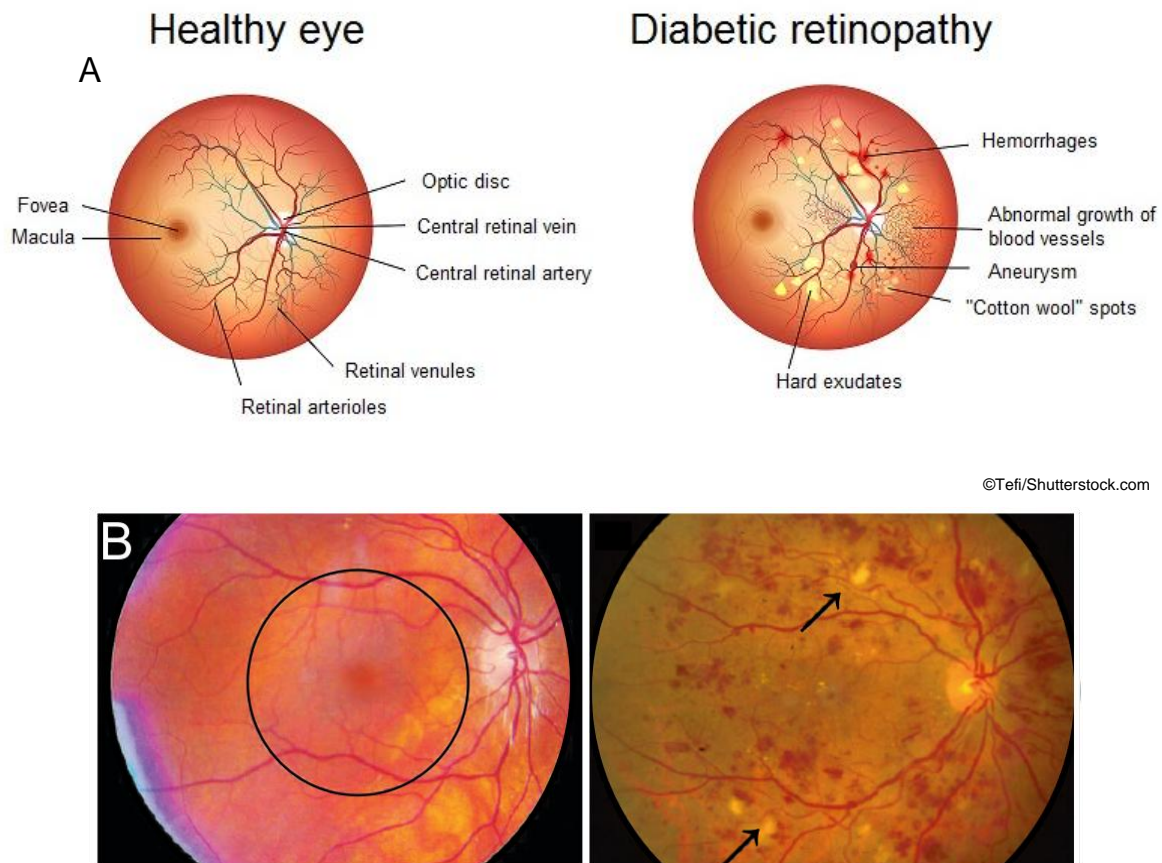


**Figure 5: Diabetic retinopathy.** **A.** Drawing of a healthy eye and an eye with diabetic retinopathy. Pathological changes like hemorrhages, abnormal growth of blood vessels, aneurysms, cotton wool spots and hard exudates can be seen in the eye with diabetic retinopathy. **B.** Funduscopy of an healthy eye (left panel, macula is marked by black circle) and an eye with severe diabetic retinopathy characterized by several widespread hemorrhages inside and outside the major vascular arcades, cotton wool spots ( black arrows ). A. Slightly modified from [www.shutterstock.com](http://www.shutterstock.com). B. Slightly modified from (Jager et al. 2008, Bandello et al. 2014).

The pathological changes which occur during diabetic retinopathy are well described, albeit the underlying molecular mechanisms remain still unclear. Undoubtedly, diabetes represents the greatest risk for developing DR. Furthermore, type I diabetes is more likely to result in vision loss than type II. Along with diabetes, further important risk factors for developing DR are race, smoking, hyperglycemia and hyperlipidemia (Das et al. 2015). A key element in the development of diabetic retinopathy is VEGF (vascular endothelial growth factor) which is clearly elevated in diabetic retinal tissue without overt retinopathy. It is presumed to be the initiator of increased

permeability of the retinal vasculature in diabetes (Amin et al. 1997, Sone et al. 1997, Clermont et al. 1997). Increased VEGF levels lead to a decreased tight junction protein expression which is strongly associated with a breakdown of the inner blood retinal barrier (Antonetti et al. 1998).

Another growth factor that may contribute to the pathogenesis of diabetic retinopathy is TGF- $\beta$ . Several studies have shown that levels of TGF $\beta$ -2 were elevated in the vitreous of patients with diabetic retinopathy, especially in those who suffer from a proliferative form of the disease (Kita et al. 2006, Hirase et al. 1998). These findings suggest that TGF- $\beta$  signaling may be involved in the molecular pathogenesis of diabetic retinopathy.

### 1.4.2 Age-related macular degeneration

In people of 50 years and older, age-related macular degeneration (AMD) supersedes diabetic retinopathy as the leading cause of severe vision loss in the developed world (Pascolini et al. 2004, Congdon et al. 2004). In general, two forms (wet and dry) of AMD can be distinguished (Bowes Rickman et al. 2013). In the early stage, the disease develops slowly and remains mostly asymptomatic for years (Coleman et al. 2008, Hogg and Chakravarthy 2006). The late stage, however, is characterized by severe vision loss (de Jong, Paulus T V M 2006, Sarks et al. 1999). Typically, focal deposition of acellular debris between the retinal pigment epithelium and the Bruch's membrane occur during aging (Bird et al. 1995). These deposits are called drusen and are usually the first clinical finding of dry age-related macular degeneration (Figure 6A) (Bird et al. 1995). They can be observed in the macula as well as in the peripheral retina. Drusen can be classified in three different stages by their diameter. There are small ( $< 63\mu\text{m}$ ), medium (between  $63\mu\text{m}$  and  $124\mu\text{m}$ ) and large drusen ( $> 124\mu\text{m}$ ) (Bird et al. 1995). Furthermore, drusen can be characterized as soft or hard, based on the appearance of their margins. While hard drusen show discrete margins, soft drusen are characterized by indistinct edges (Bird et al. 1995). Excessive formation of drusen can subsequently lead to a damage of the retinal pigment epithelium. This effect together with a chronic inflammatory response can result in areas of retinal atrophy, also known as "geographic atrophy" (Figure 6B) (de Jong, Paulus T V M 2006, Maguire and Vine 1986, Sunness et al. 1999). In the following, an induction of angiogenic cytokines like VEGF can occur, leading to the formation of choroidal neovascularization (CNV) which is accompanied by increased vascular permeability (Figure 6C). These newly formed vessels grow from the choriocapillaris through the Bruch's membrane toward and into the subretinal space (Pauleikhoff 2005, van Lookeren Campagne et al. 2014). The development of

these neovascularization is directly related to serious hemorrhages and detachment of the RPE (de Jong, Paulus T V M 2006, Jager et al. 2008).



**Figure 6: Funduscopy – age-related macular degeneration.** **A.** Funduscopy of an eye with intermediate age-related macular degeneration showing large drusen. **B.** Geographic atrophy involving the centre of the fovea, with sharply demarcated loss of normal retinal pigment epithelial cells and evidence of deeper larger choroidal vessels. **C.** Neovascular age-related macular degeneration, with retinal haemorrhage, lipids, or retinal hard exudate and subretinal fluid. Slightly modified from (Coleman et al. 2008).

The strongest risk factor for developing age-related macular degeneration is age (Mitchell et al. 1995, Klein et al. 1999, Klein et al. 1992, Friedman et al. 1999). Other than that, smoking as well as genetic factors may be involved in causing AMD (Evans et al. 2005, Thornton et al. 2005, Scholl et al. 2007, Haddad et al. 2006). A recent study could demonstrate that high temperature requirement factor A1 (HTRA1) influences the risk of AMD (Yang et al. 2010).

Recently it was shown, that HTRA1 can interact with members of the TGF- $\beta$  signaling pathway and plays a critical role in the regulation of angiogenesis via TGF- $\beta$  signaling (Friedrich et al. 2015). Growth differentiation factor 6 (GDF6), which is a member of the TGF- $\beta$  family is involved in ectoderm patterning and eye development. Furthermore, *GDF6* could be identified as a novel disease gene for AMD (Zhang et al. 2012). In summary, these findings implicate a potential role of TGF-beta signaling in the molecular pathogenesis of age related macular degeneration.

### 1.5 Aim of the study

The systemic knockout of TGF- $\beta$  is embryonically lethal, because of haematopoietic and vascular defects in the yolk sack (Dickson et al. 1995). Therefore, scientists are confronted with serious problems when investigating the role of TGF- $\beta$  signaling *in vivo* during development and in adulthood. The Cre loxP system allows to circumvent embryonic lethality, using Cre recombinases that are time-dependent or tissue specific.

To date, there is no Cre recombinase available with an ubiquitous expression of Cre that is restricted to all cells of the eye. Therefore our group established a method to obtain efficient Cre mediated recombination in the entire eye. In previous studies we could show that tamoxifen eye drops successfully achieve the activation of Cre when applied to the eyes of 4 days old mouse pups carrying an tamoxifen dependent cre recombinase which is under control of an ubiquitously expressed chicken  $\beta$  actin promotor (CAGG-Cre ER<sup>TM</sup>) (Hayashi and McMahon 2002). When crossing heterozygous CAGG-Cre ER<sup>TM</sup> mice with mice carrying loxP sites flanking exon 2 of *Tgfb2* (Chytil et al. 2002), the administration of tamoxifen led to a deletion of *Tgfb2* in all ocular tissue. The downregulation of TGF- $\beta$  signaling resulted in marked morphological changes of the retinal vasculature. Most strikingly, *Tgfb2* deficient mice (*Tgfb2* <sup>$\Delta$ eye</sup>) developed multiple microaneurysms, similar to those that can be seen in patients suffering from diabetic retinopathy. Furthermore, the expression levels of *Vegf-a* and *Hif1- $\alpha$*  were significantly increased in the retinae of 4 week-old mice. At the age of 6 weeks the mice additionally developed choroidal neovascularization (CNV) which are a hallmark for the wet form of age related macular degeneration.

The overall goal of my thesis was to characterize the newly established system of tamoxifen administration and to investigate the phenotype of *Tgfb2* deficient mice with an early and late induced deletion of the TGF- $\beta$  signaling pathway. In particular following aims were pursued:

- What is the effect of an early-induced deletion of the TGF- $\beta$  signaling pathway on the pericytes? Is the formation of microaneurysms in the *Tgfb2* <sup>$\Delta$ eye</sup> animal model a result of pericyte loss, a scenario that is called “pericyte-dropout” in diabetic retinopathy? Are there further similarities to diabetic retinopathy in humans?
- Are the choroidal neovascularization in the early-induced *Tgfb2* <sup>$\Delta$ eye</sup> animal model, a primary effect caused by the deletion of ocular TGF- $\beta$  signaling or are they a result of the irregularly developed retinal vasculature and the herein resulting hypoxia?

## Chapter 1 – General Introduction

- To discriminate these two possibilities I inhibited the TGF $\beta$ -signaling pathway after the retinal vasculature had been developed. The late-induced *Tgfb $\beta$ 2* <sup>$\Delta$ eye</sup> animal model was analyzed using a broad range of histological and molecular techniques.
- Which cell type is responsible for the formation of the choroidal neovascularization? To answer this question, I will delete *Tgfb $\beta$ 2* specifically in the retinal pigment epithelium or in the endothelial cells using appropriate inducible Cre mouse lines.

## Chapter 2

### **Tamoxifen-Containing Eye Drops Successfully Trigger Cre-Mediated Recombination in the Entire Eye**

(adapted from: Anja Schlecht\*, Sarah V. Leimbeck\*, Ernst R. Tamm, Barbara M. Braunger  
**Tamoxifen-Containing Eye Drops Successfully Trigger Cre-Mediated Recombination in the Entire Eye.** Adv Exp Med Biol. 2016;854:495-500)

\*contributed equally to the study

## **2 Tamoxifen-Containing Eye Drops Successfully Trigger Cre-Mediated Recombination in the Entire Eye**

### **2.1 Abstract**

Embryonic lethality in mice with targeted gene deletion is a major issue that can be circumvented by using Cre-loxP-based animal models. Various inducible Cre systems are available, e.g. such that are activated following tamoxifen treatment, and allow deletion of a specific target gene at any desired time point during the life span of the animal. In this study, we describe the efficiency of topical tamoxifen administration by eye drops using a Cre- reporter mouse strain (*R26R*). We report that tamoxifen-responsive *CAGG Cre-ER<sup>TM</sup>* mice show a robust Cre-mediated recombination throughout the entire eye.

### 2.2 Introduction

When working with genes associated with germline null alleles that are required for major developmental or cell maintenance pathways, scientists frequently face the problem of embryonic lethality after constitutional targeted deletion of their gene of interest (Branda and Dymecki 2004, Maddison and Clarke 2005). The use of Cre loxP- based animal models has greatly expanded the possibilities for scientists to delete essential genes in the mouse and thus circumvent the embryonic lethality, as this approach allows the generation of tissue- or cell-specific conditional deletions (Kühn and Torres 2002). Moreover, different inducible Cre systems are available, like such that are tamoxifen-responsive, and allow gene deletion at any desired time point. In this study, we used CAGG Cre-ER<sup>TM</sup> mice (Hayashi and McMahon 2002) that carry the Cre-ER<sup>TM</sup> fusion protein, which is comprised of the Cre-recombinase fused to a mutant form of the mouse estrogen receptor (Hayashi and McMahon 2002). The fusion protein is restricted to the cytoplasm and Cre- ER<sup>TM</sup> will only access the nucleus after exposure to tamoxifen. Thus, exposure to tamoxifen in a spatially-defined manner allows tissue-specific targeted gene deletion. In this article, we describe a protocol that efficiently causes Cre-mediated recombination following topical tamoxifen treatment by applying tamoxifen-containing eye drops. Using a Cre- reporter mouse strain (*R26R*), we show a robust Cre-mediated recombination throughout the entire eye.

## 2.3 Material and Methods

### 2.3.1 Mice

All procedures conformed to the tenets of the National Institutes of Health Guidelines on the Care and Use of Animals in Research, the EU Directive 2010/63/E, and institutional guidelines. Mice that were heterozygous for *CAGG Cre-ER<sup>TM</sup>* were crossed with homozygous Cre-reporter (*R26R*) (Soriano 1999) mice. *R26R* mice carry a loxP-flanked DNA segment that prevents the expression of the downstream lacZ gene. However, when *R26R* mice are crossed with a Cre transgenic strain, the Cre expression results in the removal of the loxP-flanked DNA segment and lacZ is expressed in all cells or tissues where Cre is expressed. In this study, *CAGG Cre-ER<sup>TM</sup>/R26R* mice were used as experimental mice, and *R26R* littermates as control mice. Genetic backgrounds were 129SV (*R26R*) or C57Bl6 (*CAGG Cre-ER<sup>TM</sup>*).

### 2.3.2 Tamoxifen Treatment

To induce the nuclear trans-localization of the Cre recombinase and its activation, *CAGG Cre-ER<sup>TM</sup>/R26R* mice and *R26R* littermates were treated with tamoxifen-containing eye drops. To this end, tamoxifen (Sigma) was diluted in corn oil (Sigma) to a final concentration of 5 mg/ml and the solution was pipetted as eye drops (10 µl/ drop) onto the closed eyelids of mouse pups three times per day in 4 h intervals. Our treatment started at p8 and lasted to p12, which obviously can be adjusted for other time points depending on the gene and molecular processes of interest.

### 2.3.3 PCR Analysis

Genotypes were screened by isolating genomic DNA from tail biopsies and testing for transgenic sequences by PCR as described previously (Braunger et al. 2013b). The following PCR primers were used: Cre genotyping (5'-CAC CCT GTT ACG TAT AGC-3' and 5'-CTA ATC GCC ATC TTC CAG-3') and LacZ genotyping (5'- ATC CTC TGC ATG GTC AGG TC-3' and 5'-CGT GGC CTG ATT CAT TCC-3'). The thermal cycle profile was denaturation at 96 °C for 30 s, annealing at 57 °C (Cre), or 60 °C (LacZ) for 30 s, and extension at 72 °C for 1 min for 35 cycles.

### 2.3.4 $\beta$ -galactosidase Staining

Lac-Z-staining was performed in mixed *CAGG Cre-ER<sup>TM</sup>/R26R* and *R26R* mice following a previously published protocol (Baulmann et al. 2002). Briefly, after enucleation, eyes were fixed in LacZ fixative solution (2 mM  $\text{MgCl}_2$ , 5 mM EGTA (pH 7.3), 0.2 % glutaraldehyde in 0.1 M phosphate buffer (pH 7.3) at 4 °C for 30 min. After three 10 min rinses in LacZ wash buffer (0.01 % sodium deoxycholate, 0.02 % NP-40, 2 mM  $\text{MgCl}_2$  in 0.1 M phosphate buffer (pH 7.3)),  $\beta$ -galactosidase activity was visualized in X-Gal staining solution (500 mM  $\text{K}_4\text{Fe}(\text{CN})_6 \times 3\text{H}_2\text{O}$ , 500 mM  $\text{K}_3\text{Fe}(\text{CN})_6$ , 1 mg/ml X-gal in LacZ wash buffer). The eyes were stained in X-Gal solution at 37 °C for 24 h, rinsed in LacZ wash buffer (3  $\times$  10 min) followed by one 10 min rinse in phosphate buffer and then processed to paraffin embedding. Paraffin sections (6  $\mu\text{m}$  thick) were analyzed as mentioned previously (Braunger et al. 2013a).

## 2.4 Results - Localization of Cre-mediated Recombination in Ocular Tissues

After topical tamoxifen treatment with eye drops, we used  $\beta$ -galactosidase staining to localize Cre-mediated recombination in the eye. Eyes of *CAGG Cre-ER<sup>TM</sup>/R26R* mice (Figure 7b) showed an intense  $\beta$ -galactosidase reaction throughout the entire organ while control eyes (*R26R*) were essentially negative (Figure 7a and Figure 8a, c, e, and g).

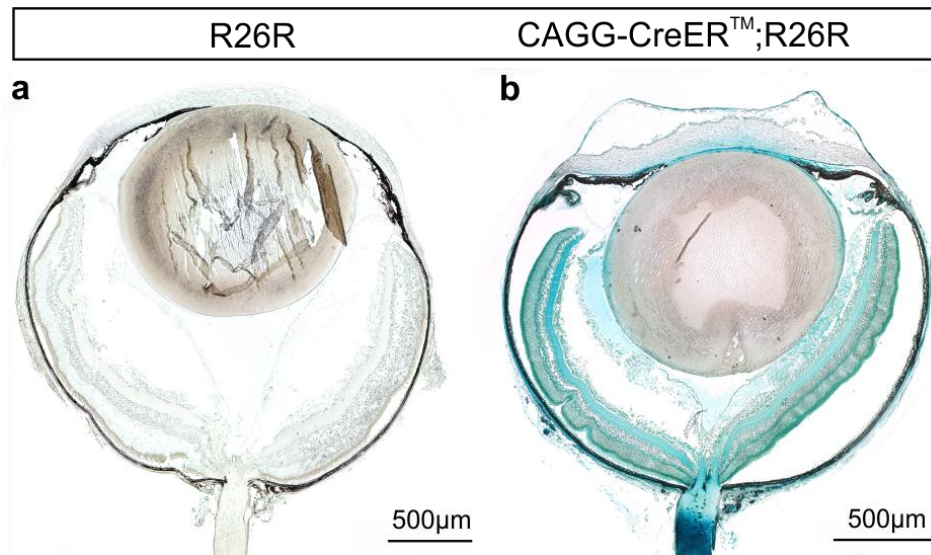


**Figure 7. Localization and activation of Cre recombinase in the eye following tamoxifen containing eye drops.** An intense  $\beta$ -galactosidase staining throughout the entire eye in 14 days old *CAGG Cre ER<sup>TM</sup>/R26R* mouse (b) indicates a successful activation of the Cre recombinase in ocular tissue following treatment with tamoxifen eye drops. Control littermates (*R26R*) (a) did not show a positive reaction. Experiment performed by Anja Schlecht and Sarah V. Leimbeck.

The detailed analysis of *CAGG Cre-ER<sup>TM</sup>/R26R* eyes showed an intense  $\beta$ -galactosidase reaction in the anterior eye segment. We observed in particular a strong  $\beta$ -galactosidase staining in the structures of the chamber angle outflow pathway, in the ciliary body (Figure 8b) and in the cornea, as well as in the epithelium of the lens (Figure 8d). In the posterior eye segment of *CAGG Cre-ER<sup>TM</sup>/R26R* eyes, the sensory retina, the retinal pigment epithelium (RPE) and the choroid (Figure 8f) stained positive for  $\beta$ -galactosidase indicating a successful Cre-mediated recombination in basically every ocular cell type. In addition, in sections where the optic nerve was cut, we observed positive staining along the sheaths surrounding the nerve indicating that tamoxifen had been distributed outside the eye (Figure 8h).

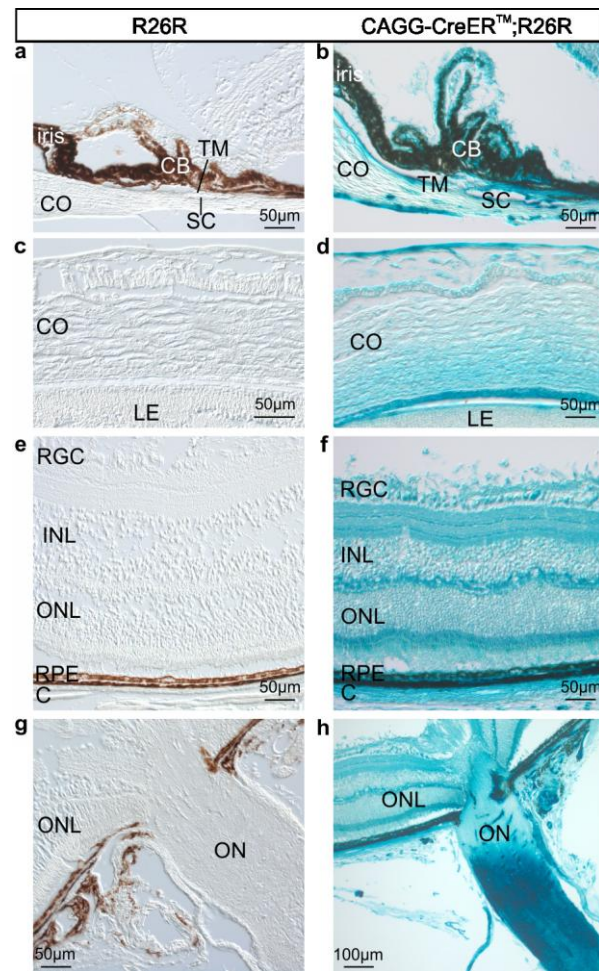


**Figure 8. Detailed localization and activation of Cre recombinase in the eye.** Detailed magnification of the  $\beta$ -galactosidase staining in the structures of the chamber angle outflow pathway (**b**), the cornea and the lens epithelium (**d**), the retina and choroid (**f**) and the optic nerve (**h**) of a 14 days old CAGG Cre-ER<sup>TM</sup>/R26R mouse. The control littermate did not show a positive reaction for  $\beta$ -galactosidase (**a**, **c**, **e** and **g**). RGC retinal ganglion cells, INL inner nuclear layer, ONL outer nuclear layer, RPE retinal pigment epithelium, C choroid, ON optic nerve, CB ciliary body, CO cornea, TM Trabecular meshwork, SC Schlemm's canal, LE lens. Experiment performed by Anja Schlecht and Sarah V. Leimbeck.

### 2.5 Discussion

Our results show that induction of Cre recombinase by using tamoxifen-containing eye drops is a suitable method to induce a tamoxifen-dependent Cre-mediated recombination in ocular tissues. The topical application of tamoxifen-containing eye drops provides several advantages. As a non-invasive method it greatly reduces or even avoids the potential risk of infections, which might eventually result from intra-peritoneal injections (Leenaars et al. 1998, Leenaars and Hendriksen 2005), which is a common method to administer tamoxifen. Intravitreal tamoxifen injections harbor the same risks of infection. Furthermore this route might influence the expression level of potential genes of interests because intravitreal injection of the vehicle alone already results in the activation of microglia and/or an elevated expression of neuroprotective molecules (Braunger 2014, Seitz and Tamm 2014). In our study, we noticed staining along the optic nerve outside the eye, a finding that appears to indicate that tamoxifen is distributed to tissues outside the eye. One could avoid this and achieve even greater spatial control of Cre expression by reducing the duration of tamoxifen treatment, e.g. from 5 days, to 3 days or maybe even less. Of course, this approach could in turn result in a Cre-mediated recombination gradient in the eye itself. This scenario might be of great interest for scientist focusing on the anterior segment of the eye like the cornea or the chamber angle outflow pathway. Here, a reduced exposure time might reduce the tamoxifen-induced Cre-mediated recombination in other parts of the eye or the body to an even greater extend. As a side note, our system also allows the usage of strong promoters like CMV or  $\beta$ -actin that would drive Cre-expression in every cell. The expression of Cre, however, can be spatially controlled, as the tamoxifen is applied topical. Finally, considering tamoxifen induced toxicity, which may influence cell viability or even promote cell death (Kim et al. 2014), the topical administration of tamoxifen using eye drops could obviously reduce this risk, too. In summary, our approach may be of great interest for scientists in the field of experimental eye research.

## Chapter 3

### **Deletion of ocular TGF- $\beta$ signaling mimics essential characteristics of diabetic retinopathy**

(adapted from: Barbara M. Braunger, Sarah V. Leimbeck, Anja Schlecht, Cornelia Volz, Herbert Jägle and Ernst R. Tamm. **Deletion of ocular TGF- $\beta$  signaling mimics essential characteristics of diabetic retinopathy**. Am J Pathol. 2015 Jun;185(6):1749-68)

### **3 Deletion of ocular TGF- $\beta$ signaling mimics essential characteristics of diabetic retinopathy**

#### **3.1 Abstract**

Diabetic retinopathy, a major cause of blindness, is characterized by a distinct phenotype. The molecular causes of the phenotype are not sufficiently clear. Here we report that deletion of TGF- $\beta$  signaling in the retinal microenvironment of newborn mice induces changes that largely mimic the phenotype of non-proliferative and proliferative diabetic retinopathy in humans. Lack of TGF- $\beta$  signaling leads to the formation of abundant microaneurysms, leaky capillaries, and retinal hemorrhages. Retinal capillaries are not covered by differentiated pericytes, but by a coat of vascular smooth muscle-like cells and a thickened basal lamina. Reactive microglia is found in close association with retinal capillaries. In older animals, loss of endothelial cells and the formation of ghost vessels are observed, findings that correlate with the induction of angiogenic molecules and the accumulation of retinal HIF-1 $\alpha$  indicating hypoxia. Consequently, retinal and vitreal neovascularization occurs, a scenario that leads to retinal detachment, vitreal hemorrhages, neuronal apoptosis and impairment of sensory function. We conclude that TGF- $\beta$  signaling is required for the differentiation of retinal pericytes during vascular development of the retina. Lack of differentiated pericytes initiates a scenario of structural and functional changes in the retina that mimics those of diabetic retinopathy strongly indicating a common mechanism.

### 3.2 Introduction

Diabetic retinopathy is a leading cause of visual impairment and blindness in the developed world (Sivaprasad et al. 2012, Congdon et al. 2003). Clinically, diabetic retinopathy begins with typical microvascular signs in the retina of an individual with diabetes mellitus. The earliest clinical signs of diabetic retinopathy include the formation of microaneurysms, small outpouchings from retinal capillaries, and of dot intraretinal hemorrhages (Frank 2004). Number and sizes of hemorrhages increase as the disease progresses. In addition, the barrier of retinal capillaries becomes impaired which may lead to retinal edema, to the deposition of plasma lipid and lipoprotein contents, and the formation of hard exudates. In parallel to the increase in vascular permeability, occlusion and loss of retinal vessels is observed, a scenario that is thought to cause the formation of ischemic infarcts of the nerve fiber layer (cotton-wool spots). Because of the high metabolic requirements of retinal neurons, capillary damage in the retina causes hypoxia and the release of potent angiogenic factors such as vascular endothelium growth factor (VEGF). As a result, diabetic retinopathy progresses from a non-proliferative stage to a fibrotic, proliferative stage that is characterized by the growth of new capillaries in retina and vitreous. Diabetic neovascularization leads to preretinal or vitreous hemorrhages, and to tractional retinal detachment caused by proliferative vitreoretinopathy (Cheung et al. 2010, Antonetti et al. 2012).

The characteristic histopathological lesion that occurs early in diabetic retinopathy, is the relative selective loss of pericytes from retinal capillaries (Kuwabara 1963). The loss of pericytes is followed by the loss of capillary endothelial cells and apoptosis is thought to be the mechanism that is largely responsible for the loss of both cell types (Mizutani et al. 1996, Barber et al. 2011). Similarly, pericyte dropout and acellular occluded capillaries were observed in numerous diabetic animal models (Hammes 2005). Pericyte loss appears to be causatively involved in capillary occlusion as genetically modified mice with specific deficiency of platelet-derived growth factor- $\beta$  (PDGF- $\beta$ ) in endothelial cells show a varying degree of pericyte loss in parallel with occlusions of retinal capillaries (Hammes 2005). Comparable findings were observed in heterozygous PDGF- $\beta$ -deficient diabetic mice (Hammes et al. 2002). Still, other characteristics of diabetic retinopathy such as sprouting of retinal capillaries and the formation of microaneurysms are not commonly observed in mice with pericyte dropout (Hammes et al. 2002). Accordingly, besides pericyte dropout, other mechanisms appear to contribute to the structural changes in diabetic retinopathy and immunological processes are likely candidates (Adamis and Berman 2008, Kern 2007).

Evidence suggests that transforming growth factor (TGF)- $\beta$  signaling plays an important role in the proliferation and the differentiation of both pericytes and endothelial cells during development (Armulik et al. 2011). The specific action of TGF- $\beta$  signaling in this context appears to depend on the respective concentrations of the TGF- $\beta$  isoforms and the availability of appropriate receptors, and may inhibit or promote proliferation and differentiation of the vascular cell types (Gaengel et al. 2009). In the retina, constitutive TGF- $\beta$  signaling appears to be important for maintaining the structure and function of retinal capillaries. Accordingly, the inhibition of TGF- $\beta$  signaling by systemic expression of soluble endoglin results in the apoptosis of vascular cells, the formation of leaky capillaries and the impairment of retinal perfusion (Walshe et al. 2009). Moreover, TGF- $\beta$  signaling is thought to serve an important immunosuppressive role in the retina (Chytil et al. 2002). Still, the role of TGF- $\beta$  signaling for the formation and maintenance of the retinal vasculature has only been incompletely studied, since the deletion of most of the different TGF- $\beta$  signaling pathway genes results in embryonic lethality during midgestation (Armulik et al. 2011, Gaengel et al. 2009). Here we report on the phenotype of mice with a conditional deletion of the essential TGF- $\beta$  type II receptor (T $\beta$ RII) in ocular tissues. We provide evidence that impairment of TGF- $\beta$  signaling in the retinal microenvironment promotes the development of structural changes in the retina that largely mimic the phenotype of non-proliferative and proliferative diabetic retinopathy. Our results point towards an important role of TGF- $\beta$  signaling in the pathogenesis of diabetic retinopathy.

### 3.3 Materials and Methods

#### 3.3.1 Mice

Mice with two floxed alleles of *Tgfb $\beta$ 2* (Chytil et al. 2002) were crossed with *Tgfb $\beta$ 2<sup>flox/flox</sup>;CAGG Cre-ER<sup>TM</sup>* animals that were heterozygous for transgenic CAGG Cre-ER<sup>TM</sup>. Resulting *Tgfb $\beta$ 2<sup>flox/flox</sup>;CAGG Cre-ER<sup>TM</sup>* animals were used as experimental mice, and littermates with two unrecombined *Tgfb $\beta$ 2<sup>fl/fl</sup>* alleles are referred to as control mice. Genetic backgrounds were 129SV (*Tgfb $\beta$ 2*) or C57Bl6 (CAGG Cre-ER<sup>TM</sup>). All mice were reared in 12 h light–12 h dark cycles (lights on at 7 am). Genotypes were screened by isolating genomic DNA from tail biopsies and testing for transgenic sequences by PCR. For Cre-PCR analysis primers were: 5'-ATGCTTCTGTCCGTT TGCCG-3' (sense) and 5'-CCTGTTTTGCACGTTCCACCG-3' (antisense). The thermal cycle profile was denaturation at 96°C for 30 s, annealing at 57°C for 30 s, and 1 min extension at 72°C for 35 cycles. For genotyping of *TGF- $\beta$ -R2<sup>flox/flox</sup>* animals, primers were 5'-GCAGGCATCAGGACCCAGTTTGATCC-3' (sense) and 5'-AGAGTGAAGCCGTGGTAGGT GAGCTTG-3' (antisense). The thermal cycle profile was denaturation at 96°C for 30 s, annealing at 61°C for 30 s, and 1 min extension at 72°C for 35 cycles. To induce Cre recombinase, mice were treated with tamoxifen (Sigma) eye drops. Tamoxifen was diluted in corn oil to a final concentration of 5 mg/ml. From P4 to P8, eye drops at a volume of 10  $\mu$ l were pipetted onto the closed eyelids of mouse pups three times a day. All procedures conformed to the tenets of the National Institutes of Health Guidelines on the Care and Use of Laboratory Animals (National Research Council (U.S.) and Institute for Laboratory Animal Research (U.S.) 2011), the EU Directive 2010/63/E, and institutional guidelines, and were approved by the local authority (Regierung der Oberpfalz, Bavaria, Germany, 54-2532.1-44/12).

#### 3.3.2 Western blot analysis

Retinal proteins were isolated following the manufacturer's instructions (Invitrogen) for TRIzol protein isolation. Proteins were separated by SDS-PAGE (6%, 8% or 10% gels, depending on the molecular weight of the protein of interest) and transferred by semidry blotting onto a polyvinyl difluoride membrane (PVDF, Milipore). PVDF membranes were incubated with TBS containing 0.1% Tween 20 (TBST; pH 7.2) and blocking reagent (Table 1) overnight. Antibodies were used as described in Table 1. After washing with TBS-T, secondary antibodies (1:2000) were added. Chemiluminescence was detected on a LAS 3000 imaging workstation. For normalization, blots were labeled with antibodies against glyceraldehyde 3-phosphate dehydrogenase (GAPDH, 1:10,000, HRP-conjugated, Cell Signaling) or  $\alpha$ -tubulin (1:5000,

Rockland). Western blots were evaluated by relative densitometry using the Aida Image Analyzer v.4.06 software (Raytest).

**Table 1. Antibodies used for Western Blot analysis**

Primary antibody	Blocking	Secondary antibody
TβRII c16 (Santa Cruz) 1:200	5% non-fat dry milk	chicken anti-rabbit coupled to horseradish peroxidase (Santa Cruz)
pSmad3 (Cell Signaling) 1:200	5% bovine serum albumin	chicken anti-rabbit coupled to horseradish peroxidase (Santa Cruz)
FGF-2 sc79 (Santa Cruz) 1:200	5% bovine serum albumin	chicken anti-rabbit coupled to horseradish peroxidase (Santa Cruz)
HIF1- α (Cayman Chemical) 1:200	5% bovine serum albumin	chicken anti-rabbit coupled to horseradish peroxidase (Santa Cruz)
Collagen IV (Rockland) 1:500	5% bovine serum albumin	goat anti-rabbit coupled to alkaline phosphatase (Santa Cruz)
Smooth muscle α-actin (Genetex) 1:500	5% bovine serum albumin	goat anti-rabbit coupled to alkaline phosphatase (Santa Cruz)
NG2 (Merck Millipore) 1:1000	5% bovine serum albumin	chicken anti-rabbit coupled to horseradish peroxidase (Santa Cruz)
GAPDH (Cell Signaling) 1:10000	5% non-fat dry milk	directly horseradish peroxidase coupled
α-tubulin (Rockland) 1:5000	5% bovine serum albumin	goat anti-rabbit coupled to alkaline phosphatase (Santa Cruz)

### 3.3.3 Microscopy and morphometry

Mice were deeply anesthetized with ketamine (120 mg/kg body weight, i.m.) and xylazine (8 mg/kg body weight), and perfused with 1 ml of modified Karnovsky's fixative (Karnovsky 1965) through the left ventricle of the heart. Eyes and optic nerves were isolated, postfixed for 24 h in the same fixative and embedded in Epon (Serva) as described elsewhere (Kritzenberger et al. 2011). Semi-thin sagittal sections (1.0 μm thick) were cut through the eyes and stained after Richardson (Richardson et al. 2009). Transmission electron microscopy was performed according to protocols published previously (Braunger et al. 2013a). Semi-thin sections of retinae and cross semi-thin sections through the optic nerve were stained with paraphenylenediamine (PPD) as described previously (Kroeber et al. 2010) to visualize lipid deposits or myelinated axons, respectively. For quantification of optic nerve axons, the number

of PPD-labeled axons in optic nerve cross sections was counted using ImageJ Cell counter as described previously (Braunger et al. 2013b). Thickness of the outer nuclear layer (ONL) was measured on semi-thin sections along the mid-horizontal (nasal-temporal) plane. The distance between *ora serrata* (OS) and optic nerve head (ONH) was divided into tenths and measured between each tenth (Braunger et al. 2013b). Fluorescence-labeled retinal whole mounts or sagittal sections were investigated on an Axiovision fluorescent microscope (Carl Zeiss) using appropriate Axiovision software 4.8 (Carl Zeiss, Jena, Germany). Analysis of retinal whole mounts by confocal microscopy was performed on a Zeiss Axiovert 200M inverted microscope combined with a LSM 510 laser-scanning device. FITC-dextran was excited using an Ar-laser at 488 nm, Cy<sup>TM</sup>-3 was excited using a HeNe laser at 543nm. The software used for image acquisition and processing was AIM 4.2 (Zeiss).

### 3.3.4 LacZ staining

Lac-Z-staining was performed in mixed CAGG CreER<sup>TM</sup>/Rosa-LacZ (Cre-reporter) or *Tgfb $\beta$ 2 <sup>$\Delta$ eye</sup>*/TOP-Gal (WNT-reporter) mice (The Jackson Laboratory) as described previously (Braunger et al. 2013a, Baulmann et al. 2002). Paraffin sections (6.0  $\mu$ m) were cut, placed on glass slides (SuperFrost/Plus; Menzel) and analyzed by light microscopy (Carl Zeiss).

### 3.3.5 Immunohistochemistry

Prior to T $\beta$ RII, pSmad3, glial fibrillary acid protein (GFAP), collagen IV and CD31 staining, eyes were fixed for 4 h in 4% paraformaldehyde (PFA), washed extensively in phosphate buffer (PP, 0.1M) and embedded in paraffin according to standard protocols. Paraffin sections (6  $\mu$ m) were deparaffinized and washed in H<sub>2</sub>O. For detection of T $\beta$ RII and pSmad3, sections were treated with boiling citrate buffer (1 x 10 min, ph 6), washed again in H<sub>2</sub>O and incubated in 0.1M PP. For detection of collagen IV and CD31, sections were pretreated with 0.05 M Tris-HCL (5 min) and covered with Proteinase K (100  $\mu$ l of Proteinase K in 57 ml Tris-HCl (0.05 M), 5 min), washed in H<sub>2</sub>O, incubated in 2 N HCl (20 min), and washed again in H<sub>2</sub>O. Sections were incubated in PP for 5 min. IBA-1, F4/80 and  $\alpha$ -smooth muscle-actin ( $\alpha$ -SMA) immunohistochemistry was performed on frozen sections. For Iba-1 and  $\alpha$ -SMA staining, eyes were fixed for 4 h in 10% glacial acetic acid, 60% methanol, and 30% chloroform, transferred to 50% and 25% methanol 30 min each, washed in phosphate buffered saline (PBS), incubated in 10%, 20%, 30% sucrose/PBS overnight at 4°C and shock frozen in tissue mounting medium (DiaTec). For F4/80 staining, eyes were fixed for 4 h in 4% PFA and washed extensively in phosphate buffer (PP,

## Chapter 3

0.1M). For immunohistochemistry, sections were washed three times in TBS (pSmad3) or PP (others) for 5 min each and blocked with 2% BSA in PP/TBS 45 min (F4/80: 1% dry milk, 0.01% Tween in PBS) at room temperature. Primary antibodies (Table 2) were diluted in a 1:10 dilution of blocking solution in PP/TBS (F4/80: 2% BSA, 0.02% NaN<sub>3</sub>, 0.01% Triton in PBS) and incubated at 4°C overnight. After three washes in PP/TBS (5 min each), biotinylated antibodies were applied for 1 h diluted in a 1:10 dilution of the blocking solution as an additional step, then anti-biotin or appropriate secondary antibodies (Table 2), diluted in a 1:10 dilution of the blocking solution, were applied for 1 h. Sections were washed again three times and cell nuclei were counterstained with DAPI (Vectashield, Vector Laboratories) 1:10 diluted in fluorescent mounting medium (Serva).

**Table 2. Antibodies used for immunohistochemistry**

Primary antibody	Fixation	Secondary antibody
TβRII- L21 (Santa Cruz) 1:20	4% paraformaldehyde (PFA)	anti-rabbit, biotinylated (Vector) 1:500, Streptavidin Alexa 488 (Invitrogen) 1:1000
pSmad3 (Cell Signaling) 1:20	4% PFA	anti-rabbit, biotinylated (Vector) 1:500, Streptavidin Alexa 488 (Invitrogen) 1:1000
Iba-1 (Wako) 1:1000	methyl-Carnoy	anti-rabbit Cy <sup>TM</sup> -3 conjugated (Jackson Immuno Research Lab) 1:2000
Collagen IV (Chemicon) 1:100	4% PFA	anti-rabbit, biotinylated (Vector) 1:500, Streptavidin Alexa 546 (Invitrogen) 1:1000
α-smooth muscle-actin (Genetex) 1:50	methyl-Carnoy (section) methanol (whole mount)	anti-rabbit Cy <sup>TM</sup> -3 conjugated (Jackson Immuno Research Lab) 1:2000
NG2 (Merck Milipore) 1:50	methanol	anti-rabbit Cy <sup>TM</sup> -3 conjugated (Jackson Immuno Research Lab) 1:2000
CD31 (RD Systems) 1:100	4% PFA	anti-goat Cy <sup>TM</sup> -3 conjugated (Jackson Immuno Research Lab) 1:2000
Collagen IV (Abcam) 1:100	4% PFA	anti-rabbit Alexa 488 (Invitrogen) 1:1000
F4/80 (Acris Antibodies) 1:600	4% PFA	anti-rat Cy <sup>TM</sup> -3 conjugated (Jackson Immuno Research Lab) 1:2000 in PBS

GFAP (DAKO) 1:1000

4% PFA

anti-rabbit Alexa 488 (Invitrogen) 1:1000

### 3.3.6 Dextran perfusion and retinal whole mounts

Mice were deeply anesthetized with ketamine (120 mg/kg body weight, i.m.) and xylazine (8 mg/kg body weight) and perfused through the left ventricle with 1 ml of phosphate buffered saline (PBS) containing 50 mg high molecular weight (MW = 2,000,000) FITC-dextran (TdB Consultancy). The eyes were enucleated and placed in 4% paraformaldehyde for 2 h. Retinae were dissected and flat mounted using fluorescent mounting medium (Serva). If sagittal sections of FITC-dextran-perfused retinae were used, the perfused eyes were fixed for 4 h in 10% glacial acetic acid, 60% methanol, and 30% chloroform, transferred to 50% and 25% methanol 30 min each, washed in phosphate-buffered saline (PBS), incubated in 10%, 20%, 30% sucrose/PBS overnight at 4°C and shock frozen in tissue mounting medium (DiaTec). Following sectioning, nuclei were counterstained with DAPI (Vectashield, Vector Laboratories) 1:10 diluted in fluorescent mounting medium (Serva). If immunohistochemical labelling was performed using retinal whole mounts, fixation was modified (Tab. 2), and antibodies were applied according to Tab. 2 and as described in the immunohistochemistry section.

### 3.3.7 Apoptosis

Apoptotic cell death was analyzed by terminal deoxynucleotidyl transferase-mediated dUTP nick end labeling using the Apoptosis Detection System (DeadEnd Fluorometric TUNEL, Promega). Paraffin sections were treated following manufacturers' instructions and protocols reported previously (Braunger et al. 2013b). For quantitative analysis, the number of TUNEL-positive nuclei in sagittal sections throughout the entire retina was counted.

### 3.3.8 Trypsin digest

Eyes were fixed for 48 h in 4% PFA. Retinae were washed in H<sub>2</sub>O for 75 min, transferred to glass slides and incubated for 90 min with 3% trypsin 0.2 M Tris-HCl at 37°C. Retinae were transferred on a new glass slide, again incubated for 120 min in 3% trypsin 0.2 M Tris-HCl at 37°C and stained with periodic acid–Schiff (PAS).

### 3.3.9 Electroretinography

Mice were dark adapted for at least 12 h before experiments and anesthetized by s.c. injection of ketamine (65 mg/kg) and xylazine (13 mg/kg). Pupils were dilated with tropicamide eyedrops (Mydriaticum Stulln; Pharma Stulln). Silver needle electrodes served as reference (forehead) and ground (tail), and gold wire ring electrodes as active electrodes. Corneregel (Bausch & Lomb) was applied to keep the eye hydrated and to maintain good electrical contact. ERGs were recorded using a Ganzfeld bowl (Ganzfeld QC450 SCX, Roland Consult) and an amplifier & recording unit (RETI-Port, Roland Consult). ERGs were recorded from both eyes simultaneously, band-pass filtered (1 to 300 Hz) and averaged. Single flash scotopic (dark adapted) responses to a series of ten LED-flash intensities ranging from -3.5 to 1.0 log cd.s/m<sup>2</sup> with an inter stimulus interval of 2 up to 20 seconds for the highest intensity were recorded. All analysis and plotting was carried out with R 2.15.2 (The R Foundation for Statistical Computing) and ggplot2 0.9.3 (Wickham 2009).

### 3.3.10 Fundus imaging and angiography

Retinal imaging was performed with a commercially available imaging system (Micron III; Phoenix Research Laboratories, Inc.). Light source path and imaging path filters (low pass and high pass at 500 nm) were used for fluorescein angiography (FLA). Mice were anesthetized by s.c. injection of ketamine (65 mg/kg) and xylazine (13 mg/kg), and their pupils were dilated with tropicamide eyedrops before image acquisition. FLA was performed using a s.c. injection of 75 mg/kg body weight fluorescein-Na (Alcon).

### 3.3.11 RNA analysis

Total RNA from neural retinae was extracted using TRIzol and first strand cDNA synthesis was performed using iScript cDNA Synthesis Kit (Bio-Rad) according to manufacturer's instructions. Quantitative real-time RT-PCR analyses were performed using the Bio-Rad iQ5 Real-Time PCR Detection System. The temperature profile was denaturation at 95°C for 10 seconds and annealing and extension at 60°C for 40 seconds for 40 cycles. All primer pairs were purchased from Invitrogen and extended over exon–intron boundaries, except for GAPDH. Sequences of primer pairs, melting temperatures and PCR product sizes are shown in Table 3. RNA that was not reverse transcribed served as negative control for real-time RT-PCR. Prior to relative quantification, mRNAs from three different potential housekeeping genes were tested: glyceraldehyde 3-phosphate dehydrogenase (Gapdh), guanine nucleotide binding protein

(Gnb2l), and ribosomal protein L32 (Rpl32). After statistical evaluation, Rpl32 was used for relative quantification. Quantification was performed using BioRad iQ5 Standard-Edition (Version 2.1) software (BioRad).

**Table 3. Primers used for quantitative real-time PCR amplification**

<b>Gene</b>	<b>Sequence forward</b>	<b>Sequence reverse</b>
<i>GAPDH</i>	5'-TGTCCGTCGTGGATCTGAC-3'	5'-CCTGCTTCACACCTTCTTG-3'
<i>GNB2L</i>	5'-TCTGCAAGTACACGGTCCAG-3'	5'-ACGATGATAGGGTTGCTGCT-3'
<i>RPL32</i>	5'-GCTGCCATCTGTTTTACGG-3'	5'-TGA CTGGTGCCTGATGAACT-3'
<i>Tgfb<math>\beta</math>2</i>	5'-AGAAGCCGCATGAAGTCTG-3'	5'-GGCAAACCGTCTCCAGAGTA-3'
<i>Tgfb<math>\beta</math>1</i>	5'-AATGTTACGCCATGAAAATATCC-3'	5'-CGTCCATGTCCCATTGTCTT-3'
<i>Smad2</i>	5'-AGGACGGTTAGATGAGCTTGAG-3'	5'-GTCCCCAAATTCAGAGCAA-3'
<i>Smad3</i>	5'-TCAAGAAGACGGGGCAGTT-3'	5'-CCGACCATCCAGTGACCT-3'
<i>Smad6</i>	5'-GTTGCAACCCCTACCACTTC-3'	5'-GGAGGAGACAGCCGAGAATA-3'
<i>Smad7</i>	5'-ACCCCCATCACCTTAGTCG-3'	5'-GAAAATCCATTGGGTATCTGGA-3'
<i>Ndp</i>	5'-CCCACTGTACAAATGTAGCTCAA-3'	5'-AGGACACCAAGGGCTCAGA-3'
<i>Ng2</i>	5'-CTTGGCCTTGTTGGTCAGAT-3'	5'-CACCTCCAGGTGGTTCTCC-3'
<i>Rgs-5</i>	5'-GCTTTGACTTGGCCCAGAAA-3'	5'-CCTGACCAGATGACTACTTGATTAGCT-3'
<i>Pdgf-R<math>\beta</math></i>	5'-ACCTCAAAGGTGTCCACGA-3'	5'-GTGTGCTCACCACTCGTAT-3'
$\alpha$ -Sma	5'-CAACCGGGAGAAAATGACC-3'	5'-CAGTTGTACGTCCAGAGGCATA-3'
<i>Vegf-R1</i>	5'-TACCTCACCGTGCAAGGAAC-3'	5'-AAGGAGCCAAAAGAGGGTCG-3'
<i>Vegf-R2</i>	5'-CAGTGGTACTGGCAGCTAGAAG-3'	5'-ACAAGCATACGGGCTTGTTT-3'

## Chapter 3

<i>Pdgfb</i>	5'-TCGAGTTGGAAAGCTCATCTC-3'	5'-GTCTTGCACTCGGCGATTA-3'
<i>Vegf-a-120</i>	5'-GGAGAGATGAGCTTCCTACAGCA-3'	5'-CTGAACAAGGCTCACAGTCATTTT-3'
<i>Vegf-a-164</i>	5'-GGAGAGATGAGCTTCCTACAGCA-3'	5'-CCTTGGCTTGTCACATTTTTTCT-3'
<i>Ang-2</i>	5'-CACACTGACCTTCCCCAACT-3'	5'-CCCACGTCCATGTCACAGTA-3'
<i>Igf-1</i>	5'-CAAAAGCAGCCCGCTCTA-3'	5'-TCGATAGGGACGGGGACT-3'
<i>Fgf2</i>	5'-GGCTCTACTGCAAGAACG-3'	5'-TGCTTGGAGTTGTAGTTTGACG-3'
<i>Ccl2</i>	5'-CATCCACGTGTTGGCTCA-3'	5'-GATCATCTTGCTGGTGAATGAGT-3'
<i>Cd68</i>	5'-CTCTCTAAGGCTACAGGCTGCT-3'	5'-TCACGGTTGCAAGAGAAACA-3'
<i>Egr1</i>	5'-CCTATGAGCACCTGACCACA-3'	5'-TCGTTTGGCTGGGATAACTC-3'
<i>Il6</i>	5'-GCTACCAAAGTGGATATAATCAGGA-3'	5'-CCAGGTAGCTATGGTACTCCAGAA-3'
<i>iNos</i>	5'-GGGCTGTCACGGAGATCA-3'	5'-CCATGATGGTCACATTCTGC-3'
<i>Tnf-<math>\alpha</math></i>	5'-TCTTCTCATTCCTGCTTGTGG-3'	5'-GGTCTGGGCCATAGAACTGA-3'
<i>Casp8</i>	5'-TTGAACAATGAGATCCCCAAA-3'	5'-CCATTTCTACAAAATTTCAAGCAG-3'
<i>Col IV a1</i>	5'-TTAAAGGACTCCAGGGACCAC-3'	5'-CCCACTGAGCCTGTCACAC-3'
<i>Col III a1</i>	5'-TCCCCTGGAATCTGTGAATC-3'	5'-TGAGTCGAATTGGGGAGAAT-3'

### 3.3.12 Statistical analysis

All results are expressed as mean  $\pm$  s.e.m. Comparisons between the mean variables of two groups were made by a two-tailed Student's t-test. *P* values  $\leq 0.05$  were considered to be statistically significant.

### 3.4 Results

#### 3.4.1 Conditional deletion of T $\beta$ RII in the eye following local tamoxifen treatment

In order to test if local tamoxifen treatment of newborn CAGG Cre-ER<sup>TM</sup> mouse pups would induce the expression of Cre to levels that are high enough to cause recombination, we crossed the animals with mice carrying the Rosa26 reporter (R26R) allele. At two weeks of age, the tamoxifen-treated eyes were stained for  $\beta$ -galactosidase. An intense positive staining was seen throughout the entire eye of CAGG Cre-ER<sup>TM</sup>; R26R mice, while ocular tissues of R26R littermates, which did not carry the CAGG Cre-ER<sup>TM</sup> transgene, were completely unstained (Figure 9A). We now generated *Tgfb $\beta$ 2<sup>fl/fl</sup>*; CAGG Cre-ER<sup>TM</sup> mice that were equally treated with tamoxifen. For simplicity, we will refer to *Tgfb $\beta$ 2<sup>fl/fl</sup>*; CAGG Cre-ER<sup>TM</sup> mice as *Tgfb $\beta$ 2 <sup>$\Delta$ eye</sup>* mice; however, littermates with two unrecombined *Tgfb $\beta$ 2<sup>fl/fl</sup>* alleles are referred to as controls. Using immunohistochemistry, a distinct immunoreactivity for T $\beta$ RII was seen in the ganglion cell layer of the control inner retina, but was barely detectable in the outer retina (Figure 9B). In contrast, in retinæ of *Tgfb $\beta$ 2<sup>eye</sup>* littermates immunoreactivity for T $\beta$ RII was almost absent. We next performed western blot analyses for T $\beta$ RII (70 kDa) in protein extracts from the tissues of the anterior eye or the retinæ of four-week-old control and conditional T $\beta$ RII-deficient *Tgfb $\beta$ 2 <sup>$\Delta$ eye</sup>* littermates (Figure 9C). By relative densitometry, the western blot band was found to be significantly less intense in both anterior eye ( $0.36 \pm 0.16$  versus  $1 \pm 0.09$ ,  $P = 0.03$ ) and retinæ ( $0.37 \pm 0.10$  versus  $1 \pm 0.16$ ,  $P = 0.02$ ) of T $\beta$ RII-deficient mice when compared to controls. To analyze the activity of TGF- $\beta$  signaling, western blot analyses of retinal proteins detected pSmad3 (54 kDa) in retinal proteins of two-week-old mice (Figure 9D) and relative densitometry confirmed the band as being significantly less intense in *Tgfb $\beta$ 2 <sup>$\Delta$ eye</sup>* mice compared to controls ( $0.30 \pm 0.04$  versus  $1 \pm 0.17$ ,  $P = 0.04$ ). Using immunohistochemistry, retinal immunoreactivity for pSmad3 was observed preferentially in the nuclei of the ganglion cell layer in control mice (Figure 9E). In contrast, nuclear immunoreactivity for pSmad3 was essentially absent in retinæ of *Tgfb $\beta$ 2 <sup>$\Delta$ eye</sup>* littermates (Figure 9E). Finally we investigated the expression of *Tgfb $\beta$ 2* and *Smad3* mRNA by real-time RT-PCR and observed significant lower amounts in RNA from *Tgfb $\beta$ 2 <sup>$\Delta$ eye</sup>* mice than in control littermates (Figure 9F). No changes were observed in the expression of mRNA for other molecules associated with TGF- $\beta$  signaling such as *Tgfb $\beta$ 1*, *Smad2*, *Smad6*, *Smad7* and *Ndp*.

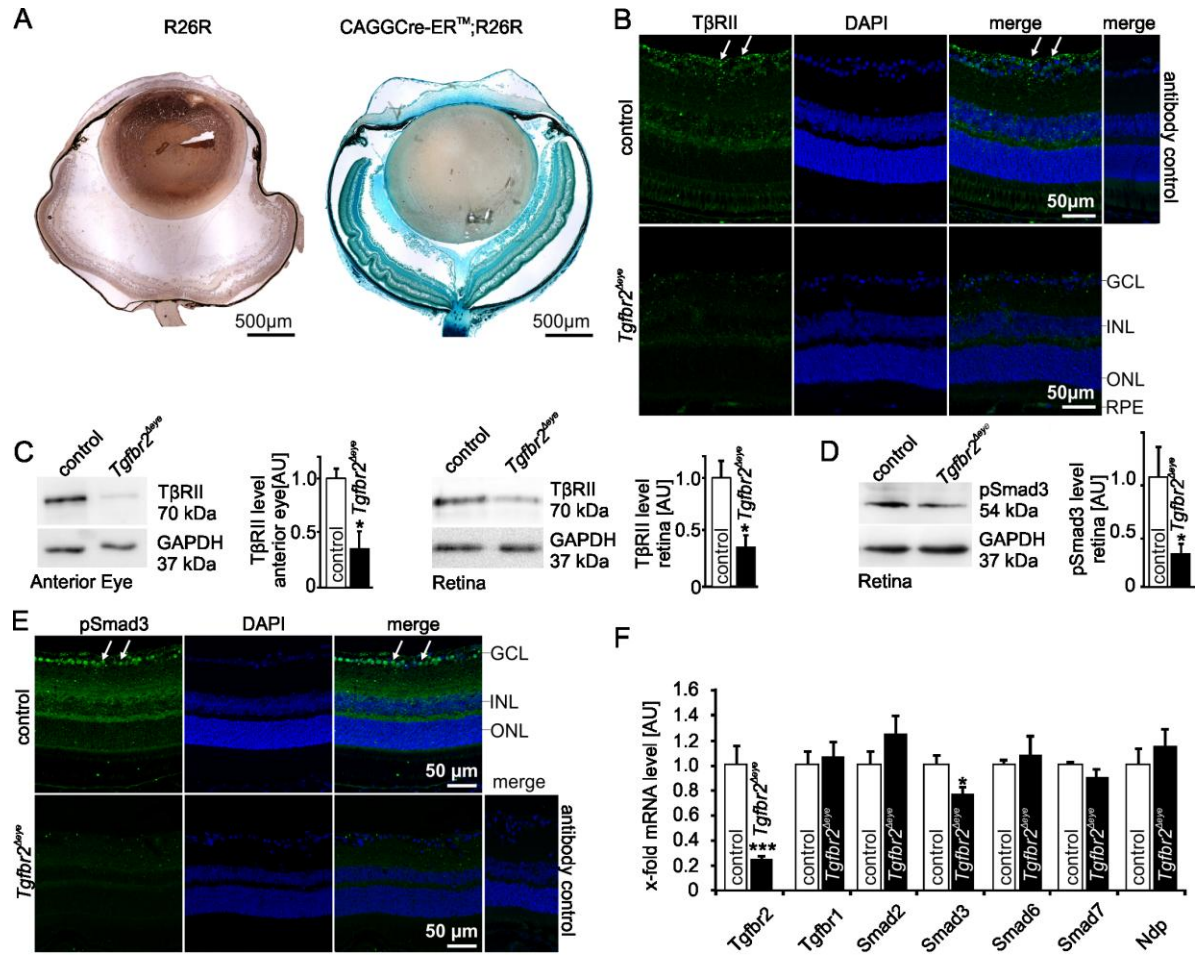


**Figure 9. TβRII deletion and inhibition of TGF-β signaling in *Tgfb2*<sup>Δeye</sup> eyes.** **A.** β-galactosidase staining is seen in the entire retina of 14-day-old double transgenic CAGG Cre-ER<sup>TM</sup> mice, but not in *R26R* control littermates. **B.** Immunoreactivity for TβRII (green) in the retina at 4 weeks of age. TβRII is detectable in the ganglion cell layer (arrows) and the inner retina in controls, but absent in the *Tgfb2*<sup>Δeye</sup> littermate. Antibody control section indicates specific staining. **C.** Western blot and densitometric analyses for TβRII in proteins from anterior eye segment or retinæ of 4-week-old animals. GAPDH was used as loading control. **D.** Western blot and densitometric analyses for pSmad3 (retina, 2-week-old). GAPDH was used as loading control. **E.** Immunoreactivity for pSmad3 (green) in the retina at 4 weeks of age. The control animal shows immunoreactivity for pSmad3 in the nuclei of the inner retina (arrows), which is considerably weaker in the *Tgfb2*<sup>Δeye</sup> littermate. **F.** Real-time RT-PCR in 2-week-old control and *Tgfb2*<sup>Δeye</sup> retinæ. Nuclei are DAPI-stained (blue). Data are expressed as mean ± SEM. Western blot analysis (C): TβRII (anterior eye segment): control: n = 3, *Tgfb2*<sup>Δeye</sup>: n = 5; TβRII (retina): control: n = 4, *Tgfb2*<sup>Δeye</sup>: n = 4; pSmad3 (retina): control: n = 3, *Tgfb2*<sup>Δeye</sup>: n = 4; Real-time RT-PCR: control: n ≥ 4, *Tgfb2*<sup>Δeye</sup>: n ≥ 7. (F, *Tgfb2*<sup>Δeye</sup>). \**P* ≤ 0.05, \*\*\**P* ≤ 0.001. AU, arbitrary unit; GAPDH, glyceraldehyde 3-phosphate dehydrogenase; GCL, ganglion cell layer; INL, Inner nuclear layer; ONL, Outer nuclear layer; RPE, Retinal pigment epithelium; R26R, Rosa26 reporter; TGF, transforming growth factor; TβRII, TGF-β type II receptor. Experiments performed by Barbara M. Braunger and Sarah V. Leimbeck.

### 3.4.2 Conditional deletion of TGF- $\beta$ signaling results in leaky retinal capillaries that form microaneurysms

Eyes of *Tgfb $\beta$ 2 $^{\Delta eye}$*  mice were investigated by funduscopy at four weeks of age and no obvious differences compared to controls were observed (Figure 10A). Still, a marked dilation of retinal vessels was observed in the eyes of *Tgfb $\beta$ 2 $^{\Delta eye}$*  mice by fluorescein angiography. The vessels were tortuous and appeared blurry indicating massive vascular leakage (Figure 10A). In contrast, retinal vessels of control littermates looked essentially normal (Figure 10A). At eight weeks of age, funduscopy exams of *Tgfb $\beta$ 2 $^{\Delta eye}$*  mice identified numerous white areas on the retina, which formed fluffy white patches or were rather dot-like. The white areas were quite reminiscent of hard exudates and cotton wool spots in human patients with diabetic retinopathy, and were not seen in control retinæ (Figure 10B). By fluorescein angiography, numerous round spots similar to capillary microaneurysms were visible in close association with retinal capillaries throughout the entire retina (Figure 10B). We next examined whole-mounted retinæ of four-week-old animals after perfusion with FITC-labeled dextran and observed abundant FITC-labeled capillary microaneurysms throughout the entire retina of *Tgfb $\beta$ 2 $^{\Delta eye}$*  mice (Figure 10C). Again, retinal capillaries of control littermates looked essentially normal (Figure 10C). At higher magnifications, microaneurysms were seen to originate laterally from capillaries or to be localized rather at the blind-ending tips of capillaries (Figure 10D). Moreover, numerous capillaries were observed from which FITC-labeled dextran had leaked corroborating the findings obtained by angiography (Figure 10D). In retinal sections, the microaneurysms were seen to have a wide lumen that was frequently filled with erythrocytes (Figure 10E). When trypsin-digested retinal capillaries were investigated, microaneurysms were found to be frequently covered by cells in which nuclear chromatin had been condensed to chromosomes indicating mitosis (Figure 10E). Retinal sections or whole mounts were studied following FITC-dextran perfusions and microaneurysms were found in capillaries from all three (superficial, intermediate and deep) vascular plexus of the retina (Figure 11A). Quite intriguingly, the capillary network of the intermediate and deep plexus was considerably denser in control animals than in *Tgfb $\beta$ 2 $^{\Delta eye}$*  mice (Figure 11A).

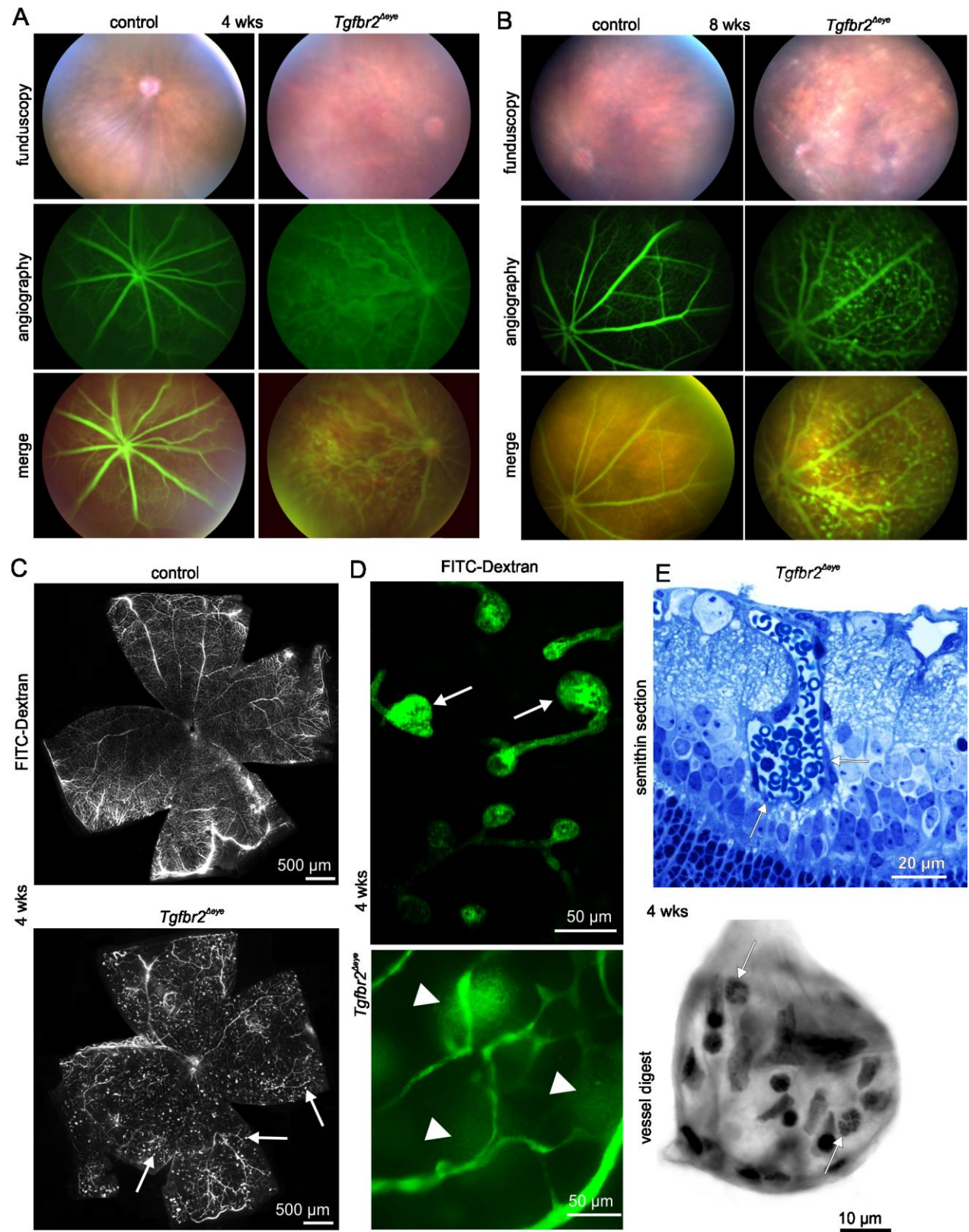


**Figure 10. Retinal vasculature after T $\beta$ RII deletion and inhibition of TGF- $\beta$  signaling in *Tgfb2<sup>Δeye</sup>* eyes.** Retinal vasculature after T $\beta$ RII deletion and inhibition of TGF- $\beta$  signaling in *Tgfb2<sup>Δeye</sup>* eyes. In vivo funduscopy and fluorescein angiography at 4 weeks (**A**) and 8 weeks (**B**) of age. **A**. Retinal vessels in

*Tgfb $\beta$ 2* <sup>$\Delta$ eye</sup> eyes are dilated, tortuous and blurry, indicating fluorescein leakage (green). **B.** Multiple microaneurysms (angiography) and white patches (funduscopy) are visible in *Tgfb $\beta$ 2* <sup>$\Delta$ eye</sup> animals. **C:** FITC-dextran-perfused retinal whole mounts of 4-week-old mice. White arrows indicate multiple microaneurysms in the *Tgfb $\beta$ 2* <sup>$\Delta$ eye</sup> mouse. **D.** Higher magnification of FITC-dextran (green)-perfused retinal vessels in a 4-week-old *Tgfb $\beta$ 2* <sup>$\Delta$ eye</sup> mouse. FITC-dextran leaks (arrowheads) from microaneurysms (arrows) and vessels. **E.** Richardson's-stained semi-thin section (1  $\mu$ m thick) of a 4-week-old *Tgfb $\beta$ 2* <sup>$\Delta$ eye</sup> mouse. The white arrows point toward a microaneurysm filled with erythrocytes. Trypsin digest of retinal vessels with magnification of a microaneurysm at 4 weeks of age. Arrows in the bottom panel point toward nuclei with condensed chromosomes, indicating mitosis. FITC, fluorescein isothiocyanate; TGF, transforming growth factor; T $\beta$ RII, TGF- $\beta$  type II receptor. Experiments performed by (A,B) Sarah V. Leimbeck, Herbert Jäggle and Cornelia Volz; (C,D) Anja Schlecht; (E,F) Barbara M. Braunger and Sarah V. Leimbeck.

### 3.4.3 Lack of pericyte differentiation upon absence of retinal TGF- $\beta$ signaling

To investigate pericyte covering of retinal capillaries in *Tgfb $\beta$ 2* <sup>$\Delta$ eye</sup> mice, we perfused animals with FITC-dextran and immunolabeled retinal whole mounts with antibodies against NG2, a marker for differentiated pericytes in the retina (Armulik et al. 2011). Retinal capillaries of control mice were densely covered by NG2-positive cells (Figure 11A). In contrast, NG2-positive cells were only rarely observed in retinal capillaries of *Tgfb $\beta$ 2* <sup>$\Delta$ eye</sup> littermates (Figure 11A) and were not found covering capillary microaneurysms (Figure 11A). We next stained retinal whole-mounts and sections with antibodies against  $\alpha$ -smooth muscle-actin ( $\alpha$ -SMA) which stains vascular smooth muscle cells, but not quiescent and differentiated pericytes (Armulik et al. 2011). In control animals, staining for  $\alpha$ -SMA actin was strictly confined to retinal arteries and arterioles (Figure 11B). In contrast, in *Tgfb $\beta$ 2* <sup>$\Delta$ eye</sup> littermates the staining extended to retinal capillaries (Figure 11B) and  $\alpha$ -SMA positive cells densely covered all FITC-dextran-filled retinal capillaries of *Tgfb $\beta$ 2* <sup>$\Delta$ eye</sup> mice (Figure 11C). Moreover, numerous  $\alpha$ -SMA-labeled capillaries were observed that were not filled with FITC-dextran, a finding that suggested the presence of non-perfused or ghost vessels (Figure 11C). The covering of  $\alpha$ -SMA positive cells was also seen along the surface of many microaneurysms (Figure 11C).

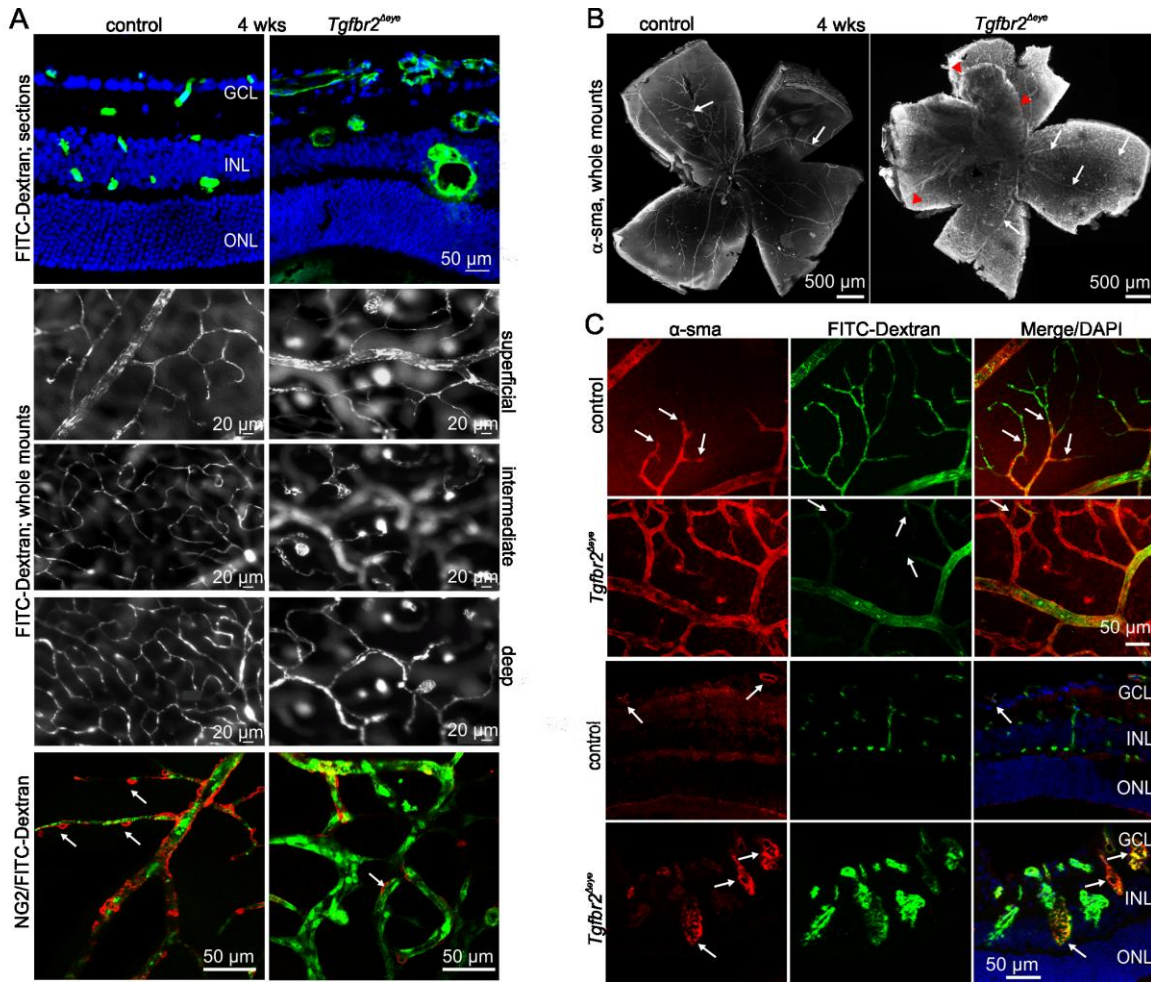


**Figure 11. Lack of pericyte differentiation in *Tgfb2*<sup>Δeye</sup> mice.** **A.** Meridional sections and whole mounts of 4-week-old FITC-dextran (green)-perfused retinæ. *Tgfb2*<sup>Δeye</sup> mice show dilated vessels and multiple microaneurysms in all (superficial, intermediate and deep) vascular plexus. The capillary network in the intermediate and deep vascular plexus of *Tgfb2*<sup>Δeye</sup> mice is less dense compared to controls. FITC-dextran-perfused (green) and NG2 (red)-labeled retinal whole mounts at 4 weeks of age. White arrows point towards NG2-positive pericytes that are markedly reduced in number in the *Tgfb2*<sup>Δeye</sup> retina. **B.** Retinal whole mounts of 4-week-old mice stained for α-SMA. In the control, staining is confined to retinal arteries and arterioles (white arrows), whereas it extends to capillaries in the *Tgfb2*<sup>Δeye</sup> mouse. Red arrowheads mark the persistent α-SMA negative hyaloid capillaries. **C.** α-SMA staining in arterioles and arteries of a 4-week-old control mouse does not extend (arrows) to FITC-dextran (green)-labeled capillaries. In the *Tgfb2*<sup>Δeye</sup> mouse, retinal capillaries are covered by α-SMA-positive cells. Perfused FITC-dextran does not enter all α-SMA-positive capillaries (arrows). Meridional sections of α-SMA (red) and FITC-dextran (green)-labeled retinæ (3-week-old). In controls, immunoreactivity for α-SMA (red) is restricted to the vessels of the superior vascular plexus. In *Tgfb2*<sup>Δeye</sup> animals, intraretinal vessels and microaneurysms are covered by α-SMA positive cells (white arrows). Nuclei are DAPI-stained (blue). FITC, fluorescein isothiocyanate; GCL, ganglion cell layer; INL, inner nuclear layer; ONL, outer nuclear layer; α-SMA, α-smooth muscle actin. Experiments performed by (A, upper and middle panel) Sarah V.

Leimbeck; (A, lower panel) Anja Schlecht; (B, C upper panel) Anja Schlecht; (C, lower panel) Barbara M. Braunger and Sarah V. Leimbeck.

Western blot analyses confirmed the results seen by immunohistochemistry (Figure 12A, B). By relative densitometry, we detected a decrease in the amounts of retinal NG2 in *Tgfb $\beta$ 2 $\Delta$ eye* mice when compared to control littermates ( $0.37 \pm 0.098$  versus  $1.0 \pm 0.25$ ,  $P = 0.042$ ) together with an increase in the amounts of retinal  $\alpha$ -SMA ( $4.70 \pm 0.99$  versus  $1 \pm 0.12$ ,  $P = 0.0029$ ). The results correlated with those obtained by real-time RT-PCR, as the amounts of retinal mRNA for Ng2 were decreased in *Tgfb $\beta$ 2 $\Delta$ eye* mice (2 weeks:  $P = 0.0023$ ; 6 weeks:  $P = 0.045$ ), while those of  $\alpha$ -Sma mRNA were increased (2 weeks:  $P = 0.0056$ ; 4 weeks:  $P = 0.012$ ) (Figure 12C). The amounts of retinal mRNA for Pdgf-R $\beta$ , a gene expressed in both pericytes and vascular smooth muscle cells were lower in 2-week-old *Tgfb $\beta$ 2 $\Delta$ eye* mice than in controls ( $P = 0.021$ ), while no differences were detected at 4 weeks of age. The levels of mRNA for Rgs-5 which is an angiogenic pericyte marker that is upregulated during physiological angiogenesis and vascular remodeling were significantly ( $P = 0.020$ ) increased in four-week-old *Tgfb $\beta$ 2 $\Delta$ eye* mice (Figure 12C).

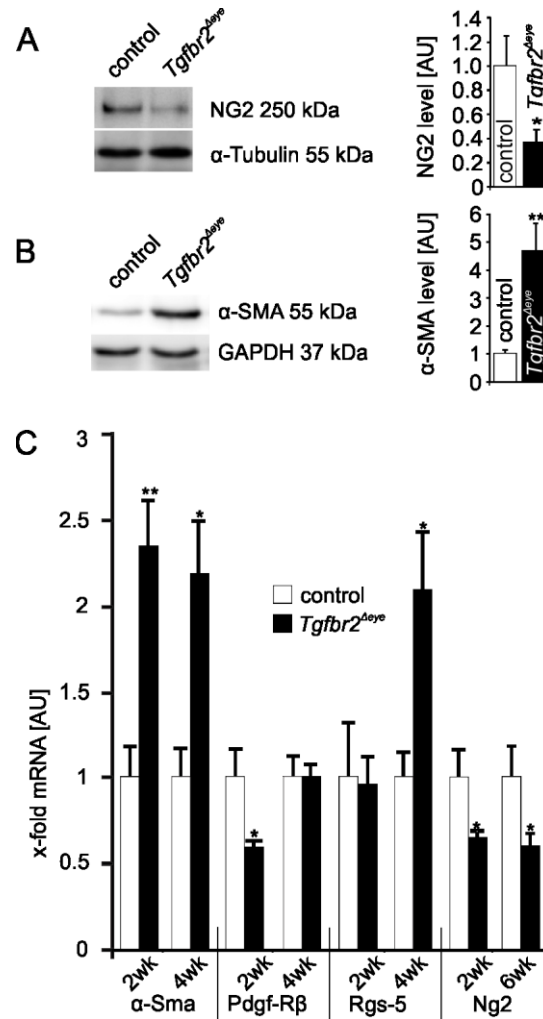


**Figure 12. Lack of pericyte differentiation in *Tgfb2<sup>Δeye</sup>* mice.** **A** and **B**. Western blot analysis and densitometry for NG2 (**A**) and α-SMA (**B**) in retinal proteins of 4-week-old mice. GAPDH and α-tubulin were used as loading control. **C**. Quantitative real-time RT-PCR in RNA from 2- and 4-week-old (6 weeks for Ng2, respectively) retinæ. Data are expressed as means ± SEM,  $n \geq 6$  (**A** and **B**);  $n \geq 4$  (**C**, control at 2 weeks);  $n \geq 6$  (**C**, *Tgfb2<sup>Δeye</sup>* 2 and 4 weeks and control at 6 weeks);  $n = 9$  (**C**, Ng2, *Tgfb2<sup>Δeye</sup>* at 6 weeks);  $n = 11$  (**C**, Ng2 control at 6 weeks). \* $P \leq 0.05$ , \*\* $P \leq 0.01$ . AU, arbitrary unit; GAPDH, glyceraldehyde 3-phosphate dehydrogenase; α-SMA, α-smooth muscle actin. Experiments performed by Anja Schlecht and Barbara M. Braunger.

We next investigated retinal capillaries by transmission electron microscopy. In sections of control capillaries, individual pericytes were regularly observed that shared the basal lamina with endothelial cells (Figure 13A). In contrast, retinal capillaries of four-week-old *Tgfb2<sup>Δeye</sup>* mice were surrounded by 1-2 complete layers of perivascular cells that contained numerous 5-6 nm actin microfilaments and showed the essential ultrastructural characteristics of vascular smooth muscle cells (Figure 13A). The cells were completely surrounded by a basal lamina which was at

least double as thick as that covering pericytes in control sections. In addition, immunostaining with antibodies against collagen type IV was more pronounced around capillaries of *Tgfb $\beta$ 2* <sup>$\Delta$ eye</sup> mice than around control capillaries corroborating the findings observed by transmission electron microscopy (Figure 13B). Staining for collagen IV showed a thicker basal lamina around capillaries of *Tgfb $\beta$ 2* <sup>$\Delta$ eye</sup> animals and was more intense in the internal limiting membrane than in control eyes (Figure 13B). Western blot analyses confirmed the higher levels of collagen type IV ( $1 \pm 0.20$  versus  $4.18 \pm 1.03$ ,  $P = 0.017$ ) in retinæ of *Tgfb $\beta$ 2* <sup>$\Delta$ eye</sup> mice (Figure 13C). Finally, we investigated by real-time RT-PCR the expression of mRNA for the collagen subunits Col4A1 and Col3A1. We observed no difference in the expression of both subunits in two-week-old animals. Still, at four weeks of age, the time when the vascular basal lamina was observed to be thicker in *Tgfb $\beta$ 2* <sup>$\Delta$ eye</sup> mice, the expression of *Col4A1* and *Col3A1* was higher ( $P = 0.0012$  or  $P = 0.032$ ) in *Tgfb $\beta$ 2* <sup>$\Delta$ eye</sup> mice than in controls (Figure 13D).

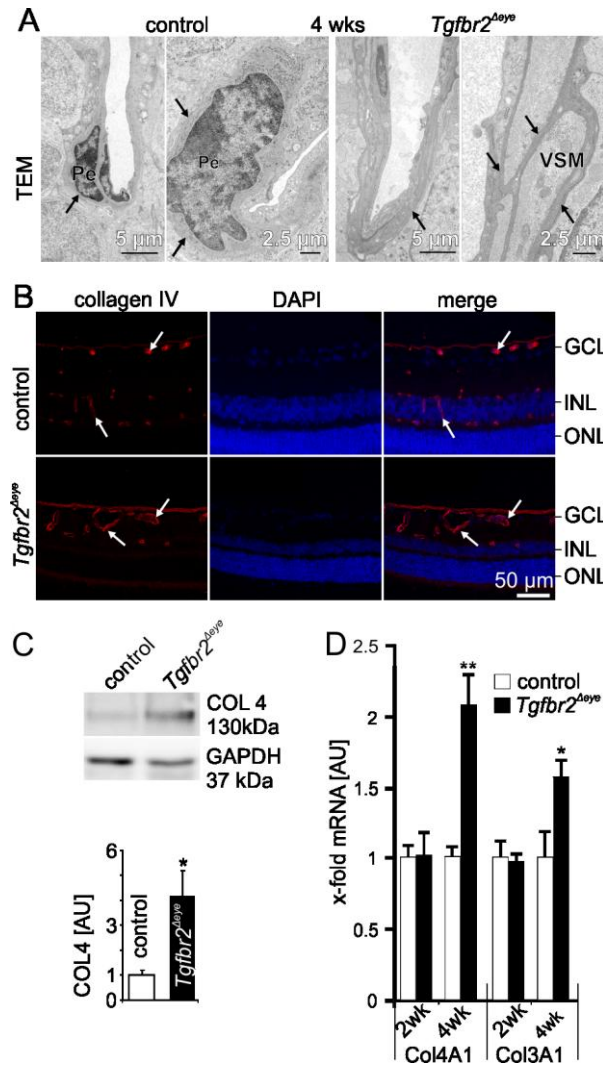


**Figure 13. Extracellular matrix accumulation in *Tgfb2*<sup>Δeye</sup> mice.** **A.** Electron micrographs of retinal capillaries in 4-week-old mice. In control eyes, pericytes share the basal lamina (arrows) with endothelial cells. Retinal capillaries of *Tgfb2*<sup>Δeye</sup> mice are surrounded by one to two complete layers of smooth muscle-like cells that are completely surrounded by a basal lamina (arrows) that is thicker than in controls. **B.** Immunoreactivity for collagen IV (red) in the retina at 4 weeks of age. Distinct immunoreactivity for collagen IV is detectable surrounding the retinal vessels (arrows) of the control mouse, but is even more intense around the vessels of the *Tgfb2*<sup>Δeye</sup> littermate. Nuclei are stained with DAPI (blue). **C.** Western blot analysis and corresponding relative densitometric analysis for collagen IV in 4-week-old retinæ. GAPDH was used as loading control. **D.** Quantitative real-time RT-PCR for mRNA of Col4a1 and Col3a1 in 2 and 4 weeks old control and *Tgfb2*<sup>Δeye</sup> retinæ. Data are expressed as mean ± SEM. n = 6 (C, control, and D, control and *Tgfb2*<sup>Δeye</sup> at 4 weeks); n = 7 (C, *Tgfb2*<sup>Δeye</sup> and D, *Tgfb2*<sup>Δeye</sup> at 2 weeks); n = 5 (D, control at 2 weeks). \**P* ≤ 0.05, \*\* *P* ≤ 0.01. AU, arbitrary unit; GAPDH, glyceraldehyde 3-phosphate dehydrogenase; GCL, ganglion cell layer; INL, inner nuclear layer; ONL, outer nuclear layer; TEM, transmission electron microscopy. Experiments performed by (A,C) Anja Schlecht and Barbara M. Braunger; (B) Sarah V. Leimbeck.

### 3.4.4 Hemorrhages and vessel loss in TGF- $\beta$ -deficient retin

Another characteristic finding concerning the ultrastructure of *Tgfb $\beta$ 2* <sup>$\Delta$ eye</sup> vessels in four-week-old mice was the presence of numerous caveolae along the luminal cell membrane of their endothelial cells (Figure 14A). Next to the vessels, we regularly observed accumulations of erythrocytes between perikarya of retinal neurons indicating intraretinal hemorrhage (Figure 14C). Regional hemorrhages were also observed between photoreceptor outer segments and cells of the retinal pigment epithelium. Cells with the typical ultrastructural characteristics of phagocytosing macrophages, such as the presence of numerous cytoplasmic phagolysosomes, were frequently associated with the hemorrhages (Figure 14C). Moreover, we regularly observed cells in close association with retinal vessels, which contained round cytoplasmic inclusions that were typically 2-2.5  $\mu$ m in diameter (Figure 14D). The inclusions stained intensely with PPD and were osmiophilic strongly indicating their lipid content (Figure 14D). Finally, we observed many capillaries in the outer plexiform layer of *Tgfb $\beta$ 2* <sup>$\Delta$ eye</sup> mice in which the lumen was markedly narrowed or absent (Figure 14B). This finding was especially evident when retin

fixed by intracardial perfusion were investigated. While in control mice capillaries had an open lumen that was surrounded by vascular endothelial cells and pericytes, the opposing vascular walls of *Tgfb $\beta$ 2* <sup>$\Delta$ eye</sup> capillaries were often in contact with each other (Figure 14B). In addition, completely occluded capillaries were identified which showed no lumen, but were still surrounded by a complete basal lamina (Figure 14B). To clarify, if endothelial cell loss was associated with the occlusion of retinal capillaries, we performed double immunohistochemistry with antibodies against both CD31 and type IV collagen. Collagen IV staining in control retin

identified a vascular basal lamina that surrounded CD31-positive cells (Figure 14E, F). In contrast in *Tgfb $\beta$ 2* <sup>$\Delta$ eye</sup> mice, type IV collagen staining identified numerous vascular basal laminae, in which CD31-staining was essentially absent indicating endothelial cell loss (Figure 14E, F).

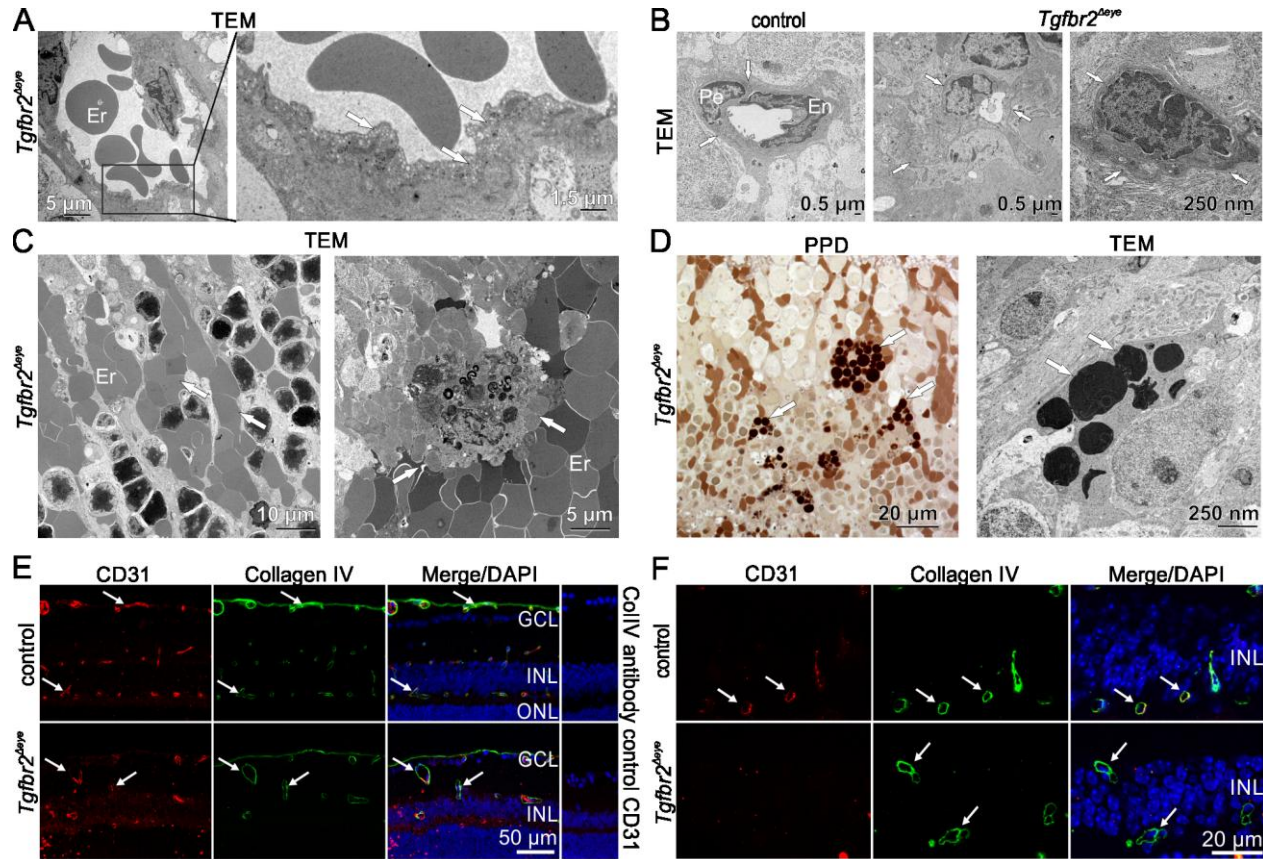


**Figure 14. Intraretinal hemorrhages and vessel loss in *Tgfb2<sup>Δeye</sup>* mice.** **A.** Electron micrographs of 4-week-old *Tgfb2<sup>Δeye</sup>* mice. Endothelial cells of intraretinal vessel show numerous caveolae (arrows). Boxed area is shown at high magnification on the right. **B.** Electron micrographs show intraretinal vessels in the OPL of an 8 week-old control (left) and *Tgfb2<sup>Δeye</sup>* (middle) mouse. In *Tgfb2<sup>Δeye</sup>* mice, the lumen of the capillaries is narrow (middle) or absent (right). **C.** Left: Extravascular erythrocytes (arrows) in the retina. Right: Phagocytosing macrophage (arrows) containing numerous cytoplasmic phagolysosomes. **D.** Left: PPD-stained semithin section of a 4-week-old *Tgfb2<sup>Δeye</sup>* mouse. Arrows point toward PPD-positive, lipid-rich, cytoplasmic inclusions. Right: Electron micrograph of the cytoplasmic inclusions (arrows). **E.** Immunoreactivity for collagen IV (green) and CD31 (red) in the retina at 4 weeks of age. The control mouse shows intense immunoreactivity for collagen IV and CD31 (arrows). In the *Tgfb2<sup>Δeye</sup>* littermate, immunoreactivity for CD31 is considerably weaker (arrows). Nuclei are DAPI-stained (blue). Antibody control sections indicate specific staining. **F.** Immunoreactivity for collagen IV (green) and CD31 (red) in the retina at 4 weeks of age with focus on the OPL. In control the mouse, collagen IV-positive vascular basal laminae (arrows) surround CD31<sup>+</sup> endothelial cells. In *Tgfb2<sup>Δeye</sup>* mice, numerous vascular basal laminae are collagen IV-positive (arrows), whereas CD31 staining is absent. Er, Erythrocyte; GCL, ganglion cell layer; INL, inner nuclear layer; ONL, outer nuclear layer; OPL, outer plexiform layer; PPD paraphenylenediamine; TEM, transmission electron microscopy. Experiments performed by Anja Schlecht and Barbara M. Braunger.

### 3.4.5 Lack of ocular TGF- $\beta$ signaling leads to hyaloid vasculature persistence

Impairment of ocular TGF- $\beta$  signaling not only affects the retinal vasculature, but also the second vascular tree in the eye, the hyaloid vasculature which is transiently present during eye development. While hyaloid vessels had completely disappeared in the normal mouse eye at around P16, they were still detectable by fluorescence angiography in eight-week-old *Tgfb $\beta$ 2* <sup>$\Delta$ eye</sup> mice (Figure 15A). The hyaloid vessels originated from the optic nerve head and formed a typical *tunica vasculosa lentis* around the lens (Figure 15B). There is evidence that regression of the hyaloid vasculature requires macrophages to initiate a cell death program in target cells by activating the canonical Wnt pathway via WNT7b as a short-range paracrine signal (Lobov et al. 2005). We therefore utilized immunohistochemistry with antibodies against IBA-1 or F4/80 to visualize macrophages. Around the persistent hyaloid vasculature of three-week-old *Tgfb $\beta$ 2* <sup>$\Delta$ eye</sup> mice, we detected numerous macrophages that were IBA-1- or F4/80-immunoreactive (Figure 15C and D). Next we crossed *Tgfb $\beta$ 2* <sup>$\Delta$ eye</sup> mice with TOP-Gal Wnt pathway reporter mice. We observed an intense staining for  $\beta$ -galactosidase around the hyaloid vessels and in the epithelial layers of lens and ciliary body of P10 *Tgfb $\beta$ 2* <sup>$\Delta$ eye</sup>/Top Gal mice (Figure 15E). In contrast, Top Gal mice crossed with control littermates of *Tgfb $\beta$ 2* <sup>$\Delta$ eye</sup> mice showed only a weak signal around the few hyaloid vessels that were still present at that age (Figure 15E). Overall, our findings strongly indicate that TGF- $\beta$  signaling is required for the regression of the hyaloid vasculature and that the activity of canonical Wnt signaling is rather increased than decreased when ocular TGF- $\beta$  signaling is absent.

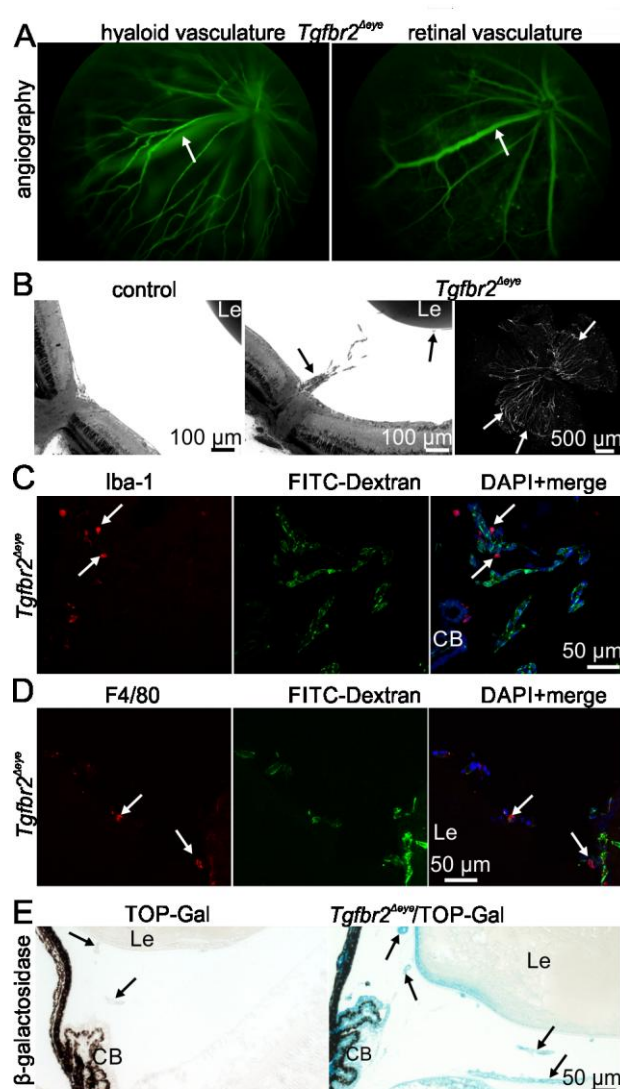


**Figure 15. Persistence of the hyaloid vasculature in *Tgfb2*<sup>Δeye</sup> mice.** **A.** *In vivo* fluorescence angiography of an 8-week-old *Tgfb2*<sup>Δeye</sup> mouse shows the hyaloid artery and the retinal vasculature (white arrow points at the retinal vessels). **B.** Richardson's- stained semithin section of a 4-week-old control and *Tgfb2*<sup>Δeye</sup> eye. In the *Tgfb2*<sup>Δeye</sup> mouse, the hyaloid artery persists (arrows) throughout the vitreous. FITC- dextran-perfused retinal whole mount of a 4-week-old *Tgfb2*<sup>Δeye</sup> mouse with hyaloid vessels located on the retinal surface (white arrows). **C.** Immunoreactivity for IBA-1 (red) and FITC-dextran (green) at the hyaloid artery of a *Tgfb2*<sup>Δeye</sup> mouse at 3 weeks of age. Nuclei are DAPI-stained (blue). **D.** Immunoreactivity for F4/80 (red) and FITC-dextran (green) at the hyaloid artery of a *Tgfb2*<sup>Δeye</sup> mouse at 2 weeks of age. Nuclei are DAPI-stained (blue). **E.** β-galactosidase staining in 10-day-old double transgenic control/TOP-Gal and *Tgfb2*<sup>Δeye</sup>/ TOP-Gal mice. In the *Tgfb2*<sup>Δeye</sup>/TOP-Gal mouse, an intense staining is present throughout the hyaloid artery. CB. Ciliary body; FITC, fluorescein isothiocyanate; Le: lens. Experiments performed by (A) Anja Schlecht, Herbert Jäggle, Cornelia Volz; (B,C) Barbara M. Braunger and Sarah V. Leimbeck; (D) Anja Schlecht and Barbara M. Braunger; (E) Sarah V. Leimbeck.

### 3.4.6 Absence of TGF- $\beta$ signaling induces microglia reactivity in the retina

The presence of numerous macrophages in the vitreous of *Tgfb $\beta$ 2* <sup>$\Delta$ eye</sup> mice prompted us to search for evidence of microglia/macrophage reactivity in the retinae. In two-week old *Tgfb $\beta$ 2* <sup>$\Delta$ eye</sup> mice, real-time RT-PCR showed a significant increase in the expression of mRNA for markers of reactive microglia such as Cd68, Tnf- $\alpha$  and Ccl-2 (Figure 16A). At four weeks of age, the expression of iNos, Il6, and Egr-1 was also significantly increased compared to control littermates (Figure 16A). By immunohistochemistry of control eyes, IBA-1-positive cells were seen in their typical localization such as the retinal surface, and the inner and outer plexiform layers in which the cells had the characteristic shape of ramified microglia (Figure 16B). IBA-1-immunoreactive cells were not obviously associated with retinal capillaries. In contrast, in *Tgfb $\beta$ 2* <sup>$\Delta$ eye</sup> retinae, IBA-1-positive cells formed a distinct and almost complete layer around the enlarged retinal capillaries (Figure 16B). Moreover, IBA-1 immunoreactive cells had changed their shape from that of ramified microglia to reactive microglia (Figure 16B). Immunohistochemistry for F4/80, a marker for macrophages and reactive microglia cells further validated this observation by showing multiple F4/80 positive cells in close association with FITC-dextran perfused capillaries of the inner retina. In contrast, in control eyes F4/80 positive cells were absent in the retina, but were observed in the choroid (Figure 16C). Finally, we labeled for GFAP to analyze reactivity of Müller cell glia. In control eyes, GFAP labeling was restricted to cells on the inner retinal surface and very likely indicated the presence of GFAP in astrocytes and/or Müller cell end-feet. In *Tgfb $\beta$ 2* <sup>$\Delta$ eye</sup> retinae, radial GFAP staining was seen throughout the retina reflecting reactivity and the typical gliosis reaction of Müller cell glia (Figure 16D). In addition, GFAP staining in the inner retina was more prominent than in controls (Figure 16D). GFAP staining did not overlap with that of IBA-1 or F4/80.

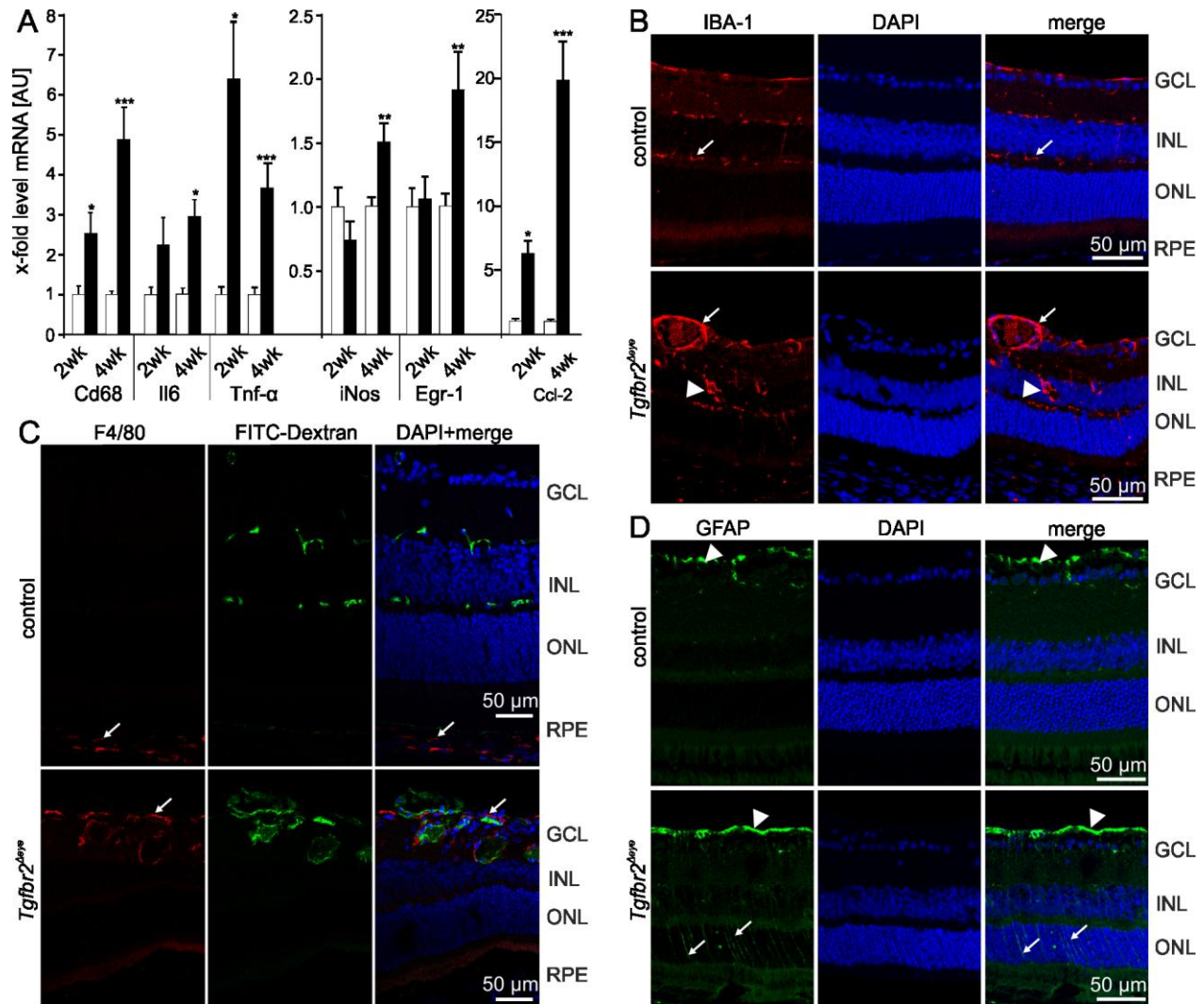


**Figure 16. Microglia reactivity in retinæ of *Tgfb2 $\Delta$ eye* mice.** **A.** Real-time RT-PCR for mRNA of Cd68, Il6, Tnf- $\alpha$ , iNOS, Egr-1 and Ccl-2 in 2- and 4-week-old retinæ. **B.** Immunoreactivity for IBA-1 (red) in the retina at 8 weeks of age. Distinct immunoreactivity for IBA-1 (arrows) is detectable in the plexiform layers of the control mouse. In the *Tgfb2 $\Delta$ eye* littermate microglia labeling is more intense, primarily localized around retinal vessels (arrows) and indicates a switch to a reactive, non-ramified phenotype (arrowhead). Nuclei are DAPI-stained (blue). **C.** Immunoreactivity for F4/80 (red) in the retina at 3 weeks of age. No immunoreactivity for F4/80 is detectable in the retina of the control mouse, whereas a distinct immunoreactivity is detectable in the choroid (arrow). In contrast, in the *Tgfb2 $\Delta$ eye* littermate F4/80 labeling is more intense and primarily localized around retinal vessels (arrows). Nuclei are DAPI-stained (blue). **D.** Immunoreactivity for GFAP (green) in the retina at 4 weeks of age. Distinct immunoreactivity for GFAP (arrowhead) is detectable at the inner retinal surface of the control mouse. In the *Tgfb2 $\Delta$ eye* littermate GFAP labeling on the retinal surface is more intense. In addition, radial staining is seen throughout the retina (arrows), indicating reactivity of Müller glia. Nuclei are DAPI-stained (blue). Data are expressed as means  $\pm$  SEM. Sample size (A): 2 weeks: control:  $n \geq 5$ , *Tgfb2 $\Delta$ eye*:  $n \geq 10$ , Il6: hardly detectable,  $n \geq 4$ ; 4

weeks: control:  $n \geq 9$ , *Tgfb $\beta$ 2* <sup>$\Delta$ eye</sup>:  $n \geq 8$ ; Il6: hardly detectable,  $n \geq 3$ . \* $P \leq 0.05$ ; \*\* $P \leq 0.01$ ; \*\*\* $P \leq 0.001$ . AU, arbitrary unit; FITC, fluorescein isothiocyanate; GCL, ganglion cell layer; GFAP, glial fibrillary acid protein; INL, inner nuclear layer; ONL, outer nuclear layer; RPE, retinal pigment epithelium. Experiments performed by (A) Barbara M. Braunger; (B,D) Sarah V. Leimbeck; (C) Anja Schlecht and Barbara M. Braunger.

### 3.4.7 Continuous lack of retinal TGF- $\beta$ signaling leads to proliferative retinopathy

At around six weeks of age, we frequently observed capillaries that penetrated the inner limiting membrane of *Tgfb $\beta$ 2* <sup>$\Delta$ eye</sup> retinæ and grew into the vitreous body to cause proliferative retinopathy (Figure 17A). To identify stimuli for the proliferation, we assessed by real-time RT-PCR the amounts of mRNA for various angiogenic growth factors. At two weeks of age, the expression of mRNA for Vegf-a-120, Vegf-a-164, Pdgf-b, Ang2, Igf1 and Fgf2 was not significantly different when RNA from *Tgfb $\beta$ 2* <sup>$\Delta$ eye</sup> retinæ was compared with that of controls (Figure 17B, C). In contrast in four-week-old animals, the expression of mRNA for Vegf-a-120, Vegf-a-164, Pdgf-b, Ang2, Igf1 and Fgf2 was significantly higher in the retinæ of *Tgfb $\beta$ 2* <sup>$\Delta$ eye</sup> mice (Figure 17B, C). As the mRNA levels for Fgf2 showed the highest (approx. 10.5-fold) increase (Figure 17C), we additionally investigated the amounts of FGF2 and observed a significant and approx. 4-10-fold increase in the amounts of the FGF2 isoforms (18 kDa, 21 kDa, and 24 kDa) when compared to controls (Figure 17D). As retinal hypoxemia might contribute to the observed effects, we investigated the amounts of HIF-1 $\alpha$  and detected retinal levels of HIF-1 $\alpha$  that were almost double as high as those in controls (Figure 17E).

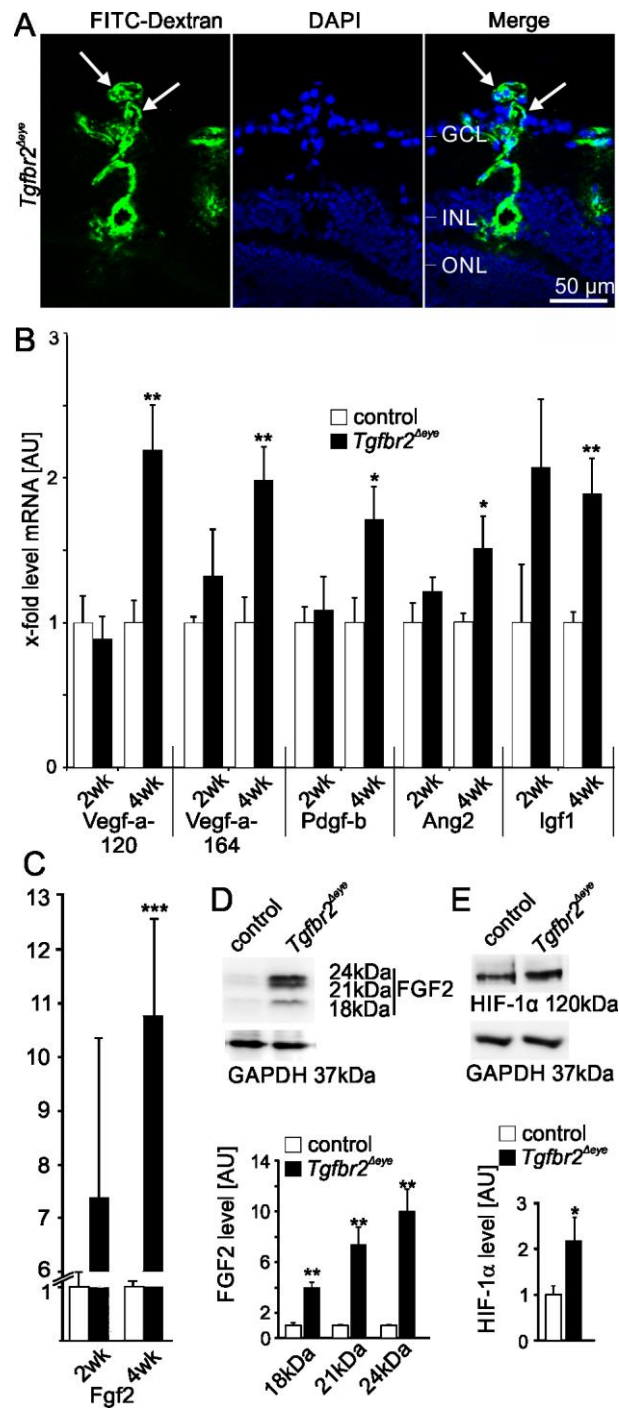


**Figure 17. *Tgfr2<sup>Δeye</sup>* mice develop proliferative retinopathy.** **A.** Meridional section of a 6-week-old FITC-dextran (green)-perfused *Tgfr2<sup>Δeye</sup>* retina shows neovascularization into the vitreous (white arrows). **B.** Real-time RT-PCR for mRNA of Vegf-a-120, Vegf-a-164, Pdgf-b, Ang-2 and Igf-1 in 2- and 4-week-old retinæ. **C.** Real-time RT-PCR for Fgf2 mRNA in 2- and 4-week old retinæ. Data are expressed as means  $\pm$  SEM (same samples as in B). **D** and **E.** Western blot and relative densitometric analyses for FGF2 (D) and HIF1- $\alpha$  in the retina of 4 week old animals. GAPDH was used as loading control. Data are expressed as mean  $\pm$  SEM. Sample size: (B) 2 weeks: control:  $n \geq 4$ , *Tgfr2<sup>Δeye</sup>*:  $n \geq 5$ ; 4 weeks:  $n \geq 7$ ; (D and E)

FGF2:  $n = 4$ , HIF1- $\alpha$ :  $n \geq 7$ ;  $*P \leq 0.05$ ;  $**P \leq 0.01$ ;  $***P \leq 0.001$ . AU, arbitrary unit; FITC, fluorescein isothiocyanate; Fgf2, basic fibroblast growth factor; GAPDH, glyceraldehyde 3-phosphate dehydrogenase GCL, ganglion cell layer; HIF, hypoxia-inducible factor; INL, inner nuclear layer; ONL, outer nuclear layer. Experiments performed by (A) Sarah V. Leimbeck; (B,C,D,E) Barbara M. Braunger.

Proliferative retinopathy resulted in the formation of epiretinal vascular membranes on the surface of *Tgfb $\beta$ 2* <sup>$\Delta$ eye</sup> retinae (Figure 18A) that were not observed in controls (Figure 18A). In four-month-old animals, we frequently observed detachment of the sensory retina which remained in contact with the underlying RPE by thin strands of presumably glial tissue (Figure 18A). Proliferative retinopathy and retinal detachment correlated with pronounced changes in the sensory retina that lost its layered structure (Figure 18A). The structural differences occurred in parallel to a loss of retinal neurons. In support of this, we observed a significant reduction in the amounts of PPD-labeled optic nerve axons that were counted in optic nerve cross sections (Figure 18B) as a measure of retinal ganglion cell number. Moreover, the thickness of the ONL was significantly reduced, again indicating neuronal loss (Figure 18C). The structural changes caused marked functional changes in the retinae of *Tgfb $\beta$ 2* <sup>$\Delta$ eye</sup> mice including a reduction in b/a-amplitude ratio indicating a more pronounced inner retinal function loss (Figure 18D). As likely reason for the neuronal loss, we identified an increase in neuronal apoptotic cell death. Accordingly, the number of retinal TUNEL-positive nuclei was significantly higher in four-week-old *Tgfb $\beta$ 2* <sup>$\Delta$ eye</sup> retinae (Figure 18E and G) as was the expression of Casp8 mRNA at two and four weeks of age (Figure 18F).

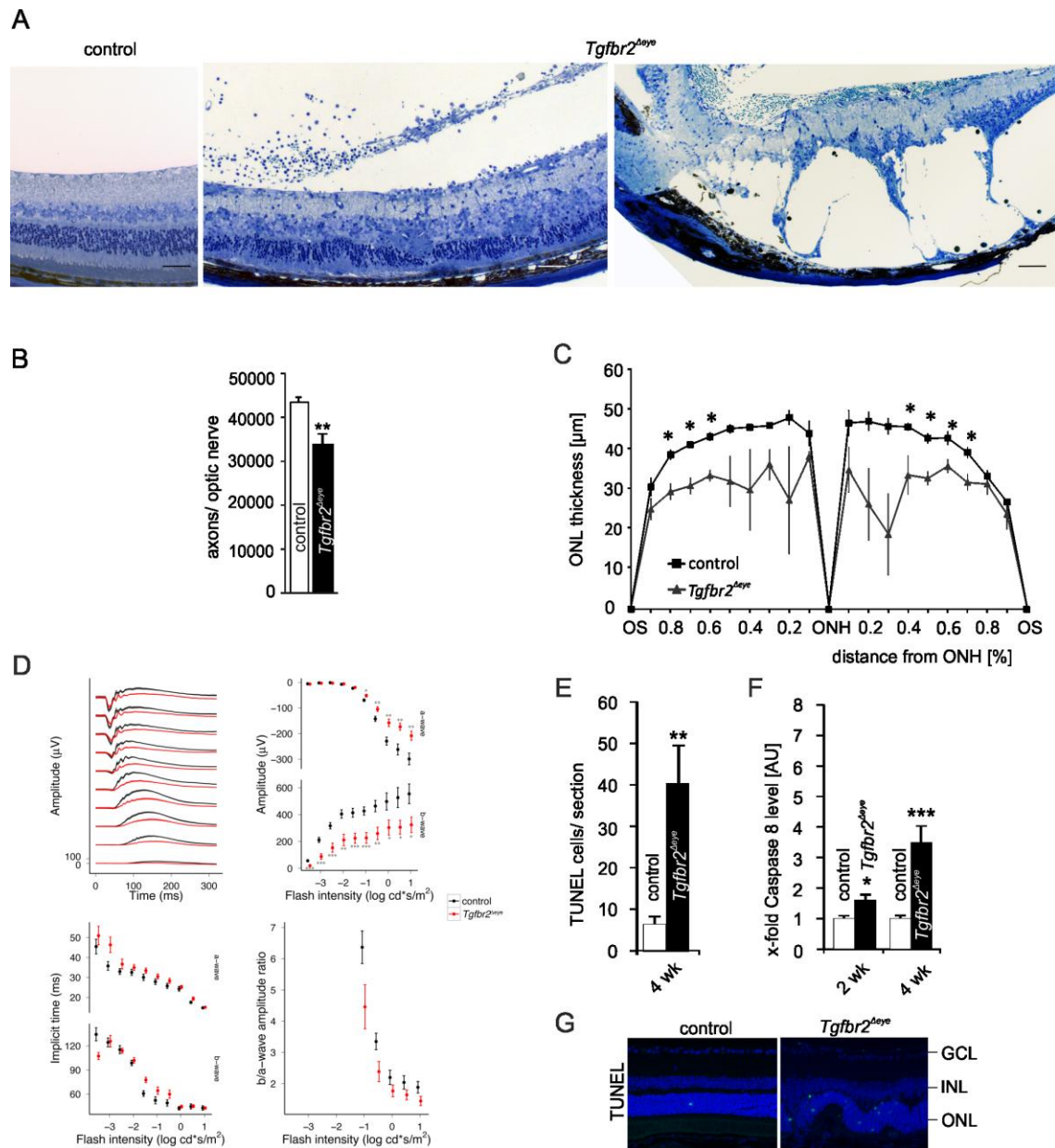


**Figure 18. *Tgfbbr2<sup>Δeye</sup>* mice develop functional and structural deficits.** **A.** Richardson's-stained semi-thin section of a 2-month-old control (left) and 3- and 4-month-old *Tgfbbr2<sup>Δeye</sup>* retina. *Tgfbbr2<sup>Δeye</sup>* mice develop intravitreal membranes (middle, 3-month-old), resulting in traction retinal detachment (right, 4 months old). **B.** Number of optic axons in 8 to 12-week-old mice. **C.** ONL thickness in 8-week-old mice. **D.** Dark adapted ERGs show similar waveforms (upper left panel) but significantly lower a- and b-wave amplitudes (upper right panel) for *Tgfbbr2<sup>Δeye</sup>* compared with control. In addition, slightly lower b/w-wave amplitude ratios (lower right panel) point toward a predominant inner retinal function loss. Implicit times are similar for both groups (lower left panel). **E.** Number of TUNEL-positive cells/meridional section. **F.** Real-time RT-PCR for mRNA of Casp8 in 2- and 4-week-old retinæ. **G.** TUNEL labeling (green) in 6-week-old retinæ. TUNEL-positive cells (arrows) are mainly localized in the ONL. Nuclei are DAPI-stained (blue). Data are expressed as mean  $\pm$  SEM.  $n = 5$  (B);  $n = 3$  (C and E);  $n = 7$  (F, control at 2 weeks);  $n =$

## Chapter 3

10 (F, *Tgfb $\beta$ 2* <sup>$\Delta$ eye</sup> at 4 weeks); n = 11 (F, *Tgfb $\beta$ 2* <sup>$\Delta$ eye</sup> at 2 weeks and control at 4 weeks). \* $P \leq 0.05$ , \*\* $P \leq 0.01$ , \*\*\* $P \leq 0.001$ . AU, arbitrary unit; ERG, electroretinography; GCL, ganglion cell layer; INL, inner nuclear layer; ONH, optic nerve head; ONL, outer nuclear layer; OS, *ora serrata*; TUNEL, terminal deoxynucleotidyl transferase-mediated dUTP nick-end labeling. Experiments performed by (A) Anja Schlecht and Sarah V. Leimbeck; (B,C) Barbara M. Braunger and Sarah V. Leimbeck; (D) Herbert Jägle; (EFG) Barbara M. Braunger.

### 3.5 Discussion

We conclude that lack of TGF- $\beta$  signaling in the retinal microenvironment of the mouse eye is sufficient to induce all the major structural and functional changes that are associated with diabetic retinopathy in humans. The cellular players that are affected by the lack of retinal TGF- $\beta$  signaling are the microvascular pericytes that largely dedifferentiate, the vascular endothelial cells that proliferate and lose their barrier function, and the microglia that changes to a reactive phenotype. The combined cellular changes directly result in a phenotype quite similar to that seen in non-proliferative retinopathy including leakiness of retinal capillaries, microhemorrhages, the formation of multiple microaneurysms, and the degeneration of retinal capillaries. The pathogenic process subsequently leads to retinal hypoxia, to the induction of angiogenic molecules resulting in retinal and vitreal neovascularization, and in the essential structural and functional characteristics of proliferative diabetic retinopathy. Our conclusions rest upon (1) the generation of mutant *Tgfr2* <sup>$\Delta$ eye</sup> animals with a tamoxifen-induced conditional deletion of T $\beta$ RII in ocular tissues, (2) the observation that retinal NG2-positive pericytes are markedly reduced in number while  $\alpha$ -SMA positive perivascular cells are massively increased, (3) the formation of abundant vascular microaneurysms in every vascular plexus in the retina, (4) the finding that retinal capillaries are leaky, and associated with extravascular erythrocytes and lipid-laden macrophages, (5) the fact that capillaries are surrounded by numerous reactive microglial cells, (6) the loss of vascular endothelial cells and the continuing closure of the retinal capillaries, (7) the increasing amounts of HIF-1 $\alpha$ , and of angiogenic molecules and their mRNA, and (8) the observation of retinal detachment, retinal and vitreal hemorrhages, neuronal apoptosis and impairment of retinal sensory function.

### 3.5.1 TGF- $\beta$ signaling determines pericyte differentiation during development of the retinal vasculature

TGF- $\beta$  signaling appears to play an essential role for vascular morphogenesis during early embryonic life (Armulik et al. 2011, Gaengel et al. 2009, Pardali et al. 2010, Jakobsson and van Meeteren 2013, Goumans et al. 2009, Patel-Hett and D'amore 2011) since mice that are defect in genes coding for various components of the TGF- $\beta$  signaling pathways such as *Tgfb1* (Dickson et al. 1995), *Tgfb2* (Oshima et al. 1996), *Tgfb1/Alk5* (Larsson et al. 2001), *Acvrl1/Alk1* (Urness et al. 2000), *Eng* (Li 1999, Dijke et al. 2008, Bourdeau et al. 1999), or *Smad5* (Chang et al. 1999, Yang et al. 1999) develop vascular abnormalities and die during early embryonic life. The approach used in the present study enabled us to conditionally delete TGF- $\beta$  signaling in the eye during early angiogenesis of the mouse retina in the first postnatal week. Our results provide evidence that TGF- $\beta$  signaling critically influences the molecular differentiation of pericytes in the retina.

Pericytes constitute a somewhat diverse cell population and no molecular marker has been identified so far, which is expressed by all pericytes (Armulik et al. 2011, Krueger and Bechmann 2010, Díaz-Flores et al. 2009). NG2 is a transmembrane chondroitin sulfate proteoglycan that is widely expressed in microvascular pericytes of newly formed blood vessels (Ozerdem et al. 2001). In the central nervous system including the retina, the majority of pericytes expresses NG2 during vascular development and, after their differentiation, throughout adulthood (Hughes and Chan-Ling 2004, Winkler et al. 2010, Bell et al. 2010, Schallek et al. 2013). In addition, NG2 localizes to the surface of retinal vascular smooth muscle cells (Krueger and Bechmann 2010, Díaz-Flores et al. 2009, Ozerdem et al. 2001, Hughes and Chan-Ling 2004, Schallek et al. 2013, Trost et al. 2013). In contrast to NG2, labeling for  $\alpha$ -SMA in the normal retina is not observed in microvascular pericytes that are associated with retinal capillaries, but is restricted to vascular smooth muscle cells that surround larger vessels such as arterioles and arteries (Hughes and Chan-Ling 2004, Trost et al. 2013, Nehls 1991). Results from studies using neural crest-specific reporter genes indicate a common neural crest origin for the vast majority of NG2-positive pericytes and  $\alpha$ -SMA-positive vascular smooth muscle cells in the mouse retina (Gage et al. 2005, Trost et al. 2013). In retinal development of the mouse eye, both cell types are first observed in the eye at around P0 when retinal angiogenesis begins. During the formation of the superficial primordial retinal vascular network in the first postnatal week, pericytes spread along retinal capillaries while vascular smooth muscle cells surround arterial vessels (Fruttiger 2002). Upon retinal *Tgfb2* deficiency, capillaries become completely surrounded by  $\alpha$ -SMA-positive

smooth muscle-like cells while NG2-positive pericytes are largely reduced in number. The observation strongly indicates that during retinal angiogenesis, TGF- $\beta$  signaling in the retinal microenvironment is important to determine the respective pericyte/vascular smooth muscle phenotype of mural cells that surround capillaries. Lack of TGF- $\beta$  signaling during vascular development of the retina favors the differentiation of mural cells towards a vascular smooth muscle cell-like fate at the expense of the formation of differentiated pericytes.

It is well established that PDGF-B released from angiogenic endothelial cells binds to PDGFR $\beta$  to induce a mural cell fate in undifferentiated mesenchymal cells and stimulates their co-migration. Accordingly, the deletion of *Pdgfb* or *Pdgfrb* in mice causes an almost complete pericyte deficiency throughout the body and leads to perinatal lethality (Hellström et al. 1999, Lindahl et al. 1997). Since TGF- $\beta$  signaling induces the expression of  $\alpha$ -SMA and other molecules characteristic for vascular smooth muscle cells in mesenchymal cells both *in vitro* and *in vivo* (Chambers et al. 2003, Chen 2003, Sieczkiewicz and Herman 2003, Kumar and Owens 2003, Darland and D'Amore 2001, Hirschi et al. 1998), a contributing role of this signaling pathway for mural cell differentiation towards a vascular smooth muscle phenotype has been suggested. While our results clearly support the concept that TGF- $\beta$  signaling is required to induce or maintain the differentiated phenotype of pericytes, they also indicate though that the lack of TGF- $\beta$  signaling does not lead to an obvious reduction of vascular smooth muscle cells.

### 3.5.2 Lack of retinal TGF- $\beta$ signaling leads to vascular leakage

Brain capillaries of mice with null and hypomorphic alleles of *Pdgfrb*, and defects in pericyte generation, are permeable to low-molecular-mass and high-molecular-mass tracers such as dextran indicating that pericytes are necessary for the formation of the blood-brain barrier (Bell et al. 2010, Armulik et al. 2010, Daneman et al. 2010). The increase in permeability is caused by an increase in transcytosis that is associated with a marked increase in the number of cytoplasmic vesicles in endothelial cells (Daneman et al. 2010, Armulik et al. 2010, Hellström et al. 2001). Quite similarly, an increased vascular permeability to fluorescein and FITC-dextran, and an accumulation of cytoplasmic vesicles in endothelial cells were observed in our study strongly supporting the concept that the  $\alpha$ -SMA-positive mural cells covering retinal capillaries in the *Tgfb2* –deficient retinae had not differentiated to functional pericytes. In addition to tracer leakage, we observed massive retinal hemorrhages and lipid-laden macrophages, all common findings seen in human diabetic retinopathy (Wu et al. 2008, Toussaint et al. 1962, Garner 1993). Clearly, the lack of capillary integrity is even more pronounced in retinae with deficiency in retinal TGF- $\beta$  signaling than in animals lacking pericytes. Factors other than lack of pericyte

differentiation appear to contribute to the severe lack of capillary integrity and *Tgfb2* deficiency in capillary endothelial cells is a likely candidate. In support of this assumption are findings in mice with deficiency of *Smad4*, an intracellular mediator of TGF- $\beta$  signaling, in brain capillary endothelial cells, which suffer from perinatal intracerebral hemorrhages and breakdown of the blood brain barrier (Li et al. 2011). Quite similarly, the selective deletion of *Tgfb2* in endothelial cells result in intracerebral hemorrhages and embryonic lethality (Nguyen et al. 2011). In the retina, inhibition of TGF- $\beta$ 1 signaling by systemic expression of soluble endoglin also induces breakdown of the blood retinal barrier, an effect that is mediated via a decreased association between the tight junction proteins zo-1 and occludin. Again, the effect on capillary integrity appears to be less pronounced than in our study since hemorrhages were not reported. Endothelial cells express the T $\beta$ RI receptors ALK1 and ALK5 which are each recruited and activated following binding of TGF- $\beta$ 1 dimers to T $\beta$ RII (Pardali et al. 2010). Soluble endoglin interferes only with ALK1-mediated TGF- $\beta$ 1 signaling, while ALK5 is not affected. ALK5 signaling is intracellularly mediated by *Smad2/3* (Pardali et al. 2010), and deletion of ALK5 or *Smad2/3* in vascular endothelial cells causes hemorrhages and embryonic lethality (Itoh et al. 2012). Our approach causes retinal deficiency of T $\beta$ RII thus interrupting both ALK1- and ALK5-mediated signaling in endothelial cells, a scenario that likely explains the more massive disruption of vascular integrity. Overall our results clearly support the concept that TGF- $\beta$  signaling induces pericyte-endothelial cell interactions that are critical for the stability of capillaries in the retina, a mechanism that likely fails in diabetic retinopathy.

It is of interest to note that both endothelial cells and  $\alpha$ -SMA-positive mural cells of *Tgfb2* – deficient retinae are covered by a basal lamina which is thicker and richer in type IV collagen than that in control littermates. Similar findings are very characteristic for diabetic retinopathy in humans (Roy et al. 1994, Garner 1993). In cell culture, TGF- $\beta$  signaling induces the expression of basal lamina proteins in vascular endothelial cells and pericytes (Neubauer et al. 1999, van Geest et al. 2010) and its increased activity has been hypothesized to be causative for the increase in basal lamina thickening in diabetic retinopathy (van Geest et al. 2010), a concept that is not supported by the phenotype observed in *Tgfb2*-deficient retinae.

### 3.5.3 Lack of retinal TGF- $\beta$ signaling induces the formation of capillary microaneurysms

A hallmark of non-proliferative diabetic retinopathy are capillary microaneurysms (Sjölvi et al. 2011) which are formed by proliferating endothelial cells (Aguilar et al. 2003). Cell culture studies indicate that TGF- $\beta$ 1 is activated upon contact between endothelial cells, and pericytes or smooth muscle cells, an effect that mediates the inhibition of endothelial cell proliferation and

migration (Sato 1989, Antonelli-Orlidge et al. 1989, Sato 1990). Accordingly, the hypothesis has been put forward that the loss of pericytes in diabetic retinopathy is a causative factor for the generation of microaneurysms. Still, the formation of retinal microaneurysms is not a prominent finding in mouse mutants that lack pericytes, even in those where more than 50% of pericytes are missing (Enge 2002, Feng et al. 2007, Hammes 2005, Hammes et al. 2002, Hammes et al. 2004). Overall, the effects of TGF- $\beta$  signaling on endothelial cell proliferation appear to depend on the relative levels of ALK1/5 expression, and on the strength and duration of the TGF- $\beta$  signal (Armulik et al. 2011, Pardali et al. 2010). ALK1 promotes endothelial cell proliferation whereas ALK5 has the opposite effect, and the balance between TGF- $\beta$ /ALK1 versus TGF- $\beta$ /ALK5 determines the pro- or anti-angiogenic effects of TGF- $\beta$ . We assume that lack of *Tgfb2* in retinal endothelial cells shifts the balance to the pro-angiogenic effects, a scenario which promotes endothelial proliferation and the formation of microaneurysms. In support of this assumption are data from mice with induced conditional inactivation of *Tgfb2* in retinal vascular endothelial cells, which develop abnormally thickened vessels (Arnold et al. 2012) or glomerular tufts (Allinson et al. 2012) during retinal angiogenesis, findings that indicate an increase in endothelial proliferation. Overall, the incomplete pericyte differentiation and the increased endothelial proliferative activity both induced by retinal lack of *Tgfb2* appear to be the essential factors that drive the formation of microaneurysms in the mice investigated in the present study. Other prominent angiogenic factors are very likely not involved since the levels of mRNAs for Vegf-a-120, Vegf-a-164, Pdgf-b, Ang2, Igf1 or Fgf2 are not significantly elevated in two-week old mice with retinal *Tgfb2* deficiency.

### 3.5.4 Lack of retinal TGF- $\beta$ signaling induces capillary closure and reactive microglia

Our results indicate that with increasing age, mice lacking retinal *Tgfb2* develop nonperfused capillary segments that are devoid of endothelial cells, a finding commonly observed in diabetic retinopathy (Toussaint et al. 1962, Hammes et al. 2011) where capillaries are reduced to endothelial cell-free tubes of basal lamina as the disease progresses (Ashton 1963, Cogan 1961, Engerman 1989). Pericyte dropout appears to play a causative role in the generation of nonperfused capillary segments in diabetes, since comparable changes were observed in mice with endothelial deficiency of *Pdgfb*, which show a 50% reduction in the number of retinal pericytes that correlates with substantial capillary regression (Enge 2002). Cell culture experiments indicate that activated TGF- $\beta$  released from pericytes plays a causative role in this process and acts as survival factor for vascular endothelial cells (Walshe et al. 2009). Indeed, systemic inhibition of TGF- $\beta$ 1 by soluble endoglin results in retinal underperfusion, loss of

capillary integrity, and ultrastructural changes of retinal capillaries that are quite similar to those observed in the present study (Walshe et al. 2009).

In the perivascular areas of affected vessels, we consistently observed macrophages and microglia with a reactive phenotype. Also the high expression of *Tnf- $\alpha$*  and of other characteristic molecules in retinal extracts indicated that microglia had changed from a ramified, resting phenotype to that of reactive microglia. Essentially similar changes are seen in human retinae with diabetic retinopathy in which microglial perivasculitis is a common finding (Zeng et al. 2008). We expect that our approach also caused *Tgfb2*-deficiency in microglia, a scenario, which in turn induced the reactive changes. In support of this assumption is the well-documented immunosuppressive role of TGF- $\beta$  signaling in the eye (Nussenblatt and Ferris 2007, Niederkorn 2006). Mediators released by reactive microglia may contribute to the capillary damage seen *Tgfb2*-deficient retinae, and TNF- $\alpha$ , which induces apoptosis of vascular endothelial cell in culture (Robaye et al. 1991), is a likely candidate. TNF- $\alpha$  is similarly increased in the retina of diabetic rodents and its suppression reduces diabetic blood-retinal barrier breakdown (Joussen et al. 2001), pericyte and endothelial cell death, and apoptosis (Joussen et al. 2009). Also data from other animal studies provided evidence for a causative role of low-grade subclinical inflammation in the pathogenesis of the vascular changes in diabetic retinopathy (Joussen et al. 2009, Joussen et al. 2004).

Cells of macrophage lineage are also involved during the ontogenetic regression of the other major capillary network in the posterior eye, the hyaloid vasculature. Apparently, the cells initiate a cell-death program in target cells by activating the canonical Wnt pathway via WNT7b as a short-range paracrine signal (Lobov et al. 2005). Since our approach caused recombination in the entire eye including the vitreous, our findings strongly indicate that vitreous TGF- $\beta$  signaling plays an equally important role during the ontogenetic regression of the hyaloid vasculature. Very likely this role is not directly related to canonical Wnt-signaling, and is required to induce capillary regression rather than preventing it as presumably in the adult retina. Apparently, the role of TGF- $\beta$  signaling for vascular maintenance depends on tissue-specific and temporal contexts.

### 3.5.5 Phenotypic changes in retinae progress to proliferative retinopathy

Non-proliferative diabetic retinopathy eventually progresses to proliferative retinopathy that is characterized by retinal edema, retinal and vitreal neovascularization, retinal detachment, and vitreal hemorrhages (Frank 2004, Cheung et al. 2010, Antonetti et al. 2012, Garner 1993). Consequently neurons die by apoptosis, a scenario that results in impairment of retinal sensory

function. Essentially similar changes are seen when mice with ocular *Tgfb $\beta$ 2*-deficiency become older, an observation that underlines the close similarity of their phenotype with that of humans suffering from diabetic retinopathy. It is more than likely that the driving factors in both conditions are similar such as capillary regression leading to hypoxia and the induction of potent angiogenic molecules such as vascular endothelium growth factor-A and FGF2.

### 3.5.6 Conclusion

We conclude that the interaction of pericytes, vascular endothelial cells and microglia is required for maintenance of retinal capillaries and that TGF- $\beta$  signaling plays an essential role in this process. Lack of TGF- $\beta$  signaling in the retinal microenvironment disrupts this interaction and leads to homeostatic changes. The changes induce all the major aspects of the phenotype of diabetic retinopathy and underline the important role of the TGF- $\beta$  signaling pathway during the pathogenesis of this disease.

### Acknowledgements

The authors greatly appreciate the excellent technical assistance of Elke Stauber, Angelika Pach, Margit Schimmel and Silvia Babl. This work has been supported by the Deutsche Forschungsgemeinschaft (FOR 1075, TP5 to ERT).

## Chapter 4

### **Ablation of endothelial TGF- $\beta$ signaling causes choroidal neovascularization**

(adapted from: Anja Schlecht, Sarah V. Leimbeck, Herbert Jägle, Annette Feuchtinger, Ernst R. Tamm and Barbara M. Braunger. **Ablation of endothelial TGF- $\beta$  signaling causes choroidal neovascularization.** Submitted to Journal of Clinical Investigation)

## **4 Ablation of endothelial TGF- $\beta$ signaling causes choroidal neovascularization**

### **4.1 Abstract**

The molecular pathogenesis of choroidal neovascularization (CNV), an angiogenic process that critically contributes to vision loss in age-related macular degeneration (AMD) is unclear. Here we analyzed the role of transforming growth factor (TGF)- $\beta$  signaling for CNV formation by generating a series of mutant mouse models with induced conditional deletion of TGF- $\beta$  signaling in the entire eye, the retinal pigment epithelium (RPE) or the vascular endothelium. Ablation of TGF- $\beta$  signaling in the eye caused CNV, irrespectively if it was ablated in newborn or three-week-old mice. Areas of CNV showed photoreceptor degeneration, multilayered RPE, basal lamina deposits and accumulations of monocytes/macrophages. The changes progressed, leading to marked structural and functional alterations of the retina. While the specific deletion of TGF- $\beta$  signaling in the RPE caused no obvious changes, specific deletion in vascular endothelial cells caused CNV and a phenotype quite similar to that observed after the deletion in the entire eye. We conclude that impairment of TGF- $\beta$  signaling in the vascular endothelium of the eye is sufficient to trigger CNV formation. Our findings highlight the importance of TGF- $\beta$  signaling as key player in the development of ocular neovascularization and indicate a fundamental role of TGF- $\beta$  signaling in the pathogenesis of AMD.

### 4.2 Introduction

The therapeutic options to treat age-related macular degeneration (AMD), the leading cause of vision loss and blindness in industrialized countries (Friedman et al. 2004, Finger et al. 2011, Klaver et al. 1998), are limited (Ambati and Fowler 2012, Lim et al. 2012). AMD is a complex disease (Fritsche et al. 2016) whose molecular pathogenesis is not well understood (Ambati and Fowler 2012, Lim et al. 2012). Vision loss in AMD is caused by choroidal neovascularization (CNV) or geographic atrophy (Ambati and Fowler 2012, Lim et al. 2012). In geographic atrophy (“late dry” AMD), the progressive atrophy of the retinal pigment epithelium (RPE) and of the choriocapillaris causes photoreceptor degeneration. Angiogenic processes that cause immature choroidal vessels to break through the RPE into the subretinal space characterize CNV. The resulting blood and plasma leakage causes fibrous scarring of the retina (“wet” AMD). The pathogenic mechanisms underlying the onset of CNV in AMD are unclear. Dysfunction of the retinal pigment epithelium (RPE) and immunovascular deregulation in region of the retinal/choroidal interface are considered as contributing factors (Ambati and Fowler 2012, Miller et al. 2013, Miller 2013).

The choroidal vasculature forms the choriocapillaris, a vascular bed of highly anastomosed capillaries that is essential for nutrition and oxygen supply of both photoreceptors and RPE (Kur et al. 2012). The capillaries have a fenestrated endothelial layer and are highly permeable (Bill et al. 1980), a substantial difference to retinal capillaries. There is evidence from several studies of genetically engineered mouse models indicating that RPE-derived vascular endothelial growth factor (VEGF) is essential for choriocapillaris maintenance. VEGF is expressed in high amounts by RPE cells during embryonic development and in adult life (Ford et al. 2011). If VEGF expression is compromised, formation of the choriocapillaris in development or its maintenance in adult eyes are severely impaired leading to choriocapillaris ablation (Kurihara et al. 2012, Marneros et al. 2005, Le et al. 2010, Saint-Geniez et al. 2009, Ohlmann et al. 2016). Other growth factors that are secreted by RPE cells in high amounts are transforming growth factor

(TGF)- $\beta$ 1 and - $\beta$ 2 (Strauss 2005) causing a concentration of both factors in the RPE/choroid complex that is more than 10-fold higher than in the retina (Pfeffer et al. 1994). In a recent study we showed that a conditional ocular deletion of TGF- $\beta$  signaling results in pronounced structural changes of retinal capillaries including the formation of abundant microaneurysms, leaky capillaries, and retinal hemorrhages. Overall a phenotype resulted very similar to that of diabetic retinopathy in humans (Braunger et al. 2015).

Since TGF- $\beta$ s are present at very high concentrations in region of the RPE/choroid interface, we wondered if TGF- $\beta$  signaling might not only be required for stability of retinal capillaries, but also for that of the choriocapillaris. To this end, we targeted the TGF- $\beta$  type II receptor (T $\beta$ RII), which is essential for TGF- $\beta$  signaling and generated a series of mutant mouse strains with an induced conditional deletion in the entire eye, the RPE or in vascular endothelial cells. Here we provide evidence that impairment of TGF- $\beta$  signaling in the vascular endothelium of the eye is sufficient for the development of CNV. Our findings highlight the importance of the TGF- $\beta$  signaling pathway as a key player in the development of ocular neovascularization and indicate a fundamental role of TGF- $\beta$  signaling in the pathogenesis of AMD.

### 4.3 Material and Methods

#### 4.3.1 Mice

All procedures conformed to the tenets of the NIH's Guidelines for the Care and Use of Laboratory Animals, the EU Directive 2010/63/E, institutional guidelines, and were approved by the local authority (Regierung der Oberpfalz, AZ 54-2532.1-44/12 and DMS 2532-2-85). All experiments were performed in mice of either sex that were tested negatively for the Rd8 mutation (Mattapallil et al. 2012).

Mice with two floxed alleles of *Tgfb $\beta$ 2* (*Tgfb $\beta$ 2<sup>fl/fl</sup>*) (Chytil et al. 2002) were crossed with CAGG Cre-ER<sup>TM</sup> (Hayashi and McMahon 2002), *VMD2<sup>rtTA</sup>* Cre (Le et al. 2008) or *VECad* Cre-ER<sup>T2</sup> (Monvoisin et al. 2006) mice that were heterozygous for the Cre recombinase. Resulting *Tgfb $\beta$ 2<sup>fl/fl</sup>*; CAGG Cre-ER<sup>TM</sup>, *Tgfb $\beta$ 2<sup>fl/fl</sup>*; *VMD2<sup>rtTA</sup>* Cre or *Tgfb $\beta$ 2<sup>fl/fl</sup>*; *VECad* Cre-ER<sup>T2</sup> mice were used as experimental mice. For simplicity, *Tgfb $\beta$ 2<sup>fl/fl</sup>*; CAGG Cre-ER<sup>TM</sup> mice will be referred to as *Tgfb $\beta$ 2 <sup>$\Delta$ eye</sup>*, *Tgfb $\beta$ 2<sup>fl/fl</sup>*; *VMD2<sup>rtTA</sup>* Cre mice will be referred to as *Tgfb $\beta$ 2 <sup>$\Delta$ RPE</sup>* and *Tgfb $\beta$ 2<sup>fl/fl</sup>*; *VECad* Cre-ER<sup>T2</sup> mice will be referred to as *Tgfb $\beta$ 2 <sup>$\Delta$ EC</sup>*. *Tgfb $\beta$ 2<sup>fl/fl</sup>* littermates with two unrecombined *Tgfb $\beta$ 2* alleles served and are referred to as controls. Genetic backgrounds were 129SV (*Tgfb $\beta$ 2<sup>fl/fl</sup>*, *VMD2<sup>rtTA</sup>* Cre, *VECad* Cre-ER<sup>T2</sup>) and C57/Bl6 (CAGG Cre-ER<sup>TM</sup>). All mice were reared in a light/dark cycle of 12 h (lights on at 7AM). Genotypes were screened by isolating genomic DNA from tail biopsies and testing for transgenic Cre sequences and floxed *Tgfb $\beta$ 2* sequences as described previously (Boneva et al. 2016, Braunger et al. 2015).

#### 4.3.2 Induction of Cre recombinase

Cre recombinase in CAGG Cre-ER<sup>TM</sup> and *VECad* Cre-ER<sup>T2</sup> mice is tamoxifen dependent. In CAGG Cre-ER<sup>TM</sup> mice, the Cre-ER<sup>TM</sup> fusion protein is ubiquitously expressed. Cre recombinase is restricted to the cytoplasm and will only access the nucleus after binding to tamoxifen (Hayashi and McMahon 2002, Feil et al. 1996). *VECad* Cre-ER<sup>T2</sup> mice carry the Cre-ER<sup>T2</sup>

expression cassette under regulatory control of the mouse VE-cadherin gene promoter region that specifically drives gene expression in the vascular endothelium (Monvoisin et al. 2006). To activate Cre recombinase in *Tgfb $\beta$ 2* <sup>$\Delta$ eye</sup> and *Tgfb $\beta$ 2* <sup>$\Delta$ EC</sup> mice, the animals and their respective control littermates were treated with tamoxifen containing eyedrops from P4 to P8 as described previously (Schlecht et al. 2016). A second stock of *Tgfb $\beta$ 2* <sup>$\Delta$ eye</sup> and control mice was treated from P21 to P25, a time when the development of the retinal vasculature is complete. For simplicity, *Tgfb $\beta$ 2* <sup>$\Delta$ eye</sup> mice that were tamoxifen treated from P4-8 will be referred to as “early-induced” and *Tgfb $\beta$ 2* <sup>$\Delta$ eye</sup> mice that were tamoxifen treated from P21-25 will be referred to as “late-induced”. Cre recombinase in *VMD2*<sup>rtTA</sup> Cre;*Tgfb $\beta$ 2*<sup>fl/fl</sup> is doxycycline dependent and under the control of the RPE-specific bestrophin promotor (Le et al. 2008). Doxycycline (AppliChem, Darmstadt, Germany) was diluted in phosphate-buffered saline (PBS) to a final concentration of 0.1 g/ml and doxycycline eye drops (10  $\mu$ l) were pipetted onto the eyes of *Tgfb $\beta$ 2* <sup>$\Delta$ RPE</sup> mice and their control littermates from P21 to P25 three times per day.

### 4.3.3 *mT/mG* reporter mice

The efficient Cre recombinase activation in *VeCad-Cre-ER*<sup>T2</sup> mice was confirmed using *mT/mG* reporter mice (Muzumdar et al. 2007), which express a membrane-targeted green fluorescent protein (mG/GFP) after Cre mediated excision. Heterozygous *VeCad Cre-ER*<sup>T2</sup> mice were crossed with homozygous *mT/mG* mice. The resulting offspring (*VeCad-Cre-ER*<sup>T2</sup>(+/-);*mT/mG*(+/-) and *wildtype;mT/mG*(+/-)) was treated with tamoxifen eyedrops from P4 to P8 according to previously published protocols (Braunger et al. 2015, Schlecht et al. 2016). Mice were killed at P10. After enucleation, the eyes were fixed in 4% PFA for 4h, washed extensively in phosphate buffer (PB), incubated in 10%, 20%, 30% sucrose over night and shock frozen in tissue mounting medium (O.C.T. Compound; DiaTec, Bamberg, Germany). Sections were washed three times in phosphate buffer (PB, 5 min each) and cell nuclei were counterstained

## Chapter 4

with DAPI (Vectashield; Vector Laboratories, Burlington, CA) 1:10 diluted in fluorescent mounting medium (Serva).

### 4.3.4 *Tgfb $\beta$ 2* deletion PCR

*Tgfb $\beta$ 2* deletion PCR screens its successful genomic deletion following Cre mediated recombination. DNA samples of the sensory retina and the choroid (including cells of the RPE) served as templates. Primer pairs and protocol are described in previously published manuscripts (Chytil et al. 2002, Braunger et al. 2013b). Actin was used as loading control.

### 4.3.5 Morphology and microscopy

The eyes were enucleated, fixed for 24 h in 2% paraformaldehyde (PFA)/2.5% glutaraldehyde and embedded in Epon (Serva, Heidelberg, Germany) as described elsewhere (Karnovsky 1965, Kugler et al. 2015). Semithin meridional sections (1  $\mu$ m thick) were cut through the eyes and stained after Richardson (Richardson et al. 2009). The sections were analyzed using an Axio Imager Z1 microscope (Carl Zeiss, Jena, Germany) and appropriate Axiovision version 4.8 software (Carl Zeiss). Ultrathin sections were processed according to protocols published previously (Braunger et al. 2014, Braunger et al. 2013a), stained with uranyl acetate and lead citrate, and analyzed on a transmission electron microscope (Libra, Zeiss).

### 4.3.6 Immunohistochemistry

Prior to T $\beta$ RII, collagen IV and VEGF-A staining, eyes were fixed for 4 h in 4% paraformaldehyde (PFA), washed extensively in PB (0.1 M, pH 7.4) and embedded in paraffin according to standard protocols. Paraffin sections (6  $\mu$ m) were deparaffinized and washed in H<sub>2</sub>O. For detection of T $\beta$ RII, sections were treated with boiling citrate buffer (1 x 10 min, pH 6), washed again in H<sub>2</sub>O and incubated in 0.1 M PB. For detection of collagen IV and VEGF-A, sections were pretreated with 0.05 M Tris-HCl (5 min) and covered with Proteinase K (100  $\mu$ l of Proteinase K in 57 ml of Tris-HCl (0.05 M), 5 min), washed in H<sub>2</sub>O, incubated in 2 N HCl (20

min), and washed again in H<sub>2</sub>O. Sections were incubated in PB for 5 min and then blocked with 2% BSA, 0.2% CWFG, 0.1% Triton X (TβRII), ) 2% BSA, 0.1% Triton X (Collagen IV) or 5% non-fat dry milk (VEGF-A) at room temperature for 60 min. Primary antibodies (Table 4) were diluted in a 1:10 dilution of blocking solution in PB.

Prior to F4/80 and PLVAP staining, eyes were fixed for 4 h in 4% paraformaldehyde (PFA), washed extensively in phosphate buffer (PB, 0.1 M), incubated in 10%, 20%, 30% sucrose/PBS overnight at 4 °C and shock frozen in tissue mounting medium (DiaTec). For immunohistochemistry, frozen sections were washed three times in PB or PBS (F4/80) for 5 min each and blocked at room temperature with 2% BSA in PB for 45 min (F4/80: 1% non-fat dry milk, 0.01% Tween in PB). Primary antibodies (Table 4) were diluted in a 1:10 dilution of blocking solution in PB (F4/80: 2% BSA, 0.02% NaN<sub>3</sub>, 0.01% Triton-X in PBS) and incubated at 4 °C overnight. After three washes in PB/PBS (5 min each), biotinylated antibodies were applied for 1 h, diluted in a 1:10 dilution of the blocking solution, then appropriate secondary antibodies (Table 4), diluted in a 1:10 dilution of the blocking solution, were applied for 1 h. Sections were washed again three times in PB/PBS and nuclei were counterstained with DAPI (Vectashield, Vector Laboratories) diluted 1:10 in fluorescent mounting medium (Serva). Sections were investigated on an Axio Imager Z1 fluorescent microscope (Carl Zeiss, Jena, Germany) and appropriate Axiovision version 4.8 software (Carl Zeiss).

**Table 4. Antibodies used for immunohistochemistry**

Primary antibody	Fixation	Secondary antibody
TβRII- L21 (Santa Cruz) 1:20	4% paraformaldehyde (PFA)	anti-rabbit, biotinylated (Vector) 1:500, Streptavidin Alexa 488 (Invitrogen) 1:1000
Collagen IV (Rockland) 1:100	4% PFA	anti-rabbit Cy <sup>TM</sup> -3 conjugated (Jackson Immuno Research Lab) 1:2000

## Chapter 4

VEGF-a	1:50	(R&D	4% PFA	anti-goat, biotinylated (Vector)	1:500,
systems)				Streptavidin Alexa 546 (Invitrogen)	1:1000
F4/80	(Acris	Antibodies)	4% PFA	anti-rat Cy <sup>TM</sup> -3 conjugated	(Jackson
1:600				Immuno Research Lab)	1:2000 in PBS
PLVAP	(Santa Cruz)	1:50	4%PFA	anti-rat Cy <sup>TM</sup> -3 conjugated	(Jackson
				Immuno Research Lab)	1:2000

### 4.3.7 Dextran Perfusion

Prior to dextran perfusion, mice were deeply anesthetized with ketamine (120 mg/kg body weight) and xylazine (8 mg/kg body weight). Afterwards mice were perfused through the left ventricle with 1 ml of PBS containing 50 mg FITC-dextran (MW = 2000 kDa, TdB Consultancy, Uppsala, Sweden). The eyes were enucleated and fixed in 4% PFA for 2 h (flatmounts)/ 4 h (sections) and washed in PB. Eyes were sectioned, placed on glass slides and counterstained with DAPI (Vectashield, Vector Laboratories) 1:10 diluted in fluorescent mounting medium. For quantification of CNV, retinal/choroidal tissue were dissected and flat mounted on glass slides using fluorescent mounting medium. FITC-dextran perfused sections and flatmounts were investigated on an Axio Imager Z1 fluorescent microscope.

### 4.3.8 Electroretinography (ERG)

Mice were dark adapted for at least 12 hours before the experiments and anesthetized by s.c. injection of ketamine (65 mg/kg) and xylazine (13 mg/kg). Pupils were dilated with tropicamide eye drops (Mydriaticum Stulln; Pharma Stulln GmbH, Stulln, Germany). Silver needle electrodes served as reference (forehead) and ground (tail), and gold wire ring electrodes served as active electrodes. ERGs were recorded with a Ganzfeld bowl (Ganzfeld QC450 SCX) and an amplifier/recording unit (RETI-Port; both Roland Consult, Brandenburg, Germany), band-pass filtered (1 to 300 Hz), and averaged. Single-flash scotopic (dark adapted) responses to a series of 10 LED-flash intensities (range: -3.5 to 1.0 log cd.s/m<sup>2</sup>) were recorded. After 10 minutes of

adaption to a white background illumination ( $20 \text{ cd/m}^2$ ) single flash photopic (light adapted) responses to three Xenon-flash intensities (1, 1.5 and  $2 \log \text{ cds/m}^2$ ) were recorded. All analysis and plotting were performed with R version 3.2.1 (The R Foundation for Statistical Computing, Vienna, Austria) and ggplot2 version 2.1.0 (Wickham 2009).

### 4.3.9 Fundus Imaging and Angiography

Imaging of the retinal vasculature was performed with a commercially available imaging system (Micron III; Phoenix Research Laboratories, Pleasanton, CA). Light source and imaging path filters (low pass and high pass at 500 nm) were used for fluorescein angiography (FLA). Mice were anesthetized by s.c. injection of ketamine (65 mg/kg) and xylazine (13 mg/kg), and their pupils were dilated with tropicamide eye drops before image acquisition. FLA was performed with s.c. injection of 75 mg/kg body weight fluorescein-Na (Alcon, Hünenberg, Switzerland).

### 4.3.10 RNA Analysis

Total RNA from retinae was extracted with TriFast, and first-strand cDNA synthesis was performed with iScript cDNA Synthesis Kit (Bio-Rad Laboratories, Inc., Hercules, CA) according to the manufacturer's guidelines. Quantitative real time RT-PCR analyses were performed with the iQ5 Realtime PCR Detection System (Bio-Rad Laboratories, Inc.). The temperature profile was denaturation at  $95^\circ\text{C}$  for 10 s and annealing and extension at  $60^\circ\text{C}$  for 40 s for 40 cycles. All primer pairs were purchased from Invitrogen and extended over exon-intron boundaries, except for *Gapdh*. Sequences of primer pairs are shown in Table 5. RNA that was not reverse transcribed served as a negative control for real time RT-PCR. Before relative quantification, mRNAs from three different potential housekeeping genes were tested: glyceraldehyde 3-phosphate dehydrogenase (*Gapdh*), guanine nucleotide binding protein (*Gnb2l*) and ribosomal protein L32 (*Rpl32*). We performed statistical analyses to confirm that none of the housekeeper

was regulated and then used the geometric mean of the crossing thresholds of all three housekeepers for relative quantification. Quantification was performed using BioRad iQ5 Standard-Edition (Version 2.1) software (Bio-Rad Laboratories GmbH, Munich, Germany) and the  $\Delta\Delta C_t$  method in Excel (Microsoft Corporation, Redmond, WA, USA) (Livak and Schmittgen 2001).

**Table 5. Primers used for real time PCR amplification**

<b>Gene</b>	<b>Sequence forward</b>	<b>Sequence reverse</b>
<i>GAPDH</i>	5'-TGTCCGTCGTGGATCTGAC-3'	5'-CCTGCTTCACCACCTTCTTG-3'
<i>GNB2L</i>	5'-TCTGCAAGTACACGGTCCAG-3'	5'-ACGATGATAGGGTTGCTGCT-3'
<i>RPL32</i>	5'-GCTGCCATCTGTTTTACGG-3'	5'-TGA CTGGTGCCTGATGAACT-3'
<i>Tgfb<math>\beta</math>2</i>	5'-AGAAGCCGCATGAAGTCTG-3'	5'-GGCAAACCGTCTCCAGAGTA-3'
<i>Ccl2</i>	5'-CATCCACGTGTTGGCTCA-3'	5'-GATCATCTTGCTGGTGAATGAGT-3'
<i>Cd68</i>	5'-CTCTCTAAGGCTACAGGCTGCT-3'	5'-TCACGGTTGCAAGAGAAACA-3'
<i>Gfap</i>	5'-TCGAGATCGCCACCTACAG-3'	5'-GTCTGTACAGGAATGGTGATGC-3'
<i>Il6</i>	5'-GCTACCAAACCTGGATATAATCAGGA-3'	5'-CCAGGTAGCTATGGTACTCCAGAA-3'
<i>iNos</i>	5'-GGGCTGTCACGGAGATCA-3'	5'-CCATGATGGTCACATTCTGC-3'
<i>Tnf-<math>\alpha</math></i>	5'-TCTTCTCATTCCTGCTTGTGG-3'	5'-GGTCTGGGCCATAGAACTGA-3'
<i>Vegf-a-120</i>	5'-AAAGCCAGCACATAGGAGAG-3'	5'-GGCTTGTCACATTTTCTGG-3'
<i>Vegf-a-164</i>	5'-GAACAAAGCCAGAAAATCACTGTG-3'	5'-CGAGTCTGTGTTTTTGCAGGAAC-3'
<i>Fgf2</i>	5'-CGGCTCTACTGCAAGAACG-3'	5'-TGCTTGGAGTTGTAGTTTGACG-3'

### 4.3.11 Deep tissue imaging by 3D light-sheet fluorescence microscopy

Mice were deeply anesthetized with ketamine (120 mg/kg body weight) and xylazine (8 mg/kg body weight) and 130  $\mu$ l of *Tomato lectin* (Perkin Elmer, Inc., Waltham, MA) were injected slowly intravenous. Mice were killed 15 min after injection by cervical dislocation. The eyes were enucleated and fixed using Paxgene Tissue Containers (Qiagen, Hilden, Germany) according to the manufacturer's recommendations and thereafter underwent a chemical procedure of optical clearing as previously described (Erturk et al. 2012). Cleared transparent whole mouse eyes were imaged on a light-sheet fluorescence microscope (UltraMicroscope II, LaVision BioTec, Bielefeld, Germany), equipped with a sCMOS camera (Andor Neo, Concord, USA) and a 2x/0.5 NA objective lens (MVPLAPO 2x, Olympus, Hamburg, Germany). The specimens were two-sided illuminated by a planar light-sheet using a white light laser (SuperK EXTREME EXW-9, NKT Photonics, Birkerød, Denmark). To visualize the specific TLectinSense680 signals for vascularization, a bandpass filter set with an excitation range of 640/30 and emission range of 690/50 was used in combination with an additional filter set (excitation: 531/40; emission: 593/40) for detection of autofluorescence (morphology). By moving the specimen chamber vertically stepwise (step-size = 4 $\mu$ m) through the laser light-sheet, optical sections were obtained. In order to ensure standardized imaging regions for each eye the scan always covered 600  $\mu$ m above to 600  $\mu$ m below the optical nerve. Maximum intensity projections were performed by InspectorPro Software (LaVision BioTec, Bielefeld, Germany).

### 4.3.12 Statistical Analysis

All results are expressed as means  $\pm$  SEM. Comparisons between the mean variables of two groups were made by a two-tailed Student's *t*-test. Significance of the ERG analyses was evaluated using a one-way ANOVA test, followed by Tukey HSD post hoc test  $P \leq 0.05$  was considered to be statistically significant.

## 4.4 Results

### 4.4.1 Deletion of ocular TGF- $\beta$ signaling in mouse pups leads to choroidal neovascularization

To investigate the role of the TGF- $\beta$  signaling pathway for the structure of retinal and choroidal vessels, we deleted the essential T $\beta$ RII receptor in the eyes via tamoxifen-induced conditional deletion. To this end, *Tgfb $\beta$ 2<sup>fl/fl</sup>;CAGG Cre-ER<sup>TM</sup>* mice were generated and treated from postnatal day (P) 4 to P8 with tamoxifen eye drops. For simplicity we will refer to *Tgfb $\beta$ 2<sup>fl/fl</sup>;CAGG Cre-ER<sup>TM</sup>* mice that received tamoxifen by this protocol as early-induced *Tgfb $\beta$ 2 <sup>$\Delta$ eye</sup>* mice and littermates with two unrecombined *Tgfb $\beta$ 2<sup>fl/fl</sup>* alleles are referred to as controls. As shown previously, the treatment results in a significant reduction of T $\beta$ RII and its mRNA in the eyes of early-induced *Tgfb $\beta$ 2 <sup>$\Delta$ eye</sup>* mice compared to controls (Braunger et al. 2015). We also observed in the previous study that the deletion of ocular TGF- $\beta$  signaling leads to the formation of abundant microaneurysms in retinal vessels and to a phenotype that largely mimics that of nonproliferative and proliferative diabetic retinopathy in humans (Braunger et al. 2015). Consequently we observed in the retina of two and three month old early-induced *Tgfb $\beta$ 2 <sup>$\Delta$ eye</sup>* mice vascular microaneurysms in the inner nuclear layer, which were characterized by thick layers of perivascular cells (Fig. 19A, B, C) (Braunger et al. 2015). In contrast, no changes were seen in control mice (Fig. 19A and B). We now turned our attention to the choroidal/retinal interface that we had not analyzed previously. Here we frequently observed focal areas in which the outer segments of photoreceptors were completely missing and the thickness of the outer nuclear layer was substantially reduced (Fig. 19B and C). Accumulations of cells were present between photoreceptors and RPE. The cells frequently surrounded vascular openings filled with erythrocytes strongly indicating their endothelial origin and an ongoing neoangiogenetic process. The RPE was multilayered in those areas, and contained cystic and amorphous inclusions (Fig. 19C).

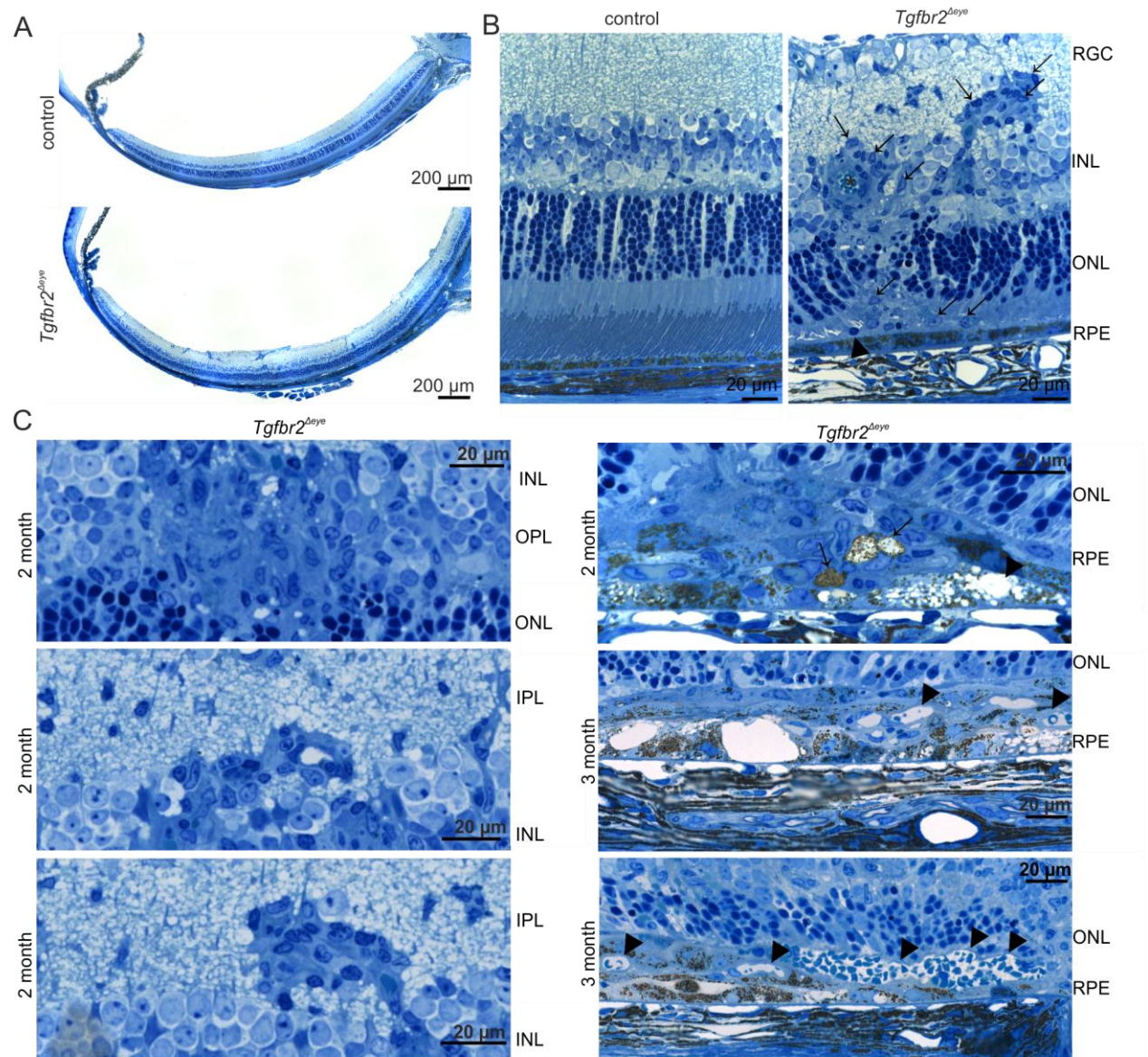


**Figure 19. Early-induced deletion of TGF- $\beta$  signaling in the eye causes structural changes in the subretinal space.** Richardson's stained semi-thin sections (1  $\mu\text{m}$  thick) of an early-induced *Tgfb2<sup>Δeye</sup>* mouse and its control littermate. **A.** Retinal hemispheres of two-month-old control and *Tgfb2<sup>Δeye</sup>* animals. **B.** Detailed magnification of the retina. The control mouse shows regular structure. In the retina of the *Tgfb2<sup>Δeye</sup>* mouse a vessel (asterisk) filled with erythrocytes is seen, which disrupts the inner (INL) and outer nuclear layer (ONL) and is surrounded by an accumulation of cells that continue into the subretinal space (arrows). In the subretinal space mononuclear cells (arrowhead) are present while photoreceptor outer segments are degenerated and the choroid is thickened. **C.** Left-handed panel. In the inner retina of two-month-old *Tgfb2<sup>Δeye</sup>* mice accumulations of endothelial cells are seen in both the outer nuclear/plexiform layer (ONL/OPL) and in the inner nuclear/plexiform layer (INL/IPL). Right-handed panel. At the retinal/choroidal interface of two- and three-month-old *Tgfb2<sup>Δeye</sup>* mice the RPE is multilayered (black arrows in upper panel) and contains cystic and amorphous inclusions (upper panel, black

arrowhead). At the age of three months erythrocyte-containing vessels fill the subretinal space (middle and lower panel, black arrowheads). IPL, inner plexiform layer; OS, outer segments; IS, inner segments; INL, inner nuclear layer; RPE, retinal pigment epithelium. Experiments performed by Sarah V. Leimbeck and Barbara M. Braunger.

To characterize the origin of the newly formed vessels in the subretinal space (between the sensory retina and the RPE) of early-induced *Tgfb $\beta$ 2* <sup>$\Delta$ eye</sup> mice, we now perfused the mice with high molecular weight FITC-dextran for vascular labeling. While the retinal and choroidal vasculature of control animals was essentially normal, distinct changes were observed in the subretinal space of early-induced *Tgfb $\beta$ 2* <sup>$\Delta$ eye</sup> mice. Here we observed vessels breaking from the choroid through Bruch's membrane (BM) across the RPE into the subretinal space (Figure 20A). We quantified the number of CNV using FITC dextrane perfused wholemounts of the retina and choroid of four to six week old animals and observed  $2.86 \pm 0.59$  CNV per wholemount ( $n = 7$ ). To confirm this observation by an independent method, we next performed 3D imaging of lectin perfused, optical cleared whole eyes (Figure 20B). The choriocapillaris did not resolve into single capillaries but rather appeared as an intense fluorescent line covering the outer surface of the retina, a fact that we attributed to the immense density and blood flow of this capillary bed (Kaufman et al. 2003). In control eyes, the three plexus of the retinal vasculature could be completely visualized and were essentially normal. In contrast, in early-induced *Tgfb $\beta$ 2* <sup>$\Delta$ eye</sup> mice, vessels that originated from the choriocapillaris entered the retina and continued into the retinal vascular bed forming obvious anastomoses with retinal vessels (Figure 20B). We now characterized the vascular wall of the newly formed vessels by transmission electron microscopy. As expected, in control mice the endothelium surrounding retinal vessels was continuous (Figure 20C) while that around the choriocapillaris was fenestrated. When we analyzed the newly formed vessels in the subretinal space of early-induced *Tgfb $\beta$ 2* <sup>$\Delta$ eye</sup> mice, distinct fenestrations covered by a typical diaphragm were regularly observed (Figure 20C). To further support this finding, we performed immunohistochemical staining for plasmalemma

vesicle-associated protein (PLVAP), a vascular protein, intrinsic component of the diaphragm of vascular fenestrae, and marker for fenestrated endothelia (Stan et al. 2001, Stan et al. 1999, Stan et al. 2012, Herrnberger et al. 2012). As expected, in control and early-induced *Tgfb $\beta$ 2* <sup>$\Delta$ eye</sup> animals the continuous endothelium of the retinal vasculature did not show any PLVAP immunoreactivity while the fenestrated endothelium of the choriocapillaris showed an intense PLVAP signal (Figure 20D). Furthermore, in early-induced *Tgfb $\beta$ 2* <sup>$\Delta$ eye</sup> mice, intense PLVAP immunoreactivity was observed in the areas of neovascularization in the subretinal space (Figure 20D). Overall our results strongly indicated that loss of TGF- $\beta$  signaling in early-induced *Tgfb $\beta$ 2* <sup>$\Delta$ eye</sup> mice caused choroidal neovascularization (CNV).

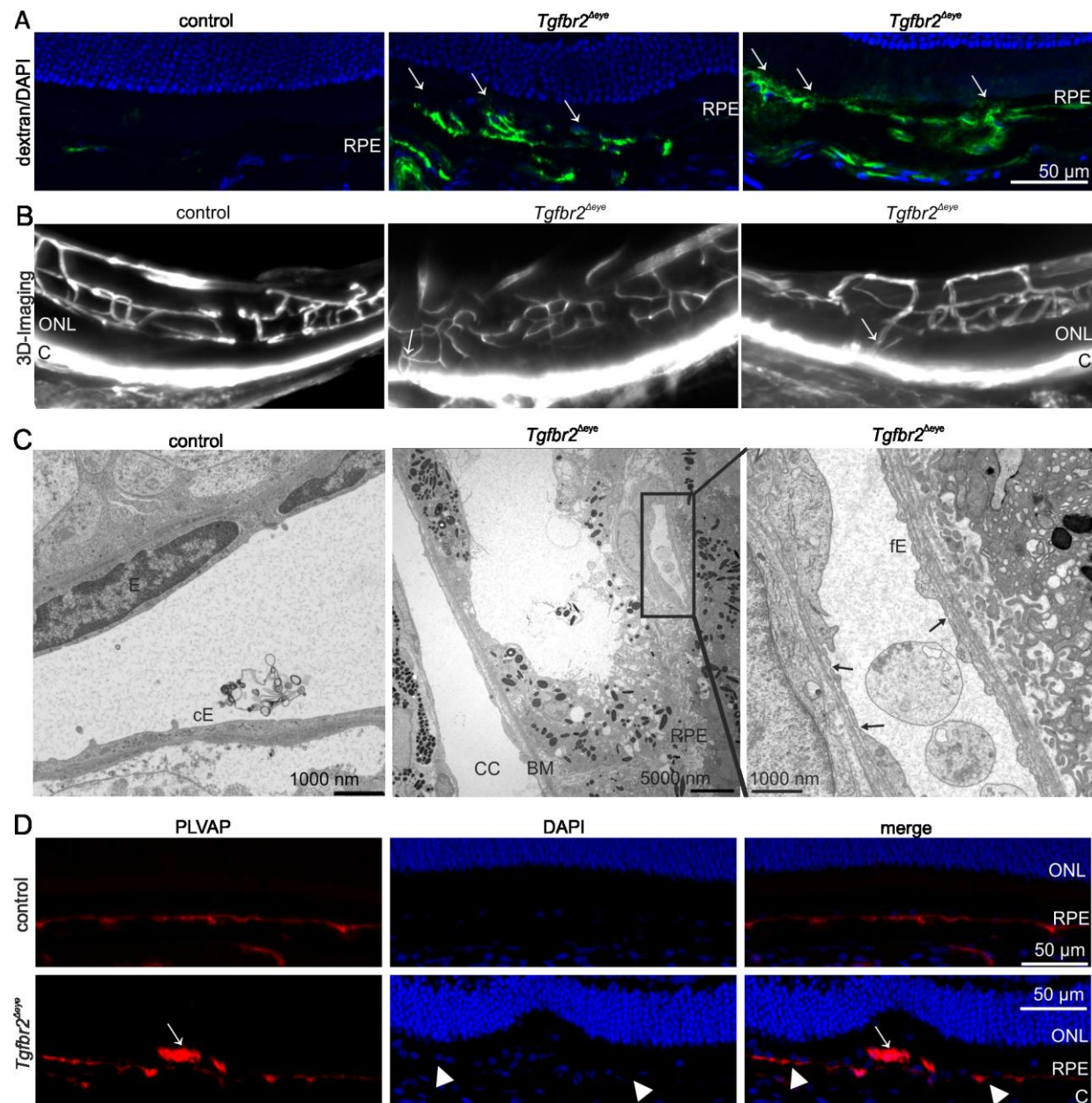


**Figure 20. Subretinal neovascularization with fenestrated endothelium following deletion of TGF- $\beta$  signaling in the eyes of early-induced *Tgfr2<sup>Δeye</sup>* mice.** **A.** FITC-dextran (green)-perfused retinal meridional section of a control and *Tgfr2<sup>Δeye</sup>* mouse at 6 weeks of age. White arrows point towards choroidal vessels breaking through Bruch's membrane and RPE into the subretinal space. Nuclei are DAPI-stained (blue). **B.** Light-sheet fluorescence microscopy of transparent eyes of six-week-old lectin-injected *Tgfr2<sup>Δeye</sup>* mice and a control littermate. The control mouse shows an essentially regular arborized retinal vasculature. The *Tgfr2<sup>Δeye</sup>* mice have an irregular arrangement of the retinal plexus and form anastomoses between retinal and choroidal vessels (arrows). **C.** Transmission electron microscopy of an intraretinal vessel outlined with a continuous endothelium (cE) in a 2.5-month-old control animal. In contrast, the subretinal neovasculation in the *Tgfr2<sup>Δeye</sup>* littermate has a fenestrated endothelium (fE,

black arrows). **D.** Immunoreactivity for PLVAP (red) in the retina at 4 weeks of age. The control and the *Tgfb $\beta$ 2* <sup>$\Delta$ eye</sup> animal show a thin, one-layered PLVAP signal in the choriocapillaris (white arrowheads). In addition, the *Tgfb $\beta$ 2* <sup>$\Delta$ eye</sup> mouse displays PLVAP-positive signals (white arrows) in RPE and subretinal space. Nuclei are DAPI-stained (blue). RGC, retinal ganglion cells; INL, inner nuclear layer; ONL, outer nuclear layer; RPE, retinal pigment epithelium; C, choroid; BM, Bruch's membrane; RPE retinal pigment epithelium; fE, fenestrated endothelium; cE, continuous endothelium; E, endothelium; CC, choriocapillaris. Experiments performed by (A) Sarah V. Leimbeck; (B) Anja Schlecht and Annette Feuchtinger; (C,D) Sarah V. Leimbeck.

### 4.4.2 TGF- $\beta$ signaling is required to prevent choroidal neovascularization in late-induced *Tgfb $\beta$ 2* <sup>$\Delta$ eye</sup> mice

Next we wondered whether the formation of CNV after T $\beta$ RII deletion might be supported by the fact that retinal vascular development is not completed in mouse pups and signaling processes are continuously ongoing that promote angiogenesis. To learn if TGF $\beta$ -signaling is also important for maintenance of the adult choriocapillaris when retinal vascular development is completed, we deleted TGF $\beta$ -signaling by an essentially comparable approach in three week old mice after the retinal vasculature had been developed. Mice were treated with tamoxifen eye drops from P21 – P25 and are further referred to as late-induced *Tgfb $\beta$ 2* <sup>$\Delta$ eye</sup> mice. The significant deletion of retinal *Tgfb $\beta$ 2* was confirmed by real time RT-PCR analyses (supplementary data Figure 29A). Next, we analyzed the ocular morphology of late-induced *Tgfb $\beta$ 2* <sup>$\Delta$ eye</sup> mice and controls at the age of three (Figure 21A and B) and six months (Figure 22A and B). Retinal structure was essentially normal in control animals (Figure 21A, B and Figure 22A, B) and no obvious changes were observed in the inner retina of three month old late-induced *Tgfb $\beta$ 2* <sup>$\Delta$ eye</sup> animals (Figure 21B). However, similar to our observations in early-induced *Tgfb $\beta$ 2* <sup>$\Delta$ eye</sup> animals, all of the late-induced *Tgfb $\beta$ 2* <sup>$\Delta$ eye</sup> mice showed structural changes in the subretinal space that were essentially comparable to that observed in early-induced *Tgfb $\beta$ 2* <sup>$\Delta$ eye</sup> mice (Figure 21A, E and Figure 22A, B and D).

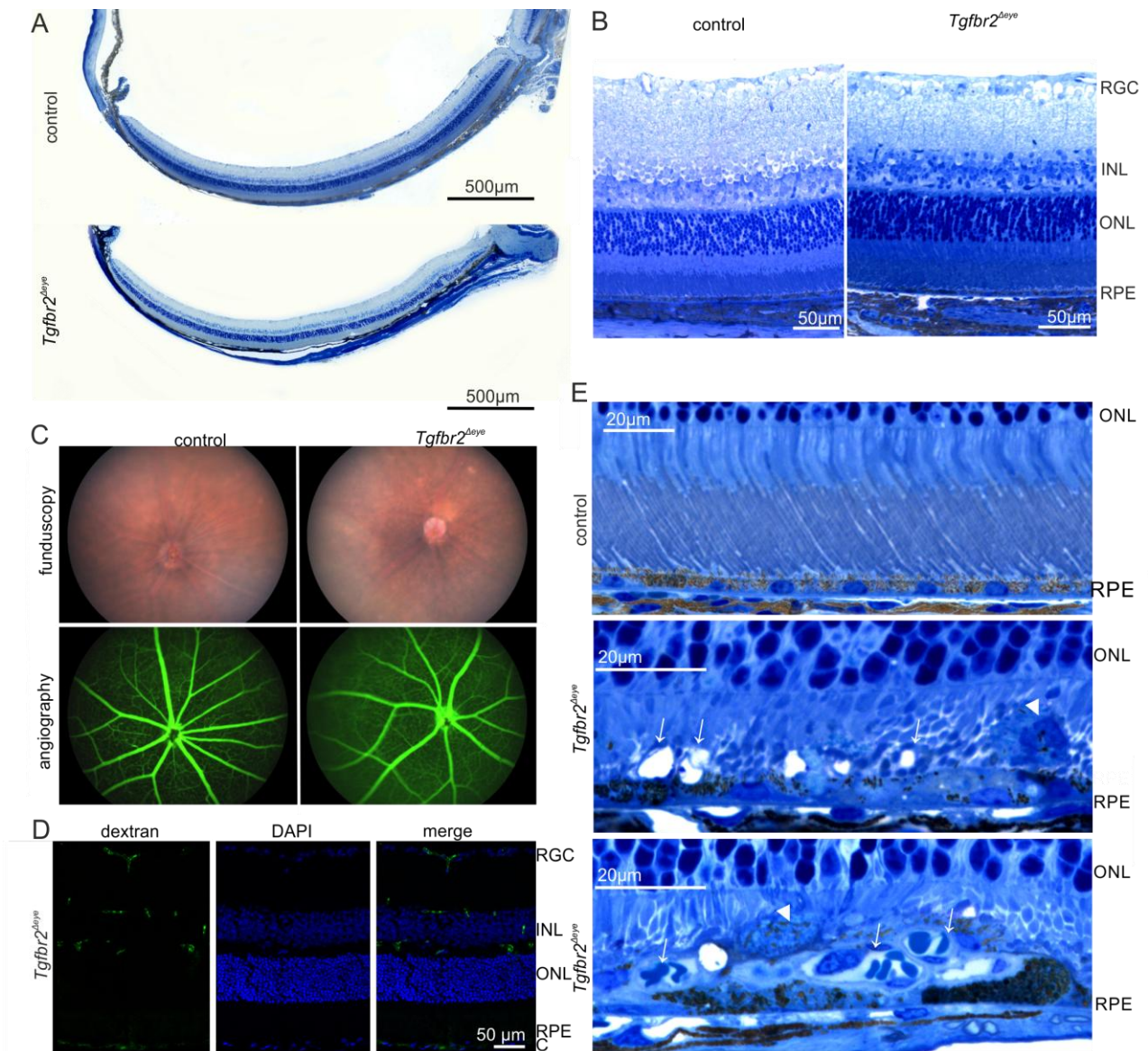


**Figure 21. Subretinal neovascularization following deletion of TGF- $\beta$  signaling in the eyes of three month old late-induced *Tgfb2<sup>Δeye</sup>* mice.** **A.** Richardson's stained semi-thin sections (1  $\mu$ m thick) of the retinal hemispheres of a three-month-old, late-induced *Tgfb2<sup>Δeye</sup>* mouse and its control littermate. **B.** Higher magnification of the retinal sections. **C.** *In vivo* funduscopy and fluorescein angiography of a three-month-old, late-induced *Tgfb2<sup>Δeye</sup>* mouse and its control littermate. The retinal vasculature and the fundus appear essentially normal. **D.** FITC-dextran (green) perfused retinal meridional section of a 2-month-old *Tgfb2<sup>Δeye</sup>* mouse. The three retinal vascular plexus are present in their correct localization. Nuclei are DAPI-stained (blue). **E.** Detailed magnification of Richardson's stained semithin sections of the retinal/choroidal interface in three-month-old *Tgfb2<sup>Δeye</sup>* mice and a control littermate. The control mouse does not show abnormalities (upper panel). In focal areas of *Tgfb2<sup>Δeye</sup>* mice, in which photoreceptor outer segments are shortened or completely missing, vessels are observed in the subretinal space. The RPE in those areas is multilayered (white arrowheads, lower panel) and frequently contains cystic and amorphous

inclusions (white arrow, middle panel). Mononuclear cells (arrowhead, middle panel) are visible in the subretinal space. INL, inner nuclear layer; ONL, outer nuclear layer; RPE, retinal pigment epithelium; C, choroid. Experiments performed by (A,B,D) Anja Schlecht and Sarah V. Leimbeck; (C) Anja Schlecht and Herbert Jägle.

In focal areas in which photoreceptor outer segments were shortened or completely missing, vessels were observed in the subretinal space. The RPE in those areas was multilayered and frequently contained cystic and amorphous inclusions. In six month old late-induced *Tgfb $\beta$ 2* <sup>$\Delta$ eye</sup> mice, the choroid was thickened and photoreceptor outer segments completely missing (Figure 22A, B and D). The RPE was reduced to a flat layer or formed focal accumulations in those areas in which subretinal vessels were present. *In vivo* imaging and fluorescein *in vivo* angiography of three-month-old animals showed a regular fundus and retinal vasculature in both control and late-induced *Tgfb $\beta$ 2* <sup>$\Delta$ eye</sup> mice (Figure 21C). To investigate the retinal vasculature in more detail, we additionally perfused two-month-old, late-induced *Tgfb $\beta$ 2* <sup>$\Delta$ eye</sup> mice with high molecular weight FITC-dextran and analyzed the vasculature on meridional sections. The retinal vasculature had a regular appearance and the vessels were in their anatomically correct localization. Furthermore, we did not observe FITC-dextran or fluorescein leaking into the vitreous, the subretinal space or the surrounding tissue (Figure 21C and D). When we analyzed the eyes at the age of six months by *in vivo* fundus imaging and fluorescein angiography, control mice showed again no pathological changes, neither in the fundus, nor in the retinal vasculature (Figure 22C). In contrast, in late-induced *Tgfb $\beta$ 2* <sup>$\Delta$ eye</sup> mice the fundus was hyperpigmented indicating RPE proliferation or dedifferentiation, and in some animals the retina had detached (Figure 22C). In parallel with the observed structural changes we detected marked functional changes by ERG that reflected the observed gradual degeneration of the retina in three month old to the six month old late-induced *Tgfb $\beta$ 2* <sup>$\Delta$ eye</sup> mice (Figure 23A-G). While in three month old *Tgfb $\beta$ 2* <sup>$\Delta$ eye</sup> mice the scotopic responses showed similar waveform but slightly lower amplitudes compared to control mice, the photopic waveform was unchanged in amplitude and implicit time.

However, the difference was not statistically significant. In six month old *Tgfb $\beta$ 2* <sup>$\Delta$ eye</sup> mice both, the scotopic and photopic response could not be distinguished from noise in almost all eyes.

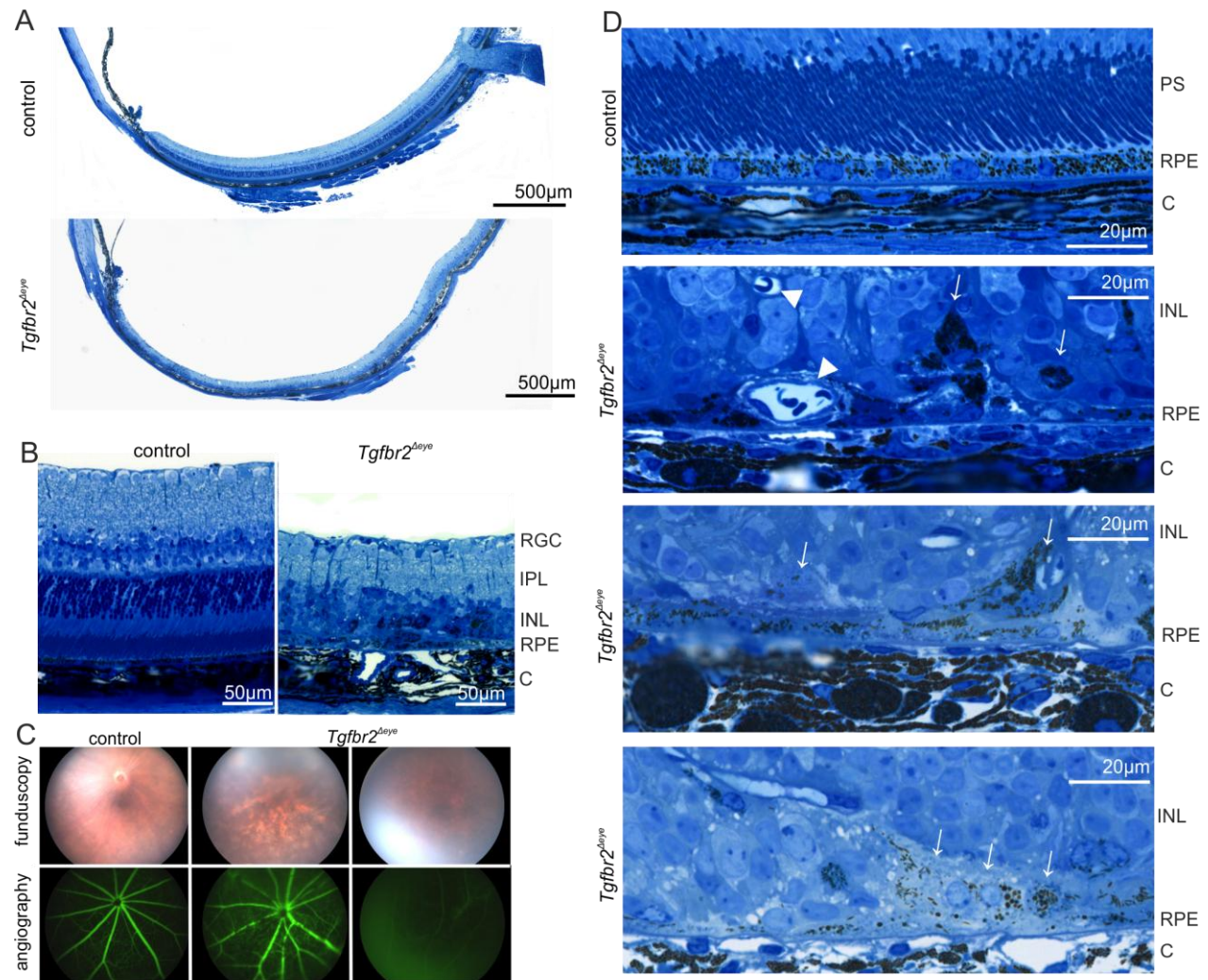


**Figure 22. Subretinal neovascularization and retinal degeneration following deletion of TGF- $\beta$  signaling in the eyes of six month old late-induced *Tgfb $\beta$ 2* <sup>$\Delta$ eye</sup> mice.** **A.** Richardson's stained semithin sections (1 $\mu$ m) of the retinal hemispheres of six-month-old animals. The control animal shows regular retinal morphology. In contrast, in the *Tgfb $\beta$ 2* <sup>$\Delta$ eye</sup> littermate photoreceptor outer segments are completely degenerated. **B.** Detailed magnification of the retina. In the *Tgfb $\beta$ 2* <sup>$\Delta$ eye</sup> mouse the retina is degenerated with a complete loss of photoreceptors. The RPE is disorganized, pigmented cells accumulate in the retina and the choroid is thickened. **C.** *In vivo* funduscopy and fluorescein angiography of the control animal are normal. *Tgfb $\beta$ 2* <sup>$\Delta$ eye</sup> mice show a hyperpigmented fundus (middle panel) or retinal detachment (right-hand panel). **D.** Detailed magnification of Richardson's stained semithin sections of the outer retina and the choroid of six-month-old *Tgfb $\beta$ 2* <sup>$\Delta$ eye</sup> mice and a control littermate. The morphology of the control mouse is normal. In contrast, the *Tgfb $\beta$ 2* <sup>$\Delta$ eye</sup> mouse has erythrocyte-filled vessels at the inner side of the RPE

(upper *Tgfb $\beta$ 2* <sup>$\Delta$ eye</sup> panel, arrowheads), thickened (middle *Tgfb $\beta$ 2* <sup>$\Delta$ eye</sup> panel) or thinned (lower *Tgfb $\beta$ 2* <sup>$\Delta$ eye</sup> panel) RPE and an accumulation of pigmented cells in the sensory retina (upper, middle and lower *Tgfb $\beta$ 2* <sup>$\Delta$ eye</sup> panel, arrows). RGC, retinal ganglion cells; INL, inner nuclear layer; IPL, inner plexiform layer; PS, photoreceptor segments; RPE, retinal pigment epithelium. C, choroid. Experiments performed by (A,B,D) Anja Schlecht; (C) Anja Schlecht and Herbert Jägle.

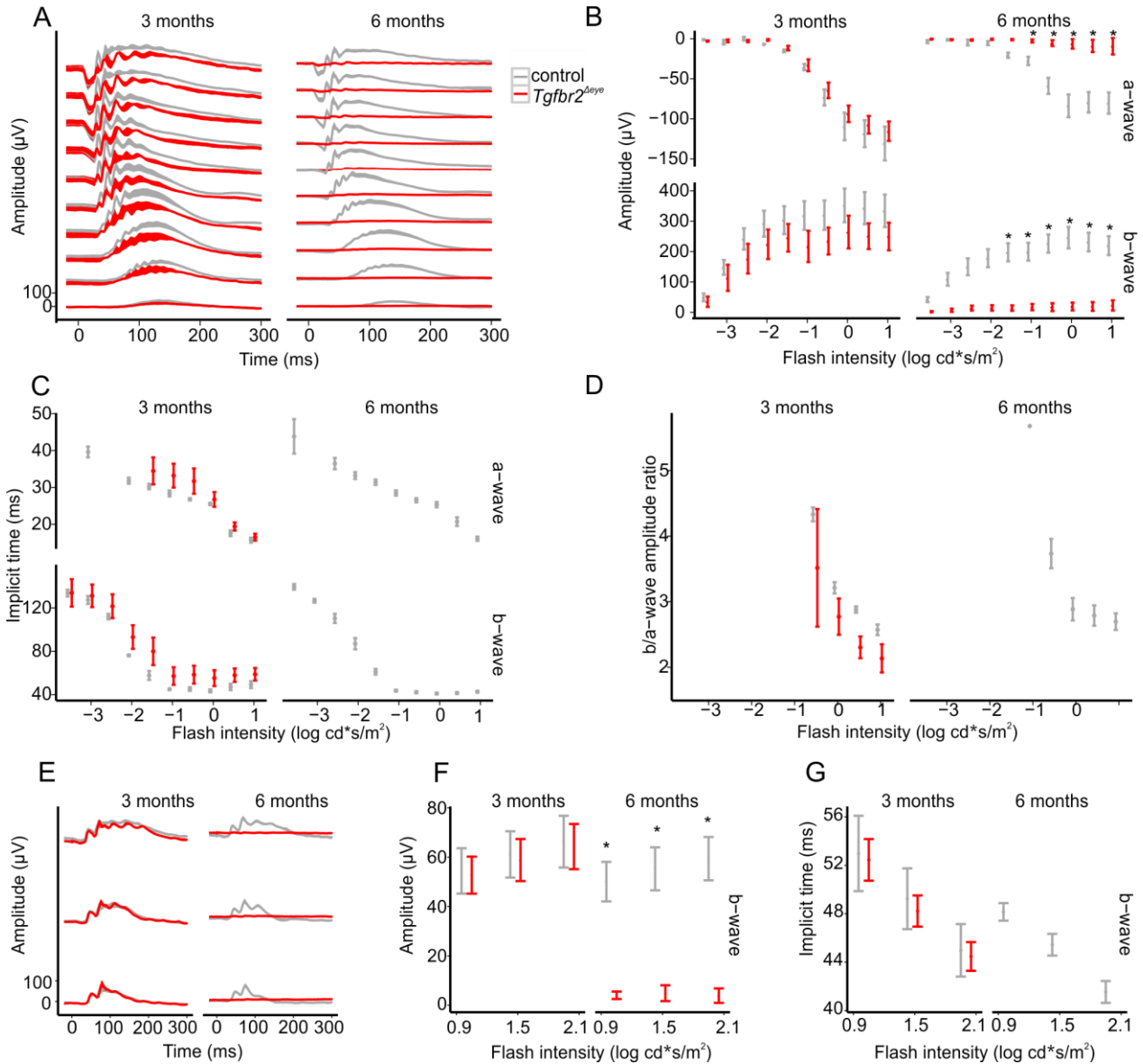


**Figure 23. Functional changes following deletion of TGF- $\beta$  signaling in the eyes of three- and six-month-old late-induced *Tgfb $\beta$ 2* <sup>$\Delta$ eye</sup> mice.** A. Dark adapted scotopic ERGs of three-month-old late-induced *Tgfb $\beta$ 2* <sup>$\Delta$ eye</sup> mice and controls show similar waveforms. The waveforms of six-month-old *Tgfb $\beta$ 2* <sup>$\Delta$ eye</sup> mice are not distinguishable from noise in almost all eyes. Compared to controls, the a- and b-wave

amplitudes of scotopic responses are reduced **B.** and implicit times are prolonged **C.** in three-month-old or at noise level in six-month-old late-induced  $Tgfb\beta 2^{\Delta eye}$  mice. **D.** In addition, a lower (three-month-old) or reduced (six-month-old) b/a-wave amplitude ratio points towards an initially predominant inner retinal function loss. **E.** Photopic ERGs show similar waveforms for three-month-old  $Tgfb\beta 2^{\Delta eye}$  mice and controls, but again in six-month-old  $Tgfb\beta 2^{\Delta eye}$  mice responses are at noise level. The b-wave amplitudes **F.** or implicit times **G.** are comparable for the three-month-old animals. Three-month-old mice: Control, n = 4,  $Tgfb\beta 2^{\Delta eye}$ , n = 4. Six-month-old mice: Control, n = 5,  $Tgfb\beta 2^{\Delta eye}$ , n = 5, \* $P \leq 0.05$ , one way ANOVA. Experiments performed by Anja Schlecht and Herbert Jägle.

### 4.4.3 Expression of angiogenic factors and immune modulating cytokines in $Tgfb\beta 2^{\Delta eye}$ mice

The “immunovascular axis”, a crosstalk of the RPE with immune and vascular cells is considered a potent driver of CNV formation (Ambati and Fowler 2012). To clarify the mechanisms behind CNV induced by  $T\beta RII$  deletion we consequently analyzed the mRNA expression levels of immune modulating cytokines and markers for the reactivity of Müller glia and microglia cells, respectively. Early-induced  $Tgfb\beta 2^{\Delta eye}$  mice showed a significant increase in retinal mRNA expression levels of *glial fibrillary acidic protein (Gfap)*, *cluster of differentiation (Cd) 68*, *inducible nitric oxide synthase (iNos)*, *interleukin (Il) -6*, *tumor necrosis factor (Tnf) - $\alpha$*  and *monocyte chemoattractant protein-1 (MCP-1/Ccl2)* at the age of six weeks compared to control littermates (Figure 24A). However, in three-month-old late-induced  $Tgfb\beta 2^{\Delta eye}$  mice, the retinal mRNA expression levels were not significantly enhanced compared to controls; in fact *Gfap* was even significantly downregulated (Figure 24B). Next, we used an antibody against F4/80 to label macrophages and microglia cells (Hume et al. 1984, Hume et al. 1983, Langmann 2007). The number of F4/80 positive cells was increased in the choroid of early-induced  $Tgfb\beta 2^{\Delta eye}$  animals when compared with controls (Figure 24C). Furthermore, in early-induced  $Tgfb\beta 2^{\Delta eye}$  animals, numerous F4/80 positive cells were seen in the subretinal space in close association with the CNV (Figure 24C). Quite similarly three-month-old late-induced  $Tgfb\beta 2^{\Delta eye}$  animals also presented a distinct accumulation of F4/80 positive cells in the choroid when compared to controls (Figure 24D). Subsequently, we focused on molecular factors that

influence vascular proliferation. In our previously published study, we already showed that early-induced four-week-old *Tgfb $\beta$ 2* <sup>$\Delta$ eye</sup> mice had significantly elevated mRNA expression levels for the angiogenic factors *Vegf-a 120*, *Vegf-a 164*, *fibroblast growth factor (Fgf) -2*, *insulin growth factor (Igf)-1*, *angiopoetin 2* and *platelet derived growth factor (Pdgf)-b* compared to control littermates (Braunger et al. 2015). We now performed immunohistochemistry for VEGF-A to localize the increased levels in the retina of early-induced *Tgfb $\beta$ 2* <sup>$\Delta$ eye</sup> mice (Figure 24E). While VEGF-A immunoreactivity was not detectable in control eyes, there was distinct and intense staining of the ganglion cell layer of early-induced *Tgfb $\beta$ 2* <sup>$\Delta$ eye</sup> mice. When we screened the retinæ of late-induced *Tgfb $\beta$ 2* <sup>$\Delta$ eye</sup> mice and their control littermates for the expression levels of the *Vegf-a* isoforms 120 and 164, the expression of *Vegf-a 120* was not altered whereas expression of *Vegf-a 164* was significantly reduced in five-week-old late-induced *Tgfb $\beta$ 2* <sup>$\Delta$ eye</sup> mice compared to controls (Figure 24F). However, at the age of six months, the retinal expression levels of both *Vegf-a 120* and 164 were significantly higher in late-induced *Tgfb $\beta$ 2* <sup>$\Delta$ eye</sup> mice compared to controls. Overall, angiogenic and immune reactivities were much higher in early than in late-induced *Tgfb $\beta$ 2* <sup>$\Delta$ eye</sup> mice.

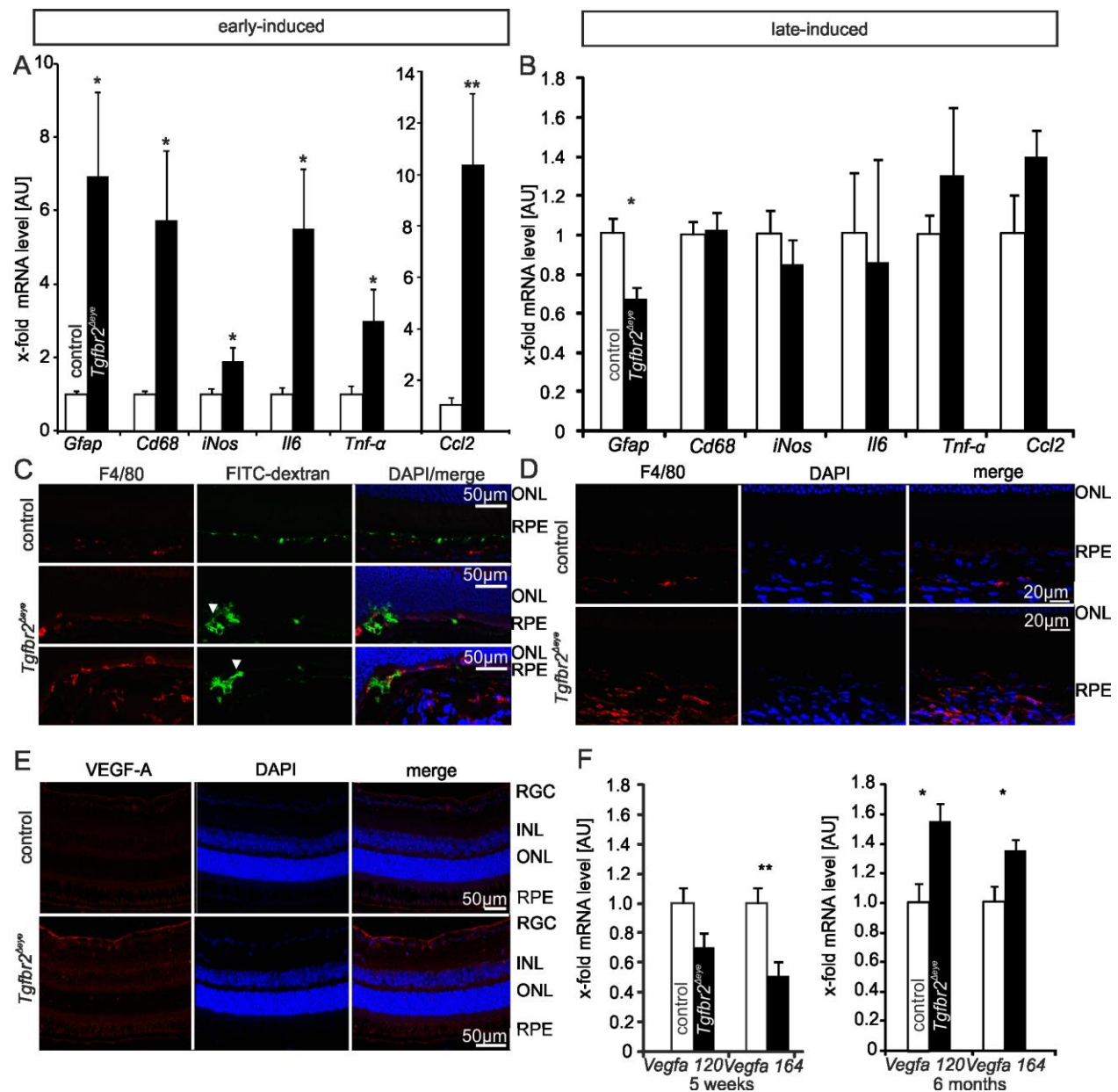


**Figure 24. Early- and late-induced inhibition of TGF- $\beta$  signaling in the eye: the expression of angiogenic factors and immune modulating cytokines.** **A/B.** Real-time RT-PCR for mRNA of *Gfap*, *CD68*, *iNOS*, *Ccl2*, *IL6*, *Tnf- $\alpha$*  in six week old early-induced *Tgfb2<sup>Δeye</sup>* mice and controls (**A.**) and five week old late-induced *Tgfb2<sup>Δeye</sup>* mice (**B.**) and controls. **C.** FITC-dextran (green) perfused and F4/80 (red) immunostained sections of a six week old early-induced *Tgfb2<sup>Δeye</sup>* mouse and control. The control mouse shows a weak immunoreactivity for F4/80 (red) positive cells in the choroid. In *Tgfb2<sup>Δeye</sup>* mice, the choroidal immunoreactivity for F4/80 (red) is more pronounced and F4/80 positive cells accumulate in the subretinal space and in close association to choroidal vessels penetrating the RPE (arrowhead). Nuclei are DAPI-stained (blue). **D.** F4/80 (red) immunostained sections of a three month old, late-induced *Tgfb2<sup>Δeye</sup>* mouse and control. A weak signal for F4/80 is visible in the choroid of the control mouse. In

contrast, the *Tgfb $\beta$ 2* <sup>$\Delta$ eye</sup> mouse shows numerous F4/80 positive cells in the choroid. Nuclei are DAPI-stained (blue). **E.** Immunoreactivity for VEGF-A (red) in early-induced four week old mice. The control mouse has a faint immunoreactivity for VEGF-A. In contrast, in the *Tgfb $\beta$ 2* <sup>$\Delta$ eye</sup> mouse it is markedly increased. Nuclei are DAPI-stained (blue). **F.** Real-time RT-PCR for mRNA of *Vegf-a 120*, *Vegf-a 164* in five week (left panel) and six month old mice (right panel). Data are expressed as mean  $\pm$  SEM. Early-induced mice: Control: n  $\geq$  7, *Tgfb $\beta$ 2* <sup>$\Delta$ eye</sup>: n  $\geq$  7. Late-induced mice (5 weeks old): Control: n  $\geq$  6, *Tgfb $\beta$ 2* <sup>$\Delta$ eye</sup>: n  $\geq$  2. Late-induced mice (six months old): Control: n = 9, *Tgfb $\beta$ 2* <sup>$\Delta$ eye</sup>: n = 7. \* $P \leq 0.05$ , \*\* $P \leq 0.01$ . Experiments performed by (A) Barbara M. Braunger; (B,D,E,F) Anja Schlecht; (C) Anja Schlecht and Barbara M. Braunger.

### 4.4.4 Formation of basal lamina deposits in *Tgfb $\beta$ 2* <sup>$\Delta$ eye</sup> mice

Since CNVs need to find their way across Bruch's membrane (BM) and through the RPE barrier, we used TEM to analyze the structure of both. Control mice showed the regular, five-layered architecture of the BM (Figure 25A and D). In early- and late-induced *Tgfb $\beta$ 2* <sup>$\Delta$ eye</sup> mice though the BM had thickened as result of an accumulation of collagen fibers and fine fibrillar extracellular material between the basal lamina of the choriocapillaris and the elastic layer of BM (Figure 25A-E). Moreover, in some areas, the RPE basal lamina had been replaced by polymorphous electron dense material that was localized between the elastic layer of BM and the RPE basal infoldings (Figure 25A). In other areas of the same eye, irregular nodules arising from the RPE basal lamina and with comparable electron density were found between the basal infoldings of the RPE (Figure 25B-C). In addition, the basal lamina was frequently found to be interrupted where nodules arised (Figure 25B, C, D). Nodules and RPE basal lamina interruptions were found very frequent in early-induced mice and more rarely in late-induced mice. The changes were essentially similar in structure to basal lamina deposits typically found in CNV in humans patients with AMD. Additionally, we found interruptions of the RPE basal lamina with an associated accumulation of electron-dense material in the adjacent RPE infoldings(Figure 25B and C). Next, we labeled the basal laminae of RPE and choriocapillaris by collagen type IV immunohistochemistry. In control mice, the basal laminae of both RPE and choriocapillaris

endothelium were continuously labeled (Figure 25F, G). In early-induced *Tgfbr2* <sup>$\Delta$ eye</sup> mice continuous staining was only seen in the basal lamina of the choriocapillaris. Staining was irregular and patchy though in region of the RPE (Figure 25F). In late-induced *Tgfbr2* <sup>$\Delta$ eye</sup> mice continuous labeling was seen in the basal lamina surrounding choriocapillaris vessels, but was incomplete underneath the RP (Figure 25G). In places, the vascular basal lamina reached between RPE cells indicating areas of CNV formation.

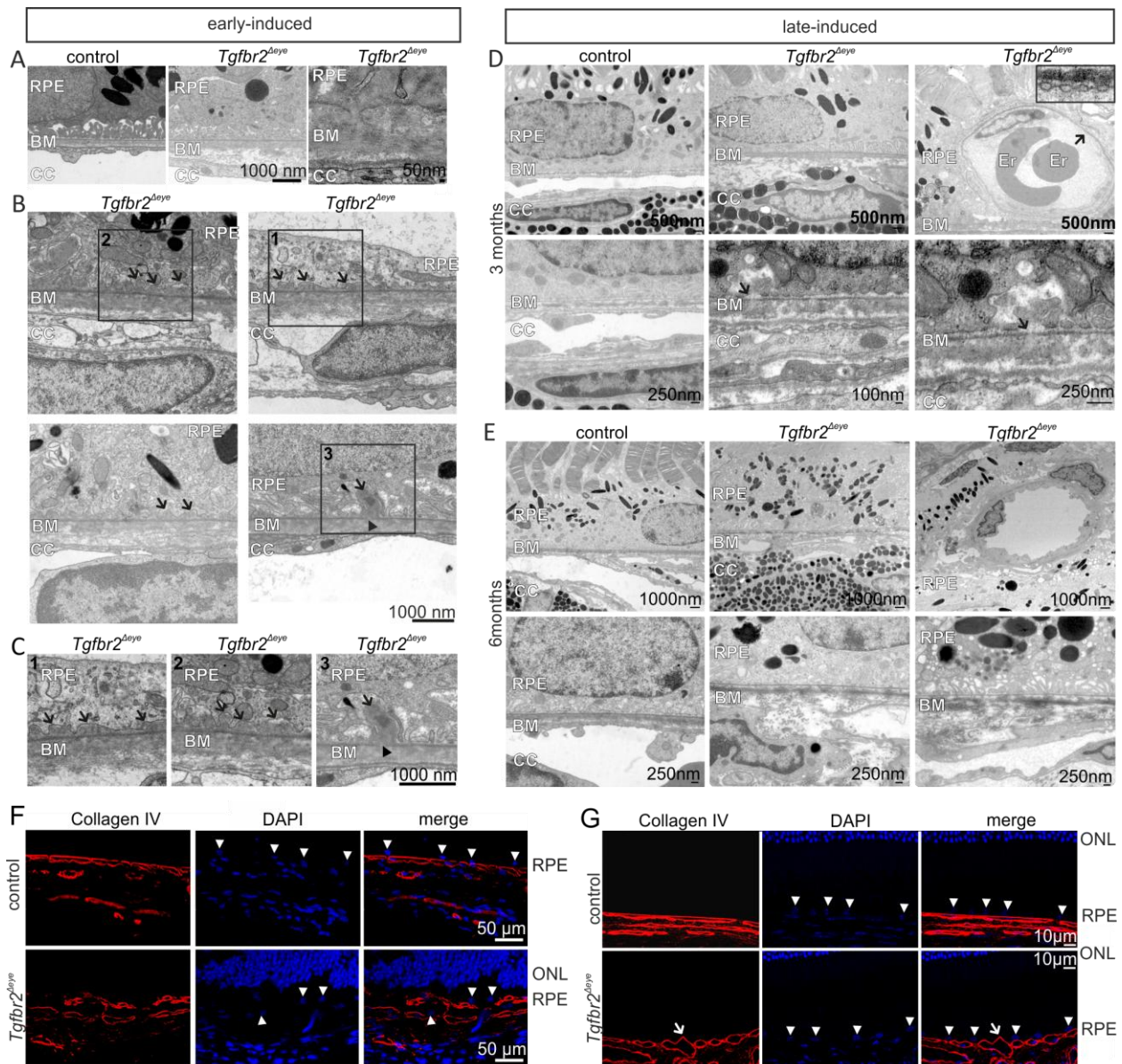


**Figure 25. Structural changes of the Bruch's membrane (BM) in early and late-induced *Tgfb2*<sup>Δeye</sup> mice.** **A.** Transmission electron microscopy (TEM) of RPE/BM in early-induced 2.5-month-old mice. The BM of the control is of regular structure, but thickened in *Tgfb2*<sup>Δeye</sup> mice as result of an accumulation of collagen fibers and fine fibrillar extracellular material between the basal lamina of the choriocapillaris and the elastic layer of BM. In some areas (right-handed panel) the RPE basal lamina is replaced by polymorphous electron dense material that reaches from the elastic layer of BM to the RPE basal infoldings. **B.** In other RPE/BM areas of early-induced *Tgfb2*<sup>Δeye</sup> mice irregular nodules arise from the RPE basal lamina (arrows) and extend between the basal infoldings of the RPE. In places (arrowhead in box 3) the RPE basal lamina is interrupted where nodules arise. **C.** Higher magnification of boxed areas (1, 2, 3) in B. **D.** TEM of RPE/BM in three-month-old late-induced *Tgfb2*<sup>Δeye</sup> mice. RPE/BM are of regular structure in control mice, but thickened in *Tgfb2*<sup>Δeye</sup> mice. Erythrocyte (Er)-filled vessels with fenestrated

endothelium are seen between RPE and photoreceptor outer segments (upper row, right-hand panel, inset). In places, the RPE basal lamina is interrupted and electron dense nodules arise to extend between the basolateral RPE infoldings (Lower row, middle panel. Higher magnification, right-handed panel). **E.** TEM of retinal/choroidal interface in six-month-old late-induced mice. While the control is of regular structure, photoreceptor outer segments are missing and the RPE forms multilayers in which vessels are seen (upper row). BM is thickened (lower row). **F.** Immunoreactivity for collagen IV (red) of the retinal/choroidal interface in early-induced, four-week-old *Tgfb $\beta$ 2* <sup>$\Delta$ eye</sup> mice. In the control, the basal laminae of RPE and choriocapillaris endothelium are labeled. In *Tgfb $\beta$ 2* <sup>$\Delta$ eye</sup> mice staining is seen in the basal lamina of the choriocapillaris. Staining is irregular and patchy in region of the RPE. Nuclei are DAPI-stained (blue). RPE nuclei are marked by arrowheads. **G.** Immunoreactivity for collagen IV (red) in the retinal/choroidal interface in late-induced, three-month-old *Tgfb $\beta$ 2* <sup>$\Delta$ eye</sup> mice. In the control, the basal laminae of RPE and choriocapillaris endothelium are continuously labeled. In *Tgfb $\beta$ 2* <sup>$\Delta$ eye</sup> mice labeling is seen in the basal lamina surrounding choriocapillaris vessels, but is incomplete underneath the RPE. In places, the vascular basal lamina continues between RPE cells (arrows) indicating areas of CNV. Nuclei are DAPI-stained (blue), RPE nuclei are marked by arrowheads. RPE, retinal pigment epithelium; BM, Bruch's membrane; CC, choriocapillaris, ONL, outer nuclear layer; Er. Erythrocyte. Experiments performed by (A,B,C,F) Sarah V. Leimbeck; (D,E,G) Anja Schlecht.

### 4.4.5 Cell-specific conditional deletion of *Tgfb $\beta$ 2* in RPE and vascular endothelium

Next we aimed at identifying the specific cell type that is responsible for CNV in *Tgfb $\beta$ 2* <sup>$\Delta$ eye</sup> mice. We focused on the RPE and the vascular endothelium, as endothelial proliferation and breakdown of the RPE barrier are essential requirements for CNV formation. To this end, we generated *Tgfb $\beta$ 2* <sup>$\Delta$ RPE</sup> mice with *Tgfb $\beta$ 2* deletion specifically in the RPE via doxycycline-driven RPE-specific expression of Cre recombinase. Successful RPE-specific T $\beta$ RII deletion was confirmed by immunohistochemistry that showed its presence in photoreceptor outer segments, RPE and choroid of control animals. In contrast, RPE immunoreactivity was not detectable in the RPE of *Tgfb $\beta$ 2* <sup>$\Delta$ RPE</sup> mice (Supplementary data Figure 29B). In addition, we confirmed recombination by PCR (Supplementary data Figure 29D). We analyzed the ocular morphology of *Tgfb $\beta$ 2* <sup>$\Delta$ RPE</sup> mice animals in detail by using essentially similar methods as used for *Tgfb $\beta$ 2* <sup>$\Delta$ eye</sup> mice, but did neither detect choroidal CNV nor other obvious structural changes (Supplementary data Figure 30). For generation of *Tgfb $\beta$ 2* <sup>$\Delta$ EC</sup> mice with specific deletion of T $\beta$ RII in vascular

endothelial cells *VeCad-Cre-ER<sup>T2</sup>* mice were used with endothelial-specific tamoxifen-inducible Cre expression. Specific recombination in retinal and choroidal vessels was confirmed by GFP immunoreactivity in *VeCad-Cre-ER<sup>T2</sup>* crossed with *mT/mG* reporter mice (Supplementary data Figure 29D). When analyzing the structure of six-week-old *Tgfb $\beta$ 2<sup>ΔEC</sup>* mice the pronounced structural changes that we had reported (Braunger et al. 2015) for early-induced *Tgfb $\beta$ 2<sup>Δeye</sup>* mice such as retinal and vitreal neovascularization, retinal detachment or vitreal hemorrhages were completely absent (Figure 26A, B). Still, similar to our results seen in early-induced *Tgfb $\beta$ 2<sup>Δeye</sup>* mice (Braunger et al. 2015), dilated vessels were frequently observed in the inner nuclear layer (Figure 26C). Quite intriguingly, at the retinal/choroidal interface, focal areas where frequently observed in which photoreceptor outer segments were degenerated or absent, the RPE multilayered and vascular endothelial cells together with extravasated erythrocytes had accumulated in the subretinal space (Figure 26D). FITC-dextran perfused ocular sections of *Tgfb $\beta$ 2<sup>ΔEC</sup>* mice showed tracer leakage from the choriocapillaris towards the RPE and choroidal vessels penetrating the RPE, indicating a breakdown of the outer blood retinal barrier and the formation of CNV (Figure 27A). In contrast to our data from *Tgfb $\beta$ 2<sup>Δeye</sup>* mice though, we did not observe an accumulation of F4/80 positive cells in the choroid of *Tgfb $\beta$ 2<sup>ΔEC</sup>* mice (Figure 27B). In addition, immunoreactivity for collagen IV in the RPE/BM region was seen in basal laminae of choriocapillaris and RPE and did not markedly differ between *Tgfb $\beta$ 2<sup>ΔEC</sup>* mice and controls (Figure 27C). TEM confirmed the findings seen by light microscopy and the presence of degenerated photoreceptor outer segments, multilayered RPE and extravasated erythrocytes (Figure 27D). Moreover, plasma-derived electron-dense material did not pass the RPE tight junctions in controls but accumulated between RPE and photoreceptor outer segments of *Tgfb $\beta$ 2<sup>ΔEC</sup>* mice indicating breakdown of the RPE barrier (Figure 27E). Overall our data obtained in *Tgfb $\beta$ 2<sup>ΔEC</sup>* mice strongly support the conclusion that deletion of TβRII in vascular endothelial cells alone is sufficient to promote the formation of CNV.

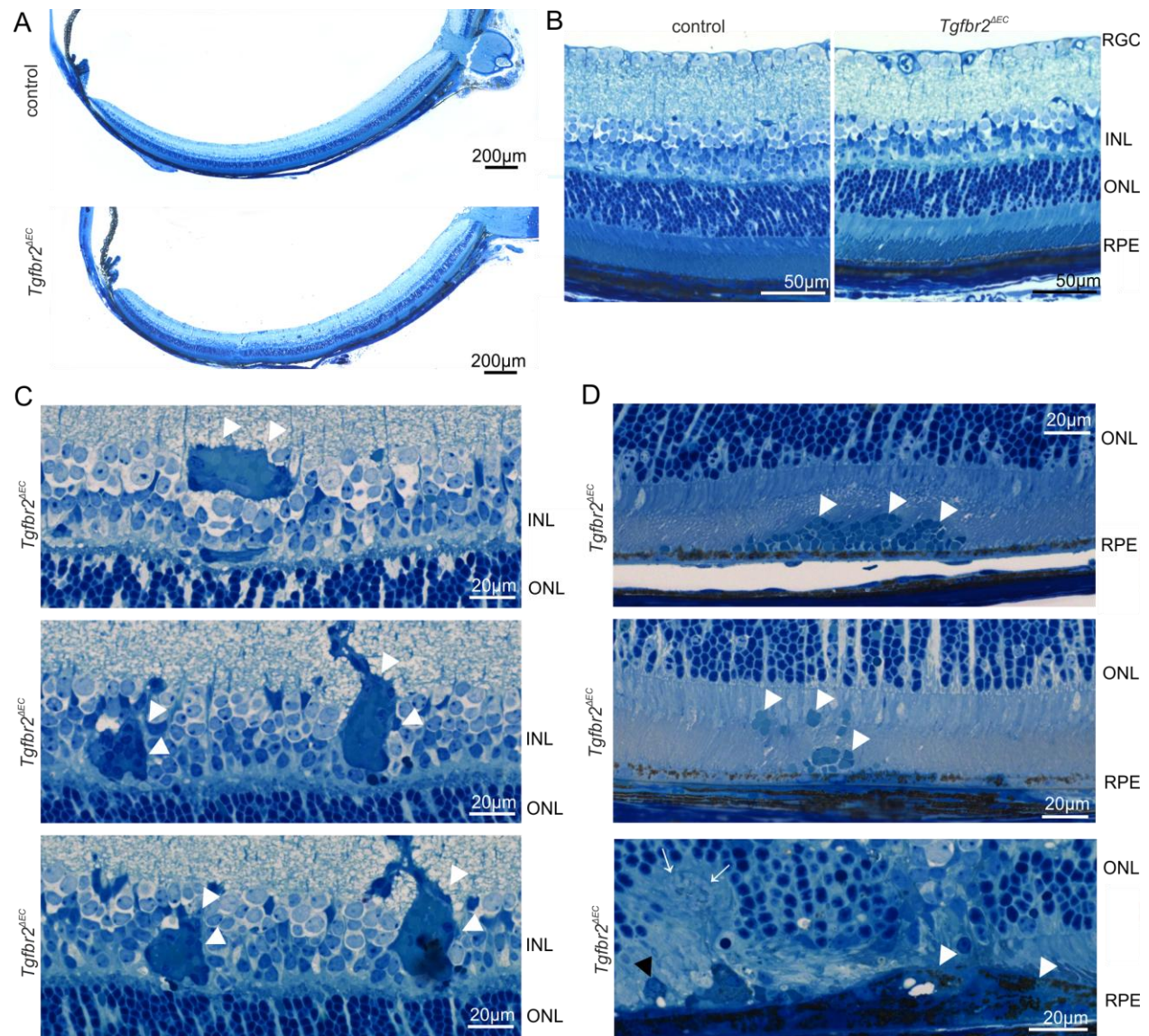


**Figure 26. Structural changes of the retina in *Tgfb2<sup>AEC</sup>* mice.** Richardson stained semi-thin sections of a six-week-old *Tgfb2<sup>AEC</sup>* mouse and its control littermate. **A.** Retinal hemispheres of the control mouse and the *Tgfb2<sup>AEC</sup>* littermate. **B.** Detailed magnification of the retina and choroid. **C.** Dilated retinal vessels are seen in the INL of *Tgfb2<sup>AEC</sup>* mice. **D.** In the retinal/choroidal interface, endothelial cells (arrow), erythrocytes (white arrowheads) and mononuclear cells (black arrowhead) are seen between degenerating photoreceptor outer segments. RGC, retinal ganglion cells; IPL, inner plexiform layer; INL, inner nuclear layer; ONL, outer nuclear layer; RPE, retinal pigment epithelium. Experiments performed by Anja Schlecht

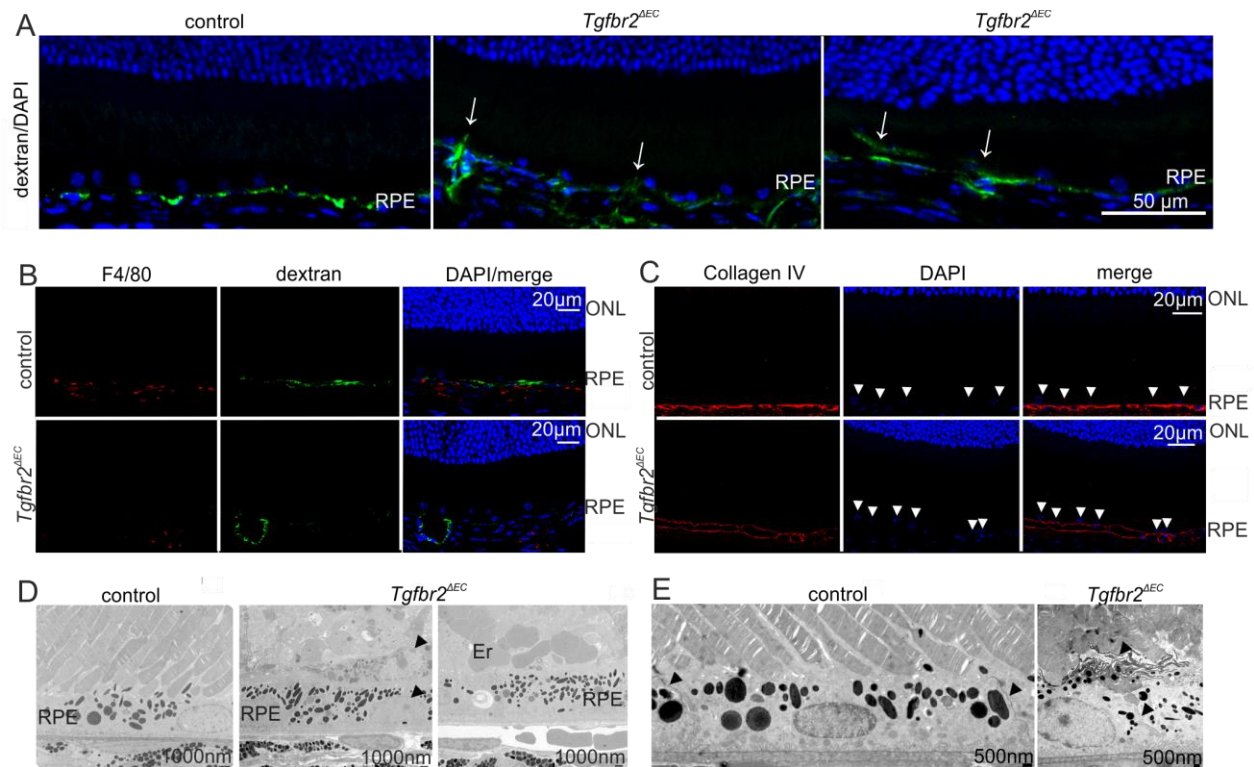


**Figure 27. Structural changes of the retinal/choroidal interface in *Tgfb2<sup>AEC</sup>* mice.** **A.** FITC-dextran perfused retinal meridional sections of a six-week-old *Tgfb2<sup>AEC</sup>* mouse and its control littermate. White arrows point towards tracer leakage in the RPE (middle panel) and choroidal vessels (right panel) invading the RPE. Nuclei are DAPI-stained (blue). **B.** FITC-dextran (green) perfused and F4/80 (red) immunostained sections. The control and the *Tgfb2<sup>AEC</sup>* littermate show immunoreactivity for F4/80 (red) positive cells in the choroid, which are not of higher number in the mutant. Nuclei are DAPI-stained (blue). **C.** Immunoreactivity for collagen IV (red) in the RPE/BM region of six-week-old mice. Basal laminae of choriocapillaris and RPE are regularly labeled in control and mutant. Nuclei are DAPI-stained (blue), RPE nuclei are marked by arrowheads. **D, E.** TEM of RPE/BM in four to six-week-old mice. **D.** In the control, photoreceptor outer segments, RPE and BM are of normal structure. In the *Tgfb2<sup>AEC</sup>* mouse, areas of degenerated photoreceptor outer segments, multilayered RPE and extravasated erythrocytes are present. **E.** Plasma-derived electron-dense material does not pass the RPE tight junctions in controls (arrowheads). In contrast, in the mutant it accumulates between RPE and photoreceptor outer segments (arrowheads). Er, erythrocytes; RPE, retinal pigment epithelium; BM, Bruch's membrane; ONL, outer nuclear layer. Experiments performed by Anja Schlecht.

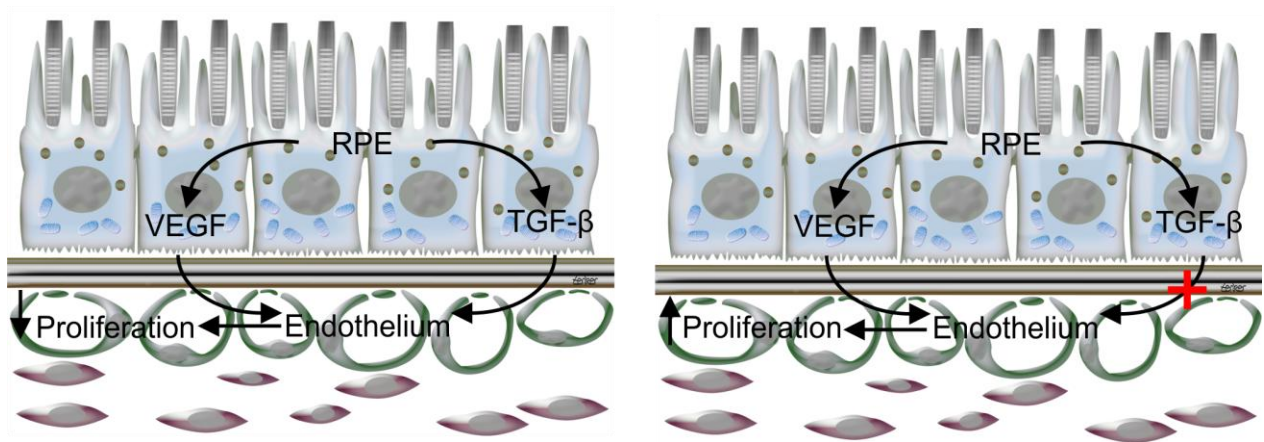


**Figure 28. Schematic of signaling events at the retinal–choroidal interface.** Normally the RPE secretes high amounts of both TGF- $\beta$  and VEGF that both ensure an appropriate physiological microenvironment for the choriocapillaris including its maintenance and inhibition of proliferation (right). The ablation of *Tgfr2* in endothelial cells results in the specific disability of TGF- $\beta$  to act on endothelial cells. This results in an imbalance of the effects of VEGF/TGF- $\beta$ , a scenario that promotes the proliferation of the vascular endothelium of the choriocapillaris in direction of the RPE and finally results in CNV. RPE, retinal pigment epithelium; TGF- $\beta$ , transforming growth factor- $\beta$ ; VEGF, vascular endothelial growth factor; CNV, choroidal neovascularization.

## 4.5 Discussion

We conclude that the ablation of TGF- $\beta$  signaling in the ocular microenvironment is sufficient to induce CNV and other phenotypic characteristics of AMD in humans. Lack of endothelial TGF- $\beta$  signaling is sufficient to trigger the onset of CNV, while its lack in the RPE is not relevant in this context. This conclusion is based on (1) the generation of mice with T $\beta$ RII deficiency in the entire microenvironment of the eye, in vascular endothelial cells, or the RPE; (2) the frequent detection of capillaries with fenestrated, PLVAP-positive endothelium that originate from the choriocapillaris and traverse the RPE to anastomose with retinal capillaries; (3) the presence of basal lamina-like deposits around the RPE basal infoldings and of areas with multilayered RPE; (4) the degeneration of photoreceptor outer segments; and (5) the finding of distinct accumulations of F4/80 positive macrophages in the choroid.

### 4.5.1 TGF- $\beta$ functions at the retinal/choroidal interface to prevent CNV

The results of our study clearly support the concept that a major function of TGF- $\beta$  signaling in choroid and retina is the stabilization of the choroidal and retinal vascular beds that are each essential for neuronal integrity in the sensory retina. This function includes the prevention of neoangiogenic processes in the two capillary beds that would otherwise cause neuronal dysfunction and death in the retina. It is of interest though that the sensitivity to the induced lack of TGF- $\beta$  signaling differs between the two vascular beds, as the formation of microaneurysms, leaky capillaries, and hemorrhages of the retinal vasculature is only seen when TGF- $\beta$  signaling is deleted in the ocular microenvironment shortly after birth (Braunger et al. 2015). In contrast, the formation of CNV is seen regardless if TGF- $\beta$  signaling is interfered with in newborn or three- to four-week-old animals. A likely explanation is the fact that the retinal vasculature of the mouse eye forms and differentiates in the first two weeks after birth (Fruttiger 2002) and may be more vulnerable to lack of TGF- $\beta$  signaling during that period. A critical contributing factor may be the

failure of pericyte differentiation around retinal capillaries that results from deficiency of TGF- $\beta$  signaling during that period (Braunger et al. 2015). Formation of the choroidal vasculature is completed in late embryonic life and the choriocapillaris is mature at birth (Rousseau 2003). Its higher sensitivity to lack of TGF- $\beta$  signaling, as opposed to the mature retinal vasculature, is likely caused by the presence of the high amounts of VEGF at the retinal/choroidal interface that are continuously secreted by the RPE, the only source of VEGF in the back of the adult eye (Saint-Geniez et al. 2006). Secretion of VEGF occurs in a polarized fashion to the RPE basolateral side facing the choriocapillaris (Blaauwgeers et al. 1999, Kannan et al. 2006) and is expected to convey a proliferative signal to endothelial cells of the choriocapillaris that are no more under the influence of constitutive TGF- $\beta$  signaling in animals with an ablation of T $\beta$ RII.

### 4.5.2 TGF- $\beta$ and VEGF as part of a homeostatic system to maintain integrity of the choriocapillaris

It is of interest to note that not only VEGF, but also TGF- $\beta$ 1 and -2 are present at high amounts at the retinal/choroidal interface (Pfeffer et al. 1994). It is very tempting to speculate that both factors are critical parts of a homeostatic system designed to maintain structure and function of the choriocapillaris. In this system, VEGF would be required to maintain the extreme high density of the choriocapillaris and their fenestrations (Esser et al. 1998, Kamba et al. 2006), while TGF- $\beta$ s antagonize any proliferative properties of VEGF signaling on the vascular endothelium. Failure in the balance of this homeostatic system would cause ablation of the choriocapillaris or induce its proliferation finally leading to CNV (Figure 28). There is direct evidence for such a homeostatic system from studies in genetically engineered mice in which lack of VEGF and/or increase in TGF- $\beta$  activity leads to ablation of the choriocapillaris (Kurihara et al. 2012, Marneros et al. 2005, Le et al. 2010, Saint-Geniez et al. 2009, Ohlmann et al. 2016), while increase in VEGF (Oshima et al. 2004, Schwesinger et al. 2001) and/or lack of TGF- $\beta$  activity (results of our present study) have direct opposite and proliferative effects. For the

initiation of CNV though, lack of TGF- $\beta$  activity appears to be more relevant than sole increase of VEGF activity, as mice with overexpression of VEGF in the RPE develop an intrachoroidal neovascularization, but no CNV (Oshima et al. 2004, Schwesinger et al. 2001). VEGF and TGF- $\beta$ s induce the transcription of one another in multiple cell types (Shi et al. 2014, Jeon et al. 2007, Nam et al. 2010, Park et al. 2013, Li et al. 2005, Lee et al. 2008) and may well do so in the RPE establishing an autoregulatory feedback system designed to maintain structure and function of the choriocapillaris.

### 4.5.3 Potential neuroprotective effects of TGF- $\beta$

Late-induced *Tgfb $\beta$ 2* <sup>$\Delta$ eye</sup> mice showed a dramatic deterioration of the retina. The prolonged presence and formation of CNV, and its detrimental effects on structure and function of the retina may explain this finding. It may also indicate though a participation of TGF- $\beta$  signaling in a neuroprotective pathway independent of the formation of CNV. We recently showed that TGF- $\beta$  signaling protects retinal neurons from developmental programmed cell death (Braunger et al. 2013b). It is well possible that it also contributes to maintenance of adult neurons by protecting them from apoptosis. In support of such a scenario are findings reported by Walshe and colleagues who neutralized TGF- $\beta$  in the adult mouse eye via expression of soluble endoglin, a TGF- $\beta$  inhibitor (Walshe et al. 2009). Apoptosis of retinal ganglion cells was observed as were functional deficits detected by ERG. Neuroprotective activities of TGF- $\beta$ s were reported for multiple types of neurons throughout the central nervous system such as in the striatum (Ma et al. 2008), spinal cord (Park et al. 2008), substantia nigra (Roussa et al. 2009) or hippocampus (Zhu et al. 2004). Quite similarly, there is increasing evidence that also VEGF signaling is important for the trophic maintenance of neurons and their survival after injury, effects that appear to be mediated via the VEGF receptor-2 (VEGFR-2) (Carmeliet and Ruiz de Almodovar 2013, Cvetanovic et al. 2011, Robinson et al. 2001, Jin et al. 2002, Ma et al. 2009b). Mice with a

constitutive high expression of VEGF in retinal ganglion cells are protected from RGC degeneration after axotomy via VEGFR-2 and downstream activation of ERK1/2 and Akt pathways (Kilic et al. 2006). While TGF- $\beta$ /VEGF are antagonists in their actions at the retinal/choroidal interface and the choriocapillaris, they may cooperate in their neuroprotective activities. Both functions would serve the ultimate goal to maintain structure and function of the retina.

### 4.5.4 The formation of BlamD-like material is not required for CNV

While CNV was consistently observed in the eyes of both early and late-induced Tgfbr2 <sup>$\Delta$ eye</sup> mice, and in that of Tgfbr2 <sup>$\Delta$ EC</sup> mice, other findings were predominant only in the eyes of early-induced Tgfbr2 <sup>$\Delta$ eye</sup> mice. This includes the formation of homogenous extracellular material between the basal infoldings of the RPE and internal to the RPE basal lamina. The material was quite similar in electron density and structure to that of basal lamina deposits (BlamD), a characteristic finding in patients with early age-related macular degeneration (van der Schaft, T L et al. 1994, Curcio et al. 2005, Loeffler and Lee 1992). BlamD-like changes were commonly observed in early-induced Tgfbr2 <sup>$\Delta$ eye</sup> mice, only rarely in late-induced Tgfbr2 <sup>$\Delta$ eye</sup> mice and not in Tgfbr2 <sup>$\Delta$ EC</sup> mice suggesting that they are not a requirement for CNV and breakdown of the RPE barrier. Our immunohistochemical data indicate that the homogenous extracellular BlamD-like material contains collagen type IV, an observation that correlates with the observation that basal lamina proteins such as collagen IV and laminin are present in BlamD in human patients with AMD (van der Schaft, T L et al. 1994, Marshall et al. 1992). BlamD formation in AMD is likely caused by RPE dysfunction (Curcio et al. 2005). A comparable dysfunction might more easily happen in early-induced Tgfbr2 <sup>$\Delta$ eye</sup> mice, in which the RPE is not yet fully differentiated. Direct ablation of TGF- $\beta$  signaling in RPE cells appears not to be relevant for formation of BlamD-like material, as it was not observed in Tgfbr2 <sup>$\Delta$ RPE</sup> mice.

### 4.5.5 Neovascularization is associated with macrophage accumulation

A common finding *Tgfb $\beta$ 2* <sup>$\Delta$ eye</sup> mice with CNV was the marked accumulation of F4/80 positive macrophages in region of the retinal/choroidal interface. Comparable findings have been described for patients suffering from AMD (Xu et al. 2009). It is reasonable to assume that signaling molecules released from proliferative capillary endothelial cells attracted the cells. Reactive macrophages might contribute to the loss of the RPE barrier in our mice and its transition from an epithelial layer to a multilayer in areas of CNV. Our findings in *Tgfb $\beta$ 2* <sup>$\Delta$ RPE</sup> mice indicate that lack TGF- $\beta$  signaling in RPE cells is not required for this process. Currently we do not know how proliferating choroidal endothelial cells manage to break down the RPE barrier, but we trust that our mouse models are appropriate tools to study this in the future. The expression of signaling molecules characteristic for reactive macrophages/microglia such *iNos*, *Il-6*, *Tnf- $\alpha$*  and *MCP-1/Ccl* was elevated in the retinal mRNA of early-induced *Tgfb $\beta$ 2* <sup>$\Delta$ eye</sup> mice, but not in late-induced, an observation that we attribute to the marked changes in the inner retina of early-induced mice that are absent in late-induced. Still, those molecules might well be elevated in the microenvironment of the choroidal/retinal interface where macrophages accumulate in mice with CNV.

### 4.5.6 TGF- $\beta$ signaling and endothelial proliferation

Retinal endothelial cells express two types of T $\beta$ RI receptors, the activin receptor-like kinase 1 (ALK1) and ALK5, which are each recruited and activated after binding of TGF- $\beta$  dimers to the T $\beta$ RII (van Geest et al. 2010, Goumans et al. 2002). Depending on which T $\beta$ RI is recruited, different SMAD signaling cascades are activated resulting either in an ALK5/SMAD2/3 mediated inhibition of endothelial cell migration and proliferation or an ALK1/SMAD1/5/8 induced proangiogenic stimulation of both processes (Goumans et al. 2002, van Geest et al. 2010, Massague 2000) In our *Tgfb $\beta$ 2* <sup>$\Delta$ EC</sup> and *Tgfb $\beta$ 2* <sup>$\Delta$ eye</sup> animal models, the deletion of T $\beta$ RII interrupts

both ALK1- and ALK5-mediated signaling cascades. We therefore hypothesize that the deficiency of T $\beta$ RII in endothelial cells shifts the ALK1/ALK5 balance towards the proangiogenic side, a scenario that finally results in the proliferation of endothelial cells promoting the development of CNV. Data obtained in mice with an inducible conditional deletion of T $\beta$ RII in retinal endothelial cells further support the concept of an increased endothelial proliferation following an interruption of the TGF- $\beta$  signaling pathway. The mice demonstrated a significant increase in vascular branch point density, the area of retina covered by vascular endothelial cells, the number of proliferating endothelial cells and glomerular tuft formation during retinal angiogenesis (Arnold et al. 2012, Allinson et al. 2012). The fact that we observed a leakage of high molecular weight FITC-dextran and erythrocytes in the retina and in the sub-retinal space in both animal models, e.g. mice with an early-induced deletion of the TGF- $\beta$  signaling pathway in the entire eye (Braunger et al. 2015) and with a deletion of the TGF- $\beta$  signaling pathway specifically in endothelial cells (present study), implicates a disruption of the inner and outer blood retinal barriers. Deficiency of the TGF- $\beta$  signaling pathway in endothelial cells is likely the major contributor in this scenario. Data obtained in mice with an endothelial specific deficiency of SMAD4, an intracellular downstream mediator of TGF- $\beta$  signaling, or data from mice with a deletion of T $\beta$ RII specifically in endothelial cells in the brain (Li et al. 2011, Nguyen et al. 2011) are in agreement with our results as both conditions caused perinatal intracerebral hemorrhages and a breakdown of the blood brain barrier. Furthermore, the virus-driven expression of soluble endoglin resulted in an inhibition of TGF- $\beta$ 1 signaling in the murine retina, a situation that also caused a breakdown of the blood retinal barrier, most likely mediated through a decreased association of the tight junction proteins occludin and zona occludens (ZO)-1 (Walshe et al. 2009).

### 4.5.7 TGF- $\beta$ signaling in human patients with AMD

Several independent case-control genome-wide association studies detected an association of two synonymous polymorphisms in exon 1 of the high-temperature requirement A1 (*HTRA1*) gene with a high risk to develop AMD (Fritsche et al. 2013, Yang et al. 2006, Dewan et al. 2006). The gene product HTRA1 appears to play a causative role in CNV (Vierkotten et al. 2011, Zhang et al. 2012, Nakayama et al. 2014). Quite intriguingly a recent study provided evidence that the two synonymous HTRA1 variants influence their protein interaction with TGF- $\beta$ 1 leading to an impairment of TGF- $\beta$  signaling (Friedrich et al. 2015). Moreover, a collaborative genome-wide association study identified *TGFBR1* the gene encoding for the TGF- $\beta$ 1 type I receptor, as a new susceptibility gene for AMD further highlighting the importance of the TGF- $\beta$  signaling pathway in the context of AMD (Fritsche et al. 2013).

### 4.5.8 Conclusion

Our findings emphasize the importance of TGF- $\beta$  signaling as a key player in the development of ocular neovascularization and implicate a fundamental role of TGF- $\beta$  signaling in the pathogenesis of AMD. A more thorough understanding of this role at the retinal/choroidal interface has the distinct potential to lead to the development of novel treatments strategies preventing CNV in patients suffering from AMD.

### Acknowledgements

The authors thank Elke Stauber, Margit Schimmel, Angelika Pach, Silvia Babl and Elfriede Eckert for their excellent technical assistance. This work was funded by the DFG Forschergruppe (FOR 1075).

## 4.6 Supplementary Data

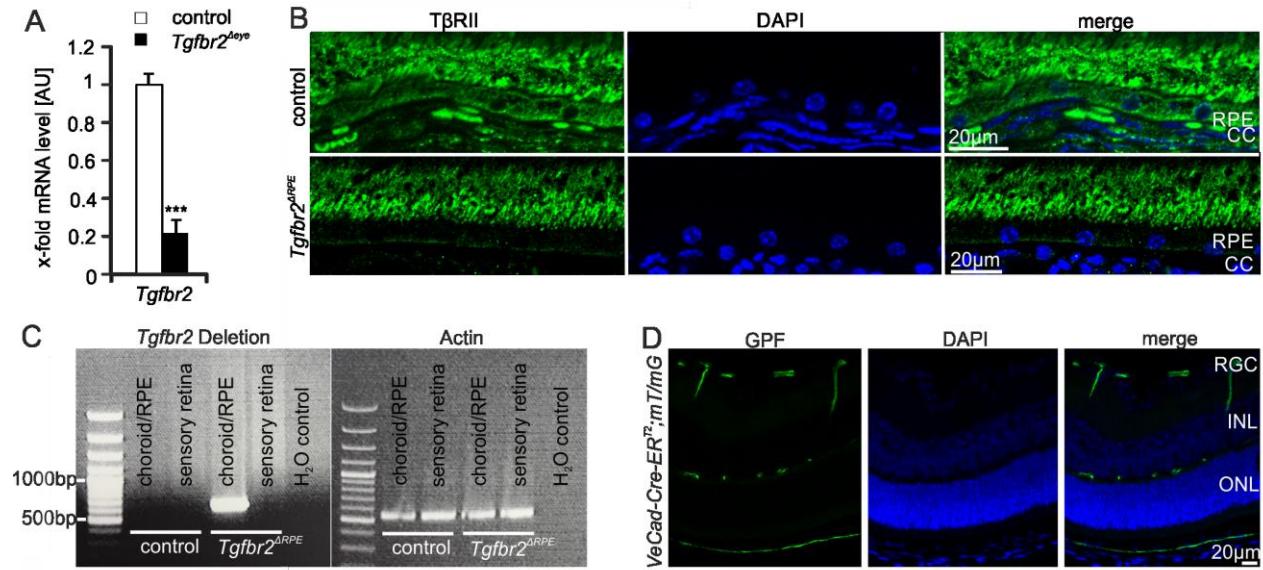


**Figure 29. Deletion of TβRII in late-induced *Tgfr2*<sup>Δeye</sup>, *Tgfr2*<sup>ΔRPE</sup> and *Tgfr2*<sup>ΔEC</sup> mice.** **A.** Real time RT-PCR for mRNA of *Tgfr2* in four-week-old control and late-induced *Tgfr2*<sup>Δeye</sup> mice. Data are expressed as mean±SEM; control: n = 9, *Tgfr2*<sup>Δeye</sup>: n = 4; \*\*\*P ≤ 0.001. **B.** Immunoreactivity for TβRII (green) in the RPE in four week old *Tgfr2*<sup>ΔRPE</sup> and control littermates. The control shows a distinct immunoreactivity for TβRII in the RPE which is essentially absent in the *Tgfr2*<sup>ΔRPE</sup> animal. Nuclei are DAPI-stained (blue). **C.** *Tgfr2* deletion PCR of a four week old *Tgfr2*<sup>ΔRPE</sup> mouse and its control littermate using the sensory retina and RPE/choroid as genomic DNA samples. Due to their different product sizes (product size control: 3974bp, product size after *Tgfr2* deletion: 636bp) and the PCR elongation time of 1 min, the *Tgfr2* PCR product was only amplified after Cre mediated recombination. As expected, in the *Tgfr2*<sup>ΔRPE</sup> mouse the recombination occurred only in RPE/choroidal sample but not in the retina. **D.** A distinct GFP signal in 10 day old *VeCad-Cre-ER*<sup>T2</sup>;mT/mG mice indicates a successful activation of the Cre recombinase in retinal and choroidal endothelial cells following tamoxifen treatment. RGC, retinal ganglion cells; INL, inner nuclear layer; ONL, outer nuclear layer; TβRII, TGF-β type II receptor; CC, choriocapillaris; RPE, retinal pigment epithelium. Experiments performed by Anja Schlecht.

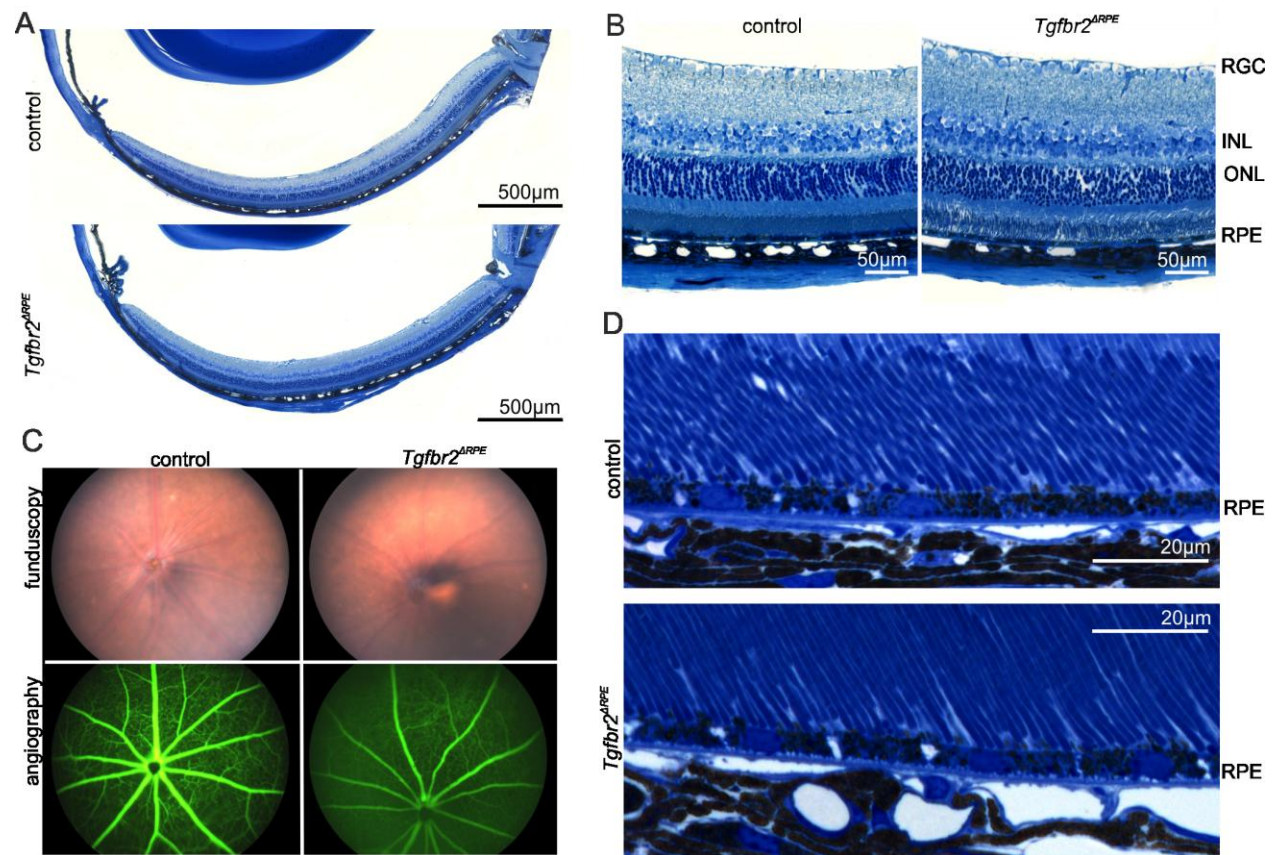


**Figure 30. Inhibition of TGF $\beta$ -signaling in the RPE: the morphology of the eye.** Richardson's stained semithin sections. **A.** Retinal hemispheres of six month old animals. The control mouse and the *Tgfb2<sup>ARPE</sup>* mouse do not obviously differ in structure. **B.** Detailed magnification of the retina/choroid of a *Tgfb2<sup>ARPE</sup>* mouse and its control littermate showing an essentially normal morphology. **C.** *In vivo* funduscopy and fluorescein angiography show no obvious alterations in the *Tgfb2<sup>ARPE</sup>* mouse compared to the control. **D.** Detailed magnifications of the interface of the outer retina, RPE and choroid, again showing a regular morphology in the *Tgfb2<sup>ARPE</sup>* mice and controls. RGC, retinal ganglion cells; INL, inner nuclear layer; ONL, outer nuclear layer; RPE, retinal pigment epithelium. Experiments performed by (A,B,D) Anja Schlecht; (C) Anja Schlecht and Herbert Jägle.

## 5 General discussion

TGF- $\beta$  signaling plays an important role in many cellular processes including cell growth, differentiation and apoptosis (Heldin et al. 1997, Massagué 2012, Braunger et al. 2015, Braunger et al. 2013b). Throughout the past years, great research efforts have been made to further investigate the effects and functions of TGF- $\beta$  signaling *in vivo*. Since the systemic constitutive deletion of the TGF- $\beta$  signaling pathway is embryonic lethal (Dickson et al. 1995), the development of the Cre-loxP system greatly enhanced the possibilities to study TGF- $\beta$  *in vivo* as different time- and/or cell type-specific Cre recombinases are available.

In our group, we aimed to investigate the role of TGF- $\beta$  signaling during development and maintenance of the ocular vasculature. Therefore, we deleted the TGF- $\beta$  signaling pathway in the entire eye. To circumvent the embryonic lethality, we decided to use an inducible, tamoxifen dependent Cre recombinase expressing mouse line (CAGG Cre-ER<sup>TM</sup>). CAGG Cre-ER<sup>TM</sup> mice carry a Cre recombinase which is fused to a mutant form of an estrogen receptor binding domain (ER<sup>TM</sup>) (Hayashi and McMahon, 2002). The fusion leads to a sequestration of the Cre in the cytoplasm and Cre-ER<sup>TM</sup> will only translocate to the nucleus after binding to tamoxifen (Feil et al. 1997, Hayashi and McMahon 2002).

In this study, we provide evidence that the topical administration of tamoxifen eye drops in CAGG-Cre ER<sup>TM</sup> mice leads to a successful activation of the Cre recombinase in the entire eye (Schlecht et al. 2016). Furthermore, we were able to show that an early-induced deletion of *Tgfr2* (tamoxifen treatment starting at P4) in the eye resulted in a phenotype mimicking essential characteristics of diabetic retinopathy (Braunger et al. 2015). In addition, we observed that a late-induced deletion of *Tgfr2*, after development of the retinal vasculature (tamoxifen treatment starting on P21), resulted in the formation of choroidal neovascularization, a hallmark of age-related macular degeneration.

### **5.1 Tamoxifen eye drops: A new delivery method without side effects?**

A frequently used standard protocol to activate tamoxifen-dependent Cre recombinases describes the administration of up to 1mg tamoxifen via a single or repeated intraperitoneal injections, depending on the used Cre recombinase (Kuhbandner et al. 2000, Leone et al. 2003, Kim et al. 2004, Indra et al. 1999). These procedures harbor the risk of infections as a result of the intraperitoneal injections (Leenaars et al. 1998, Leenaars and Hendriksen 2005). Intravitreal tamoxifen injections still go along with the risk of an ocular infection. Furthermore, studies could show that intravitreal injections of the vehicle alone can lead to a reactivity of microglia cells and elevated expression levels of neuroprotective molecules (Braunger 2014, Seitz and Tamm 2014).

In the current study, we aimed to establish an efficient recombination of the Cre recombinase in CAGG Cre-ER<sup>TM</sup> mice by using tamoxifen containing eye drops. We provide substantial evidence that tamoxifen administration via eye drops (duration of treatment was five consecutive days, eye drops were given three times per day, either from P4 – P8, or from P21 – P25) results in successful activation of the Cre recombinase in ocular tissue of CAGG Cre-ER<sup>TM</sup> mice.

It is of interest to mention that our group could show that the mentioned negative side effects of an invasive tamoxifen administration can be avoided by the use of tamoxifen eye drops. We demonstrated that Cre expression itself, or topical tamoxifen treatment does not result in detectable changes in the retinal morphology and function, the expression levels of neuroprotective molecules, neuronal vulnerability or glial reactivity (Boneva et al. 2016).

After verifying the reliability of this newly established method, we also wanted to know if the activation of the Cre via tamoxifen containing eye drops is restricted to ocular tissue only or if Cre had also been activated in other organs. To answer this question, we crossed heterozygous CAGG Cre-ER<sup>TM</sup> mice with homozygous mT/mG double fluorescent Cre reporter mice (Muzumdar et al. 2007). These reporter mice express GFP (green fluorescent protein) in each

cell in which the Cre is active. We sampled and sectioned organs from CAGG Cre-ER<sup>TM</sup>;mT/MG and control;mT/mG mice that had been treated with tamoxifen eye drops from p4 – p8. As shown in Figure 31 mice carrying the Cre recombinase present an intense GFP signal in all investigated organs: the brain, the lung, the liver, the kidney, the heart and the intestine. The control littermates did not show a GFP reaction, we only observed DAPI-labeled nuclei. This outcome indicates that the application of tamoxifen eye drops does not only result in a successful activation of the Cre in ocular tissue, but also in other parts of the body. This effect might be the result of the five-day duration of the treatment. Perhaps, a shorter timeframe of e.g. three days would be sufficient to result in a successful activation of Cre in ocular tissue, without distributing tamoxifen to any other parts of the body. We conclude, that tamoxifen eye drops are a save and non-invasive method to activate the Cre recombinase without running the risk of infections e.g. due to intraperitoneal injections or inducing the expression of neuroprotective factors or the reactivity of micro- and macroglia cells. Furthermore, we are convinced that the topical application of tamoxifen via eye drops might be an interesting approach for scientists to investigate gene function outside the eye, too.

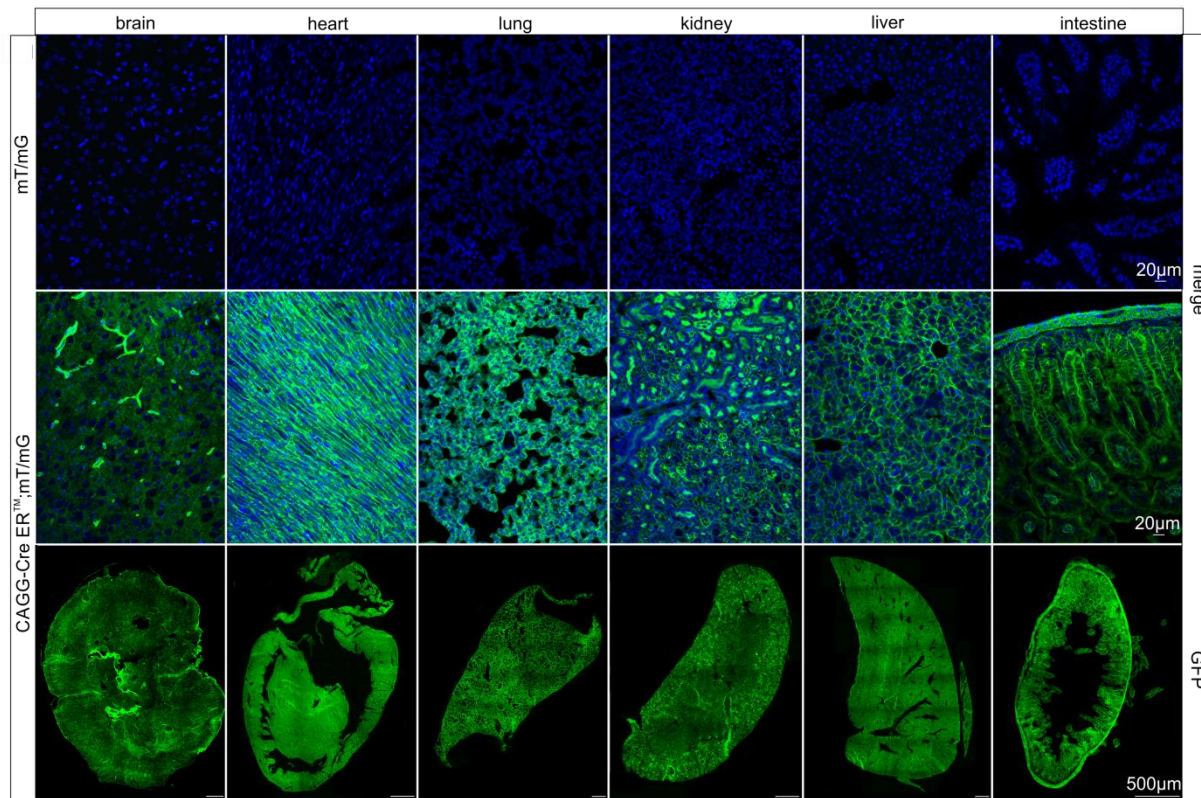


**Figure 31. Activation of the Cre recombinase after the administration of tamoxifen eye drops.** The 10 days old double transgenic CAGG Cre-ER<sup>TM</sup>/mTmG mice show a strong green fluorescence in all examined organs. In contrast, in the control littermate (mTmG) only the DAPI-labeled nuclei are visible.

## 5.2 TGF- $\beta$ signaling is required for pericyte differentiation

A general pan-pericyte marker does not exist to date, due to the diverse characteristics, functions and locations of pericytes. There are several commonly used markers for defining pericytes like alpha-smooth-muscle actin ( $\alpha$ -SMA), regulator of G protein signaling 5 (RGS-5), neuron-glia 2 (NG2) or platelet-derived growth factor receptor beta (PDGFR $\beta$ ). However, the expression patterns of these markers vary, depending on the tissue or on the developmental or angiogenic stage of a blood vessel (Bergers and Song 2005). In the retina, NG2 is mostly expressed in pericytes during vascular development and after the pericytes' differentiation (Schallek et al. 2013, Trost et al. 2013).  $\alpha$ -SMA expression in the retina is normally restricted to vascular smooth muscle cells surrounding larger vessels like arteries and arterioles and mostly

absent in retinal capillaries (Hughes and Chan-Ling 2004, Trost et al. 2013, Nehls 1991). RGS-5 and PDGFR- $\beta$  were identified as markers for developing pericytes (Bondjers et al. 2003, Lindahl et al. 1997). When we used these markers for pericytes in our immunohistochemical analyses, Tgfbr2-deficient mice showed only few NG2-positive pericytes covering retinal capillaries. However, these capillaries were densely covered with  $\alpha$ -SMA-positive smooth muscle-like cells. As pericytes and smooth muscle cells originate from the same precursors, our results indicate that, during the development of the retinal vasculature, TGF- $\beta$  signaling is essential for determining the cell fate of mural cells surrounding retinal capillaries.

### **5.3 Early-induced deletion of ocular TGF- $\beta$ signaling leads to formation of multiple microaneurysms**

The loss of pericytes and the formation of capillary microaneurysms are hallmarks of diabetic retinopathy (Cogan 1961). Proliferation of endothelial cells is thought to be a trigger for the formation of microaneurysms (Aguilar et al. 2003). *In vitro* studies showed that pericytes can control endothelial cell proliferation. This effect is discussed to be mediated by the activation of TGF- $\beta$ 1 upon contact between endothelial cells and pericytes (Sato et al. 1990, Antonelli-Orlidge et al. 1989, Hirschi et al. 1998). In addition to the proliferation of the endothelium, the early loss of pericytes is hypothesized to be a causative factor for the generation of microaneurysms. However, the fact that in mouse mutants that lack more than 50% of pericytes, microaneurysms are rare, may point towards a synergistic effect between the loss of pericytes and the proliferation of endothelial cells (Enge 2002, Hammes et al. 2002, Hammes et al. 2004, Hammes 2005). Our data show that the inhibition of ocular TGF- $\beta$  signaling leads to the formation of microaneurysms. The observed dedifferentiation of pericytes in Tgfbr2-deficient mice concomitant with an increased proliferation of endothelial cells is a very likely explanation for this scenario. It is worthwhile to mention that endothelial cells express two different TGF- $\beta$  type I

receptors (T $\beta$ RI), i.e. ALK1 and ALK5. Recruitment and activation of ALK1 leads to intracellular phosphorylation of Smad1/5/8 which results in stimulation of endothelial cell migration and proliferation. ALK5 signaling, however, is intracellularly mediated via Smad2/3 and leads to an inhibition of these two processes (Goumans et al. 2003, Goumans et al. 2002). The balance between these two possibilities determines the pro- or antiangiogenic effects of TGF- $\beta$  in endothelial cells. Our results indicate that the lack of Tgfr2 in retinal endothelial cells shifts the balance towards the proangiogenic side, resulting in endothelial proliferation. To our understanding, the proliferation of endothelial cells and the dedifferentiated pericyte population promote the formation of microaneurysms.

### **5.4 Early-induced deletion of ocular TGF- $\beta$ signaling results in non-perfused capillaries and activation of the ocular immune system**

Based on our results we provide evidence that a deletion of ocular TGF- $\beta$  signaling results in non-perfused capillaries that lack endothelial cells. Again, comparable morphological findings are described for patients suffering from diabetic retinopathy (Garner 1993, Hammes et al. 2011). In support to our findings are data obtained in mice that lack 50% of retinal pericytes. These animals also developed vascular occlusion and regression, which indicates that capillary regression is caused by pericyte dropout (Enge 2002). Furthermore, *in vitro* experiments showed that pericytes release active TGF- $\beta$ 1 which is necessary for survival of vascular endothelial cells (Walshe 2010). In Tgfr2 deficient mice, endothelial cells lack the Tgfr2, which is essential for TGF- $\beta$  signaling. Thus TGF- $\beta$ 1 cannot promote the survival of endothelial cells in this model.

It is well-known that TGF- $\beta$  signaling plays an important immunosuppressive role in the eye (Nussenblatt and Ferris 2007, Niederkorn 2006). The deletion of Tgfr2 via tamoxifen eye drops in Tgfr2 deficient mice affects the whole ocular microenvironment; hence microglia cells are also affected by the deletion of Tgfr2. It is very likely that the observed accumulation of

macrophages and reactive microglia in close association with the retinal vessels and a significant induction of immune modulating cytokines are a direct effect of the *Tgfr2* deletion on micro-and macroglia cells. Similar to our data, studies demonstrated that patients with diabetic retinopathy frequently show microglia with a reactive phenotype which clusters around the retinal vessels, especially next to dilated veins, microaneurysms and intraretinal hemorrhages (Zeng et al. 2008).

### **5.5 Early-induced deletion of ocular TGF- $\beta$ signaling causes vitreal neovascularization, impaired retinal function and retinal detachment**

The presence of non-perfused capillaries most likely triggered the significant elevation of HIF-1 $\alpha$ , which is a marker for hypoxia. Subsequently, in *Tgfr2* deficient mice, the expression levels of potent angiogenic molecules were significantly elevated, too. This resulted in vitreal neovascularization, comparable to patients suffering from proliferative diabetic retinopathy (Frank 2004, Antonetti et al. 2012, Cheung et al. 2010). Furthermore, we observed the formation of membranes in the vitreous, an increased number of apoptotic cells in the retina, an impaired retinal function and finally retinal detachment. Similar changes can be seen in humans with late-stage proliferative diabetic retinopathy: Patients show an impaired sensory function and the formation of tractional membranes which can lead to retinal detachment (Garner 1993, Frank 2004).

### **5.6 Early-induced deletion of ocular TGF- $\beta$ signaling leads to an AMD-like phenotype**

It is well known, that the Bruch's membrane plays an essential role in the exchange of diverse substances between the retina, the RPE and the choriocapillaris (Hamilton and Leach 2011). Animal models in which CNV is induced by laser induced disruption of the Bruch's membrane demonstrate that the loss of the integrity of the Bruch's membrane can lead to choroidal

neovascularization (Dobi et al. 1989, Ryan 1982). Researchers propose that throughout time abnormal molecules accumulate within the RPE due to failures in the cells' digestive mechanisms. These molecules hinder the normal metabolism, leading to an aggregation of cellular debris within the Bruch's membrane which results in the formation of basal linear deposits (BlinD), basal laminar deposits (BlamD) and drusen (Young 1987, Loffler and Lee 1986). This may lead in the following to a thickening of the Bruch's membrane (Young 1987). In general, drusen are discussed to correlate with the risk of developing AMD (Ambati et al. 2013). In our study, we provide evidence that an early-induced deletion of TGF- $\beta$  signaling in the retinal microenvironment induces substantial changes of the Bruch's membrane, similar to those of patients suffering from AMD. We observed that alterations in the Bruch's membrane, the formation of BlinDs and BlamDs, and finally the development of choroidal neovascularization. Another important factor contributing to the pathogenesis of AMD is the ocular immune system. Several studies showed that animal models with an impaired immune cell trafficking develop an AMD-like phenotype (Ambati et al. 2003, Combadiere et al. 2007, Ross et al. 2008). Furthermore, the observed accumulation of microglia in the subretinal space in patients suffering from AMD is discussed to be both a symptom of inflammatory damage and a beneficial response to injury (Xu et al. 2009). In addition, the recruitment of microglia and/or macrophages have been shown to support the growth of neovascular lesions (Espinosa-Heidmann et al. 2003, Sakurai et al. 2003, Ma et al. 2009a). In our study, we could also observe an accumulation of macrophages in the subretinal region and the choroid of Tgfr2-deficient mice and an increased expression of immune modulating cytokines in the retina.

### **5.7 Late-induced deletion of ocular TGF- $\beta$ signaling results in CNV and alterations of the Bruch's membrane**

Next we investigated whether the development of CNV in T $\beta$ RII deficient mice might be a direct effect of the conditional deletion of the TGF- $\beta$  signaling pathway or if CNV occurs as a consequence of developmental vascular pathologies e.g. the persistence of the hyaloid artery and the presence of non-perfused capillaries, and the herein resulting retinal hypoxia in the early-induced *Tgfbr2* <sup>$\Delta$ eye</sup> mice

To discriminate between these two possibilities, we decided to inhibit the TGF- $\beta$  signaling pathway after the retinal vasculature had been developed. Thus, we treated the mice with tamoxifen eye drops from P21 – P25 and analyzed the phenotype of these mice. The retinal vasculature was regular with all three retinal plexus in the correct localization. However, we still found alterations of the Bruch's membrane, CNV, an accumulation of macrophages in the choroid, an impairment of the sensory function and retinal degeneration. Therefore, our data clearly shows that TGF- $\beta$  signaling is essential for maintaining the ocular vasculature and microenvironment, and that deleting T $\beta$ RII is sufficient to induce changes similar to those seen in human patients with AMD. Still, the question remains whether an impaired TGF- $\beta$  signaling pathway may contribute to the molecular pathogenesis of AMD in humans.

Genome wide association studies showed that HTRA1 (high temperature requirement factor A1) is a risk factor for developing AMD (Deangelis et al. 2008, Fritsche et al. 2013, Dewan et al. 2006). Interestingly, it has been shown that HTRA1 is an important regulator of the TGF- $\beta$  signaling pathway. The AMD-associated polymorphism in HTRA1 results in a reduced affinity for TGF- $\beta$ 1 and a decreased ability to control TGF- $\beta$  signaling (Friedrich et al. 2015). Another genome-wide association study in 2013 identified TGFBR1 as a risk gene for developing AMD (Fritsche et al. 2013). This data together with the results obtained in our study clearly point towards an involvement of TGF- $\beta$  signaling in the pathogenesis of AMD.

### **5.8 Deletion of endothelial TGF- $\beta$ signaling leads to development of CNV and changes in the Bruch's membrane**

Next we aimed to identify the specific cell population which might be responsible for the observed choroidal neovascularization in *Tgfb $\beta$ 2*<sup>*Δeye*</sup> mice. Herein, we focused on the RPE and the endothelium, as the basement membranes of both directly contribute to the formation of BM (Booij et al. 2010). To this end, we used a doxycycline-inducible Cre mouse with a cell specific expression of the Cre recombinase in the RPE (Le et al. 2008) and a tamoxifen-dependent Cre mouse with the Cre recombinase under the control of the endothelial specific cadherin 5 promotor element (Monvoisin et al. 2006). We provide evidence that a specific deletion of T $\beta$ RII in the cells of the RPE is not sufficient to trigger the development of CNV. In contrast, mice with an endothelial deletion of T $\beta$ RII, showed an altered Bruch's membrane that lost its organized, five-layered morphology and the development of CNV. This indicates that a deletion of endothelial TGF- $\beta$  signaling, most likely of the choriocapillaris, leads to a disruption of the Bruch's membrane integrity and in the following to the formation of CNV. Furthermore, the accumulation of erythrocytes in the retina and in the subretinal space indicates a breakdown of the inner and outer blood retinal barriers. In contrast to our data obtained in mice with an ocular deletion of T $\beta$ RII in the entire eye, we did not observe an accumulation of immune cells in the retina and/or the choroid in endothelial specific *Tgfb $\beta$ 2* knockouts. Clearly, the endothelial deletion of T $\beta$ RII does not directly affect the microglia cells or macrophages. Therefore, these cells can still respond to the high levels of TGF- $\beta$ 2 that maintain the ocular immune privilege (Streilein 1999). Consequently, the observed reactivity and accumulation of microglia cells in mice with a deletion of *Tgfb $\beta$ 2* in the entire eye pinpoints towards a direct effect of the deletion on these cells.

We hypothesize that the development of CNV in mice with an endothelial specific deletion of the TGF- $\beta$  signaling pathway may be the result of an increased endothelial cell proliferation concomitant with a disruption of the BM integrity. This theory is strengthened by data obtained

from mice with an endothelial deletion of T $\beta$ RII. These mice showed an increase in vascular branch point density, the number of proliferating endothelial cells and glomerular tuft formation (Allinson et al. 2012, Arnold et al. 2012)

Most likely, the deletion of endothelial T $\beta$ RII shifts the ALK1/ALK5 balance towards a proangiogenic and pro-proliferative effect, quite comparable to the situation in our *Tgfb $\beta$ 2* <sup>$\Delta$ eye</sup> mice. In summary, our data obtained in *Tgfb $\beta$ 2* <sup>$\Delta$ EC</sup> mice strongly support the conclusion that a deletion of T $\beta$ RII in endothelial cells is sufficient to promote an AMD-like phenotype

## 6 Summary

Two of the leading causes of blindness worldwide are diabetic retinopathy and age-related macular degeneration. Both diseases are associated with pathological changes in the ocular vasculature. In the pathogenesis of diabetic retinopathy, a proliferation of the retinal vessels can be observed whereas in the wet form of age-related macular degeneration the choroidal vessels penetrate the retinal pigment epithelium and grow into the retina. The molecular mechanisms leading to these changes are mostly unknown, however there is evidence, that TGF- $\beta$  signaling is involved in the pathogenesis of these diseases.

To study the exact role of TGF- $\beta$  signaling during development and maintenance of the ocular vasculature, we generated mice with an ocular deletion of *Tgfb2*, using CAGG Cre-ER<sup>TM</sup> mice with two floxed alleles for *Tgfb2*, and activated the Cre recombinase by applying tamoxifen eye drops.

The tamoxifen treatment via eye drops resulted in efficient activation of the Cre recombinase in all ocular tissue. When tamoxifen application started on postnatal day P4, the lack of *Tgfb2* in the eye caused a phenotype that mimics essential characteristics of diabetic retinopathy. We observed the formation of multiple microaneurysms, leaky capillaries and hemorrhages. Immunohistochemical staining could show that the retinal capillaries were no longer covered by pericytes, but were densely coated by vascular smooth muscle-like cells. The basal lamina between endothelial cells and pericytes was markedly thickened. In addition, we found microglia with a reactive phenotype in close association with the retinal vessels correlating with the induction of immunomodulating cytokines. Furthermore, we found an induction of angiogenic molecules and an accumulation of retinal HIF-1 $\alpha$  which suggests local hypoxia. In the following, we could observe neuronal apoptosis and an impairment of sensory function and vitreal neovascularization which lead to the formation of vitreal membranes and finally retinal detachment.

## 6 Summary

In addition to the already mentioned structural and functional changes that mimic the phenotype of diabetic retinopathy, we found that these mice also show choroidal neovascularization (CNV), alterations of the Bruch's membrane and the formation of basal laminar as well as basal linear deposits. All findings are similar to those seen in the wet form of AMD. A later deletion of TGF $\beta$ -signaling (at P21, after development of the retinal vasculature) resulted in a normal retinal vasculature but still in the formation of CNV. To investigate which cell type is responsible for the choroidal neovascularization, we generated mice with a specific deletion of Tgfr2 in cells of the retinal pigment epithelium and mice with a specific deletion in endothelial cells. The deletion of Tgfr2 in the RPE did not result in structural changes e.g. choroidal neovascularization. However, mice with a deletion of TGF- $\beta$  signaling in endothelial cells developed alterations in the Bruch's membrane, hemorrhages and CNV.

We conclude that the lack of ocular TGF- $\beta$  signaling leads to a phenotype that shows characteristics of both diabetic retinopathy and age-related macular degeneration. These results strongly suggest that TGF- $\beta$  signaling plays an important role in the molecular pathogenesis of these ocular diseases.

## 7 Table of Figures

Figure 1: TGF- $\beta$ signaling pathway.....	3
Figure 2: Tamoxifen-inducible Cre-loxP system.....	4
Figure 3: Composition of capillaries.....	5
Figure 4: Development of the retinal vasculature in the mouse.....	7
Figure 5: Diabetic retinopathy.....	10
Figure 6: Funduscopy – age-related macular degeneration.....	12
Figure 7. Localization and activation of Cre recombinase in the eye following tamoxifen containing eye drops. ....	20
Figure 8. Detailed localization and activation of Cre recombinase in the eye.....	21
Figure 9. T $\beta$ RII deletion and inhibition of TGF- $\beta$ signaling in <i>Tgfb2</i> <sup><math>\Delta</math>eye</sup> eyes.....	36
Figure 10. Retinal vasculature after T $\beta$ RII deletion and inhibition of TGF- $\beta$ signaling in <i>Tgfb2</i> <sup><math>\Delta</math>eye</sup> eyes. ....	38
Figure 11. Lack of pericyte differentiation in <i>Tgfb2</i> <sup><math>\Delta</math>eye</sup> mice.....	40
Figure 12. Lack of pericyte differentiation in <i>Tgfb2</i> <sup><math>\Delta</math>eye</sup> mice.....	42
Figure 13. Extracellular matrix accumulation in <i>Tgfb2</i> <sup><math>\Delta</math>eye</sup> mice.....	44
Figure 14. Intraretinal hemorrhages and vessel loss in <i>Tgfb2</i> <sup><math>\Delta</math>eye</sup> mice.....	46
Figure 15. Persistence of the hyaloid vasculature in <i>Tgfb2</i> <sup><math>\Delta</math>eye</sup> mice.....	48
Figure 16. Microglia reactivity in retinæ of <i>Tgfb2</i> <sup><math>\Delta</math>eye</sup> mice.....	50
Figure 17. <i>Tgfb2</i> <sup><math>\Delta</math>eye</sup> mice develop proliferative retinopathy. ....	52
Figure 18. <i>Tgfb2</i> <sup><math>\Delta</math>eye</sup> mice develop functional and structural deficits.....	54
Figure 19. Early-induced deletion of TGF- $\beta$ signaling in the eye causes structural changes in the subretinal space. ....	76
Figure 20. Subretinal neovascularization with fenestrated endothelium following deletion of TGF- $\beta$ signaling in the eyes of early-induced <i>Tgfb2</i> <sup><math>\Delta</math>eye</sup> mice. ....	79

## 7 Table of Figures

Figure 21. Subretinal neovascularization following deletion of TGF- $\beta$ signaling in the eyes of three month old late-induced <i>Tgfb<math>\beta</math>2</i> <sup><math>\Delta</math>eye</sup> mice. ....	81
Figure 22. Subretinal neovascularization and retinal degeneration following deletion of TGF- $\beta$ signaling in the eyes of six month old late-induced <i>Tgfb<math>\beta</math>2</i> <sup><math>\Delta</math>eye</sup> mice. ....	83
Figure 23. Functional changes following deletion of TGF- $\beta$ signaling in the eyes of three- and six-month -old late-induced <i>Tgfb<math>\beta</math>2</i> <sup><math>\Delta</math>eye</sup> mice.....	84
Figure 24. Early- and late-induced inhibition of TGF- $\beta$ signaling in the eye: the expression of angiogenic factors and immune modulating cytokines. ....	87
Figure 25. Structural changes of the Bruch's membrane (BM) in early and late-induced <i>Tgfb<math>\beta</math>2</i> <sup><math>\Delta</math>eye</sup> mice. ....	90
Figure 26. Structural changes of the retina in <i>Tgfb<math>\beta</math>2</i> <sup><math>\Delta</math>EC</sup> mice. ....	93
Figure 27. Structural changes of the retinal/choroidal interface in <i>Tgfb<math>\beta</math>2</i> <sup><math>\Delta</math>EC</sup> mice. ....	94
Figure 28. Schematic of signaling events at the retinal–choroidal interface. ....	95
Figure 29. Deletion of T $\beta$ RII in late-induced <i>Tgfb<math>\beta</math>2</i> <sup><math>\Delta</math>eye</sup> , <i>Tgfb<math>\beta</math>2</i> <sup><math>\Delta</math>RPE</sup> and <i>Tgfb<math>\beta</math>2</i> <sup><math>\Delta</math>EC</sup> mice.....	103
Figure 30. Inhibition of TGF $\beta$ -signaling in the RPE: the morphology of the eye. ....	104
Figure 31. Activation of the Cre recombinase after the administration of tamoxifen eye drops. ....	108

## 8 List of Tables

Table 1. Antibodies used for Western Blot analysis .....	28
Table 2. Antibodies used for immunohistochemistry .....	30
Table 3. Primers used for quantitative real-time PCR amplification .....	33
Table 4. Antibodies used for immunohistochemistry .....	70
Table 5. Primers used for real time PCR amplification.....	73

## 9 References

- Adamis AP, Berman AJ (2008) Immunological mechanisms in the pathogenesis of diabetic retinopathy. *Seminars in immunopathology* 30(2):65–84
- Aguilar E, Friedlander M, Gariano RF (2003) Endothelial proliferation in diabetic retinal microaneurysms. *Archives of ophthalmology (Chicago, Ill. : 1960)* 121(5):740–741
- Allinson KR, Lee HS, Fruttiger M, McCarty JH, McCarty J, Arthur HM (2012) Endothelial expression of TGF $\beta$  type II receptor is required to maintain vascular integrity during postnatal development of the central nervous system. *PloS one* 7(6):e39336
- Ambati J, Anand A, Fernandez S, Sakurai E, Lynn BC, Kuziel WA, Rollins BJ, Ambati BK (2003) An animal model of age-related macular degeneration in senescent Ccl-2- or Ccr-2-deficient mice. *Nature medicine* 9(11):1390–1397
- Ambati J, Atkinson JP, Gelfand BD (2013) Immunology of age-related macular degeneration. *Nature reviews. Immunology* 13(6):438–451
- Ambati J, Fowler BJ (2012) Mechanisms of age-related macular degeneration. *Neuron* 75(1):26–39
- Amin RH, Frank RN, Kennedy A, Elliott D, Puklin JE, Abrams GW (1997) Vascular endothelial growth factor is present in glial cells of the retina and optic nerve of human subjects with nonproliferative diabetic retinopathy. *Investigative ophthalmology & visual science* 38(1):36–47
- Anand-Apte B, Hollyfield JG (2010) Developmental Anatomy of the Retinal and Choroidal Vasculature. In: *Encyclopedia of the eye Encyclopedia of the eye*. Elsevier, Amsterdam, pp 9–15
- Antonelli-Orlidge A, Saunders KB, Smith SR, D'Amore PA (1989) An activated form of transforming growth factor beta is produced by cocultures of endothelial cells and pericytes. *Proceedings of the National Academy of Sciences of the United States of America* 86(12):4544–4548

## 9 References

- Antonetti DA, Barber AJ, Khin S, Lieth E, Tarbell JM, Gardner TW (1998) Vascular permeability in experimental diabetes is associated with reduced endothelial occludin content: vascular endothelial growth factor decreases occludin in retinal endothelial cells. Penn State Retina Research Group. *Diabetes* 47(12):1953–1959
- Antonetti DA, Klein R, Gardner TW (2012) Diabetic Retinopathy. *N Engl J Med* 366(13):1227–1239
- Armulik A, Genové G, Betsholtz C (2011) Pericytes: developmental, physiological, and pathological perspectives, problems, and promises. *Developmental cell* 21(2):193–215
- Armulik A, Genové G, Mäe M, Nisancioglu MH, Wallgard E, Niaudet C, He L, Norlin J, Lindblom P, Strittmatter K, Johansson BR, Betsholtz C (2010) Pericytes regulate the blood-brain barrier. *Nature* 468(7323):557–561
- Arnold TD, Ferrero GM, Qiu H, Phan IT, Akhurst RJ, Huang EJ, Reichardt LF (2012) Defective retinal vascular endothelial cell development as a consequence of impaired integrin  $\alpha V\beta 8$ -mediated activation of transforming growth factor- $\beta$ . *The Journal of neuroscience : the official journal of the Society for Neuroscience* 32(4):1197–1206
- Ashton N (1963) Studies of the retinal capillaries in relation to diabetic and others. *The British journal of ophthalmology* 47:521–538
- Ashton N (1970) Retinal angiogenesis in the human embryo. *British medical bulletin* 26(2):103–106
- Bandello F, Lattanzio R, Zucchiatti I, Petruzzi G Non-proliferative Diabetic Retinopathy, pp 19–63
- Bandello F, Lattanzio R, Zucchiatti I, Petruzzi G (2014) Non-proliferative Diabetic Retinopathy. In: *Clinical Strategies in the Management of Diabetic Retinopathy Clinical Strategies in the Management of Diabetic Retinopathy: A step-by-step Guide for Ophthalmologists*. Springer Berlin Heidelberg, Berlin, Heidelberg, s.l., pp 19–63

## 9 References

- Barber AJ, Gardner TW, Abcouwer SF (2011) The significance of vascular and neural apoptosis to the pathology of diabetic retinopathy. *Investigative ophthalmology & visual science* 52(2):1156–1163
- Baulmann DC, Ohlmann A, Flügel-Koch C, Goswami S, Cvekl A, Tamm ER (2002) Pax6 heterozygous eyes show defects in chamber angle differentiation that are associated with a wide spectrum of other anterior eye segment abnormalities. *Mechanisms of development* 118(1-2):3–17
- Bell RD, Winkler EA, Sagare AP, Singh I, LaRue B, Deane R, Zlokovic BV (2010) Pericytes control key neurovascular functions and neuronal phenotype in the adult brain and during brain aging. *Neuron* 68(3):409–427
- Bergers G, Song S (2005) The role of pericytes in blood-vessel formation and maintenance. *Neuro-oncology* 7(4):452–464
- Bill A, Tornquist P, Alm A (1980) Permeability of the intraocular blood vessels. *Transactions of the ophthalmological societies of the United Kingdom* 100(3):332–336
- Bird AC, Bressler NM, Bressler SB, Chisholm IH, Coscas G, Davis MD, Jong P de, Klaver C, Klein B, Klein R, Mitchell P, Sarks JP, Sarks SH, Soubrane G, Taylor HR, Vingerling JR (1995) An international classification and grading system for age-related maculopathy and age-related macular degeneration. *Survey of Ophthalmology* 39(5):367–374
- Blaauwgeers HG, Holtkamp GM, Rutten H, Witmer AN, Koolwijk P, Partanen TA, Alitalo K, Kroon ME, Kijlstra A, van Hinsbergh VW, Schlingemann RO (1999) Polarized vascular endothelial growth factor secretion by human retinal pigment epithelium and localization of vascular endothelial growth factor receptors on the inner choriocapillaris. Evidence for a trophic paracrine relation. *The American journal of pathology* 155(2):421–428
- Bondjers C, Kalén M, Hellström M, Scheidl SJ, Abramsson A, Renner O, Lindahl P, Cho H, Kehrl J, Betsholtz C (2003) Transcription Profiling of Platelet-Derived Growth Factor-B-

## 9 References

- Deficient Mouse Embryos Identifies RGS5 as a Novel Marker for Pericytes and Vascular Smooth Muscle Cells. *The American journal of pathology* 162(3):721–729
- Boneva SK, Gross TR, Schlecht A, Schmitt SI, Sippl C, Jagle H, Volz C, Neueder A, Tamm ER, Braunger BM (2016) Cre recombinase expression or topical tamoxifen treatment do not affect retinal structure and function, neuronal vulnerability or glial reactivity in the mouse eye. *Neuroscience* 325:188–201
- Booij JC, Baas DC, Beisekeeva J, Gorgels, T G M F, Bergen AAB (2010) The dynamic nature of Bruch's membrane. *Progress in retinal and eye research* 29(1):1–18
- Bourdeau A, Dumont DJ, Letarte M (1999) A murine model of hereditary hemorrhagic telangiectasia. *The Journal of clinical investigation* 104(10):1343–1351
- Bowes Rickman C, Farsiu S, Toth CA, Klingeborn M (2013) Dry age-related macular degeneration: mechanisms, therapeutic targets, and imaging. *Investigative ophthalmology & visual science* 54(14):ORSF68-80
- Branda CS, Dymecki SM (2004) Talking about a revolution: The impact of site-specific recombinases on genetic analyses in mice. *Developmental cell* 6(1):7–28
- Braunger BM (2014) Molecular analysis of the neuroprotective role of Norrin for photoreceptors in the mammalian retina
- Braunger BM, Ademoglu B, Koschade SE, Fuchshofer R, Gabelt BT, Kiland JA, Hennes-Beann EA, Brunner KG, Kaufman PL, Tamm ER (2014) Identification of adult stem cells in Schwalbe's line region of the primate eye. *Investigative ophthalmology & visual science* 55(11):7499–7507
- Braunger BM, Leimbeck SV, Schlecht A, Volz C, Jäggle H, Tamm ER (2015) Deletion of ocular transforming growth factor  $\beta$  signaling mimics essential characteristics of diabetic retinopathy. *The American journal of pathology* 185(6):1749–1768
- Braunger BM, Ohlmann A, Koch M, Tanimoto N, Volz C, Yang Y, Bösl MR, Cvekl A, Jäggle H, Seeliger MW, Tamm ER (2013a) Constitutive overexpression of Norrin activates Wnt/ $\beta$ -

## 9 References

- catenin and endothelin-2 signaling to protect photoreceptors from light damage.  
Neurobiology of disease 50:1–12
- Braunger BM, Pielmeier S, Demmer C, Landstorfer V, Kawall D, Abramov N, Leibinger M, Kleiter I, Fischer D, Jäggle H, Tamm ER (2013b) TGF- $\beta$  signaling protects retinal neurons from programmed cell death during the development of the mammalian eye. The Journal of neuroscience : the official journal of the Society for Neuroscience 33(35):14246–14258
- Cai J, Boulton M (2002) The pathogenesis of diabetic retinopathy. Old concepts and new questions. Eye 16(3):242–260
- Cai X, McGinnis JF (2016) Diabetic Retinopathy. Animal Models, Therapies, and Perspectives. Journal of Diabetes Research 2016(10):1–9
- Carmeliet P, Ruiz de Almodovar C (2013) VEGF ligands and receptors: implications in neurodevelopment and neurodegeneration. Cellular and molecular life sciences : CMLS 70(10):1763–1778
- Chambers RC, Leoni P, Kaminski N, Laurent GJ, Heller RA (2003) Global Expression Profiling of Fibroblast Responses to Transforming Growth Factor- $\beta$ 1 Reveals the Induction of Inhibitor of Differentiation-1 and Provides Evidence of Smooth Muscle Cell Phenotypic Switching. The American journal of pathology 162(2):533–546
- Chang H, Huylebroeck D, Verschueren K, Guo Q, Matzuk MM, Zwijsen A (1999) Smad5 knockout mice die at mid-gestation due to multiple embryonic and extraembryonic defects. Development (Cambridge, England) 126(8):1631–1642
- Chen M, Hou P, Tai T, Lin BJ (2008) Blood-Ocular Barriers. Tzu Chi Medical Journal 20(1):25–34
- Chen S (2003) Smad proteins regulate transcriptional induction of the SM22 $\alpha$  gene by TGF- $\beta$ . Nucleic Acids Research 31(4):1302–1310
- Chen S, Lechleider RJ (2004) Transforming growth factor- $\beta$ -induced differentiation of smooth muscle from a neural crest stem cell line. Circulation research 94(9):1195–1202

## 9 References

- Cheung N, Mitchell P, Wong TY (2010) Diabetic retinopathy. *The Lancet* 376(9735):124–136
- Chytil A, Magnuson MA, Wright CVE, Moses HL (2002) Conditional inactivation of the TGF-beta type II receptor using Cre:Lox. *Genesis (New York, N.Y. : 2000)* 32(2):73–75
- Clermont AC, Aiello LP, Mori F, Bursell S (1997) Vascular Endothelial Growth Factor and Severity of Nonproliferative Diabetic Retinopathy Mediate Retinal Hemodynamics In Vivo. A Potential Role for Vascular Endothelial Growth Factor in the Progression of Nonproliferative Diabetic Retinopathy. *American Journal of Ophthalmology* 124(4):433–446
- Cogan DG (1961) Retinal Vascular Patterns. *Arch Ophthalmol* 66(3):366
- Coleman HR, Chan C, Ferris FL, Chew EY (2008) Age-related macular degeneration. *The Lancet* 372(9652):1835–1845
- Combadiere C, Feumi C, Raoul W, Keller N, Rodero M, Pezard A, Lavalette S, Houssier M, Jonet L, Picard E, Debre P, Sirinyan M, Deterre P, Ferroukhi T, Cohen S, Chauvaud D, Jeanny J, Chemtob S, Behar-Cohen F, Sennlaub F (2007) CX3CR1-dependent subretinal microglia cell accumulation is associated with cardinal features of age-related macular degeneration. *The Journal of clinical investigation* 117(10):2920–2928
- Congdon N, O'Colmain B, Klaver CC, Klein R, Munoz B, Friedman DS, Kempen J, Taylor HR, Mitchell P (2004) Causes and prevalence of visual impairment among adults in the United States. *Archives of ophthalmology (Chicago, Ill. : 1960)* 122(4):477–485
- Congdon NG, Friedman DS, Lietman T (2003) Important causes of visual impairment in the world today. *JAMA* 290(15):2057–2060
- Cunha-Vaz J (2009) The Blood–Retinal Barrier in Retinal Disease. *European Ophthalmic Review* 03(02):105
- Cunha-Vaz J, Bernardes R, Lobo C (2011) Blood-retinal barrier. *EJO* 21(Suppl. 6):3–9
- Cunha-Vaz JG (1976) The blood-retinal barriers. *Doc Ophthalmol* 41(2):287–327

## 9 References

- Curcio CA, Presley JB, Millican CL, Medeiros NE (2005) Basal deposits and drusen in eyes with age-related maculopathy: evidence for solid lipid particles. *Experimental Eye Research* 80(6):761–775
- Cvetanovic M, Patel JM, Marti HH, Kini AR, Opal P (2011) Vascular endothelial growth factor ameliorates the ataxic phenotype in a mouse model of spinocerebellar ataxia type 1. *Nature medicine* 17(11):1445–1447
- Daneman R, Zhou L, Kebede AA, Barres BA (2010) Pericytes are required for blood-brain barrier integrity during embryogenesis. *Nature* 468(7323):562–566
- Darland DC, D'Amore PA (2001) TGF beta is required for the formation of capillary-like structures in three-dimensional cocultures of 10T1/2 and endothelial cells. *Angiogenesis* 4(1):11–20
- Das A, McGuire PG, Rangasamy S (2015) Diabetic Macular Edema. *Pathophysiology and Novel Therapeutic Targets*. *Ophthalmology* 122(7):1375–1394
- de Jong, Paulus T V M (2006) Age-related macular degeneration. *The New England journal of medicine* 355(14):1474–1485
- Deangelis MM, Ji F, Adams S, Morrison MA, Harring AJ, Sweeney MO, Capone A, JR, Miller JW, Dryja TP, Ott J, Kim IK (2008) Alleles in the HtrA serine peptidase 1 gene alter the risk of neovascular age-related macular degeneration. *Ophthalmology* 115(7):1209-1215.e7
- Dewan A, Liu M, Hartman S, Zhang SS, Liu DTL, Zhao C, Tam POS, Chan WM, Lam DSC, Snyder M, Barnstable C, Pang CP, Hoh J (2006) HTRA1 promoter polymorphism in wet age-related macular degeneration. *Science (New York, N.Y.)* 314(5801):989–992
- Díaz-Flores L, Gutiérrez R, Madrid JF, Varela H, Valladares F, Acosta E, Martín-Vasallo P (2009) Pericytes. Morphofunction, interactions and pathology in a quiescent and activated mesenchymal cell niche. *Histology and histopathology* 24(7):909–969
- Dickson MC, Martin JS, Cousins FM, Kulkarni AB, Karlsson S, Akhurst RJ (1995) Defective haematopoiesis and vasculogenesis in transforming growth factor-beta 1 knock out mice. *Development (Cambridge, England)* 121(6):1845–1854

## 9 References

- Diez-Roux G, Lang RA (1997) Macrophages induce apoptosis in normal cells in vivo. *Development (Cambridge, England)* 124(18):3633–3638
- Dijke P ten, Goumans M, Pardali E (2008) Endoglin in angiogenesis and vascular diseases. *Angiogenesis* 11(1):79–89
- Ding R, Darland DC, Parmacek MS, D'amore PA (2004) Endothelial-mesenchymal interactions in vitro reveal molecular mechanisms of smooth muscle/pericyte differentiation. *Stem cells and development* 13(5):509–520
- Dobi ET, Puliafito CA, Destro M (1989) A new model of experimental choroidal neovascularization in the rat. *Archives of ophthalmology (Chicago, Ill. : 1960)* 107(2):264–269
- Doetschman T, Gossler A, Kemler R (1987) Blastocyst-Derived Embryonic Stem Cells as a Model for Embryogenesis. In: *Future Aspects in Human In Vitro Fertilization Future Aspects in Human In Vitro Fertilization*. Springer Berlin Heidelberg, Berlin, Heidelberg, pp 187–195
- Dorrell MI, Aguilar E, Friedlander M (2002) Retinal vascular development is mediated by endothelial filopodia, a preexisting astrocytic template and specific R-cadherin adhesion. *Investigative ophthalmology & visual science* 43(11):3500–3510
- Engel M (2002) Endothelium-specific platelet-derived growth factor-B ablation mimics diabetic retinopathy. *The EMBO journal* 21(16):4307–4316
- Engerman RL (1989) Pathogenesis of Diabetic Retinopathy. *Diabetes* 38(10):1203–1206
- Erturk A, Becker K, Jahrling N, Mauch CP, Hojer CD, Egen JG, Hellal F, Bradke F, Sheng M, Dodt H (2012) Three-dimensional imaging of solvent-cleared organs using 3DISCO. *Nature protocols* 7(11):1983–1995
- Espinosa-Heidmann DG, Suner IJ, Hernandez EP, Monroy D, Csaky KG, Cousins SW (2003) Macrophage depletion diminishes lesion size and severity in experimental choroidal neovascularization. *Investigative ophthalmology & visual science* 44(8):3586–3592

## 9 References

- Esser S, Wolburg K, Wolburg H, Breier G, Kurzchalia T, Risau W (1998) Vascular endothelial growth factor induces endothelial fenestrations in vitro. *The Journal of Cell Biology* 140(4):947–959
- Evans JR, Fletcher AE, Wormald RPL (2005) 28,000 Cases of age related macular degeneration causing visual loss in people aged 75 years and above in the United Kingdom may be attributable to smoking. *The British journal of ophthalmology* 89(5):550–553
- Feil R, Brocard J, Mascrez B, LeMeur M, Metzger D, Chambon P (1996) Ligand-activated site-specific recombination in mice. *Proceedings of the National Academy of Sciences of the United States of America* 93(20):10887–10890
- Feil R, Wagner J, Metzger D, Chambon P (1997) Regulation of Cre recombinase activity by mutated estrogen receptor ligand-binding domains. *Biochemical and biophysical research communications* 237(3):752–757
- Feng Y, Vom Hagen F, Pfister F, Djokic S, Hoffmann S, Back W, Wagner P, Lin J, Deutsch U, Hammes H (2007) Impaired pericyte recruitment and abnormal retinal angiogenesis as a result of angiopoietin-2 overexpression. *Thrombosis and haemostasis* 97(1):99–108
- Finger RP, Fimmers R, Holz FG, Scholl HPN (2011) Incidence of blindness and severe visual impairment in Germany: projections for 2030. *Investigative ophthalmology & visual science* 52(7):4381–4389
- Ford KM, Saint-Geniez M, Walshe T, Zahr A, D'amore PA (2011) Expression and role of VEGF in the adult retinal pigment epithelium. *Investigative ophthalmology & visual science* 52(13):9478–9487
- Frank RN (2004) Diabetic retinopathy. *The New England journal of medicine* 350(1):48–58
- Friedman DS, Katz J, Bressler NM, Rahmani B, Tielsch JM (1999) Racial differences in the prevalence of age-related macular degeneration. *Ophthalmology* 106(6):1049–1055

## 9 References

- Friedman DS, O'Colmain BJ, Munoz B, Tomany SC, McCarty C, de Jong, Paulus T V M, Nemesure B, Mitchell P, Kempen J (2004) Prevalence of age-related macular degeneration in the United States. *Archives of ophthalmology* (Chicago, Ill. : 1960) 122(4):564–572
- Friedrich U, Datta S, Schubert T, Plossl K, Schneider M, Grassmann F, Fuchshofer R, Tiefenbach K, Langst G, Weber BHF (2015) Synonymous variants in HTRA1 implicated in AMD susceptibility impair its capacity to regulate TGF-beta signaling. *Human molecular genetics* 24(22):6361–6373
- Fritsche LG, Chen W, Schu M, Yaspan BL, Yu Y, Thorleifsson G, Zack DJ, Arakawa S, Cipriani V, Ripke S, Igo RP, JR, Buitendijk GHS, Sim X, Weeks DE, Guymer RH, Merriam JE, Francis PJ, Hannum G, Agarwal A, Armbrecht AM, Audo I, Aung T, Barile GR, Benchaboune M, Bird AC, Bishop PN, Branham KE, Brooks M, Brucker AJ, Cade WH, Cain MS, Campochiaro PA, Chan C, Cheng C, Chew EY, Chin KA, Chowers I, Clayton DG, Cojocaru R, Conley YP, Cornes BK, Daly MJ, Dhillon B, Edwards AO, Evangelou E, Fagerness J, Ferreyra HA, Friedman JS, Geirsdottir A, George RJ, Gieger C, Gupta N, Hagstrom SA, Harding SP, Haritoglou C, Heckenlively JR, Holz FG, Hughes G, Ioannidis JPA, Ishibashi T, Joseph P, Jun G, Kamatani Y, Katsanis N, Keilhauer C, Khan JC, Kim IK, Kiyohara Y, Klein BEK, Klein R, Kovach JL, Kozak I, Lee CJ, Lee KE, Lichtner P, Lotery AJ, Meitinger T, Mitchell P, Mohand-Said S, Moore AT, Morgan DJ, Morrison MA, Myers CE, Naj AC, Nakamura Y, Okada Y, Orlin A, Ortube MC, Othman MI, Pappas C, Park KH, Pauer GJT, Peachey NS, Poch O, Priya RR, Reynolds R, Richardson AJ, Ripp R, Rudolph G, Ryu E, Sahel J, Schaumberg DA, Scholl HPN, Schwartz SG, Scott WK, Shahid H, Sigurdsson H, Silvestri G, Sivakumaran TA, Smith RT, Sobrin L, Souied EH, Stambolian DE, Stefansson H, Sturgill-Short GM, Takahashi A, Tosakulwong N, Truitt BJ, Tsironi EE, Uitterlinden AG, van Duijn CM, Vijaya L, Vingerling JR, Vithana EN, Webster AR, Wichmann H, Winkler TW, Wong TY, Wright AF, Zelenika D, Zhang M, Zhao L, Zhang K, Klein ML, Hageman GS, Lathrop GM, Stefansson K, Allikmets R, Baird PN, Gorin MB, Wang JJ, Klaver CCW, Seddon

## 9 References

- JM, Pericak-Vance MA, Iyengar SK, Yates JRW, Swaroop A, Weber BHF, Kubo M, Deangelis MM, Leveillard T, Thorsteinsdottir U, Haines JL, Farrer LA, Heid IM, Abecasis GR (2013) Seven new loci associated with age-related macular degeneration. *Nature genetics* 45(4):433-9, 439e1-2
- Fritsche LG, Igl W, Bailey JNC, Grassmann F, Sengupta S, Bragg-Gresham JL, Burdon KP, Hebbaring SJ, Wen C, Gorski M, Kim IK, Cho D, Zack D, Souied E, Scholl HPN, Bala E, Lee KE, Hunter DJ, Sardell RJ, Mitchell P, Merriam JE, Cipriani V, Hoffman JD, Schick T, Lechanteur YTE, Guymer RH, Johnson MP, Jiang Y, Stanton CM, Buitendijk GHS, Zhan X, Kwong AM, Boleda A, Brooks M, Gieser L, Ratnapriya R, Branham KE, Foerster JR, Heckenlively JR, Othman MI, Vote BJ, Liang HH, Souzeau E, McAllister IL, Isaacs T, Hall J, Lake S, Mackey DA, Constable IJ, Craig JE, Kitchner TE, Yang Z, Su Z, Luo H, Chen D, Ouyang H, Flagg K, Lin D, Mao G, Ferreyra H, Stark K, Strachwitz CN von, Wolf A, Brandl C, Rudolph G, Olden M, Morrison MA, Morgan DJ, Schu M, Ahn J, Silvestri G, Tsironi EE, Park KH, Farrer LA, Orlin A, Brucker A, Li M, Curcio CA, Mohand-Said S, Sahel J, Audo I, Benchaboune M, Cree AJ, Rennie CA, Goverdhan SV, Grunin M, Hagbi-Levi S, Campochiaro P, Katsanis N, Holz FG, Blond F, Blanche H, Deleuze J, Igo RP, JR, Truitt B, Peachey NS, Meuer SM, Myers CE, Moore EL, Klein R, Hauser MA, Postel EA, Courtenay MD, Schwartz SG, Kovach JL, Scott WK, Liew G, Tan AG, Gopinath B, Merriam JC, Smith RT, Khan JC, Shahid H, Moore AT, McGrath JA, Laux R, Brantley MA, JR, Agarwal A, Ersoy L, Caramoy A, Langmann T, Saksens NTM, Jong EK de, Hoyng CB, Cain MS, Richardson AJ, Martin TM, Blangero J, Weeks DE, Dhillon B, van Duijn CM, Doheny KF, Romm J, Klaver CCW, Hayward C, Gorin MB, Klein ML, Baird PN, den Hollander AI, Fauser S, Yates JRW, Allikmets R, Wang JJ, Schaumberg DA, Klein BEK, Hagstrom SA, Chowers I, Lotery AJ, Leveillard T, Zhang K, Brilliant MH, Hewitt AW, Swaroop A, Chew EY, Pericak-Vance MA, DeAngelis M, Stambolian D, Haines JL, Iyengar SK, Weber BHF, Abecasis GR, Heid IM

## 9 References

- (2016) A large genome-wide association study of age-related macular degeneration highlights contributions of rare and common variants. *Nature genetics* 48(2):134–143
- Fruttiger M (2002) Development of the mouse retinal vasculature: angiogenesis versus vasculogenesis. *Investigative ophthalmology & visual science* 43(2):522–527
- Fruttiger M (2007) Development of the retinal vasculature. *Angiogenesis* 10(2):77–88
- Gaengel K, Genové G, Armulik A, Betsholtz C (2009) Endothelial-mural cell signaling in vascular development and angiogenesis. *Arteriosclerosis, thrombosis, and vascular biology* 29(5):630–638
- Gage PJ, Rhoades W, Prucka SK, Hjalt T (2005) Fate maps of neural crest and mesoderm in the mammalian eye. *Investigative ophthalmology & visual science* 46(11):4200–4208
- Gariano RF (2003) Cellular mechanisms in retinal vascular development. *Progress in retinal and eye research* 22(3):295–306
- Garner A (1993) Histopathology of diabetic retinopathy in man. *Eye (London, England)* 7 (Pt 2):250–253
- Goumans M, Liu Z, Dijke P ten (2009) TGF-beta signaling in vascular biology and dysfunction. *Cell research* 19(1):116–127
- Goumans M, Valdimarsdottir G, Itoh S, Rosendahl A, Sideras P, Dijke P ten (2002) Balancing the activation state of the endothelium via two distinct TGF-beta type I receptors. *The EMBO journal* 21(7):1743–1753
- Goumans MJ, Valdimarsdottir G, Itoh S, Lebrin F, Larsson J, Mummery C, Karlsson S, Dijke P ten (2003) Activin receptor-like kinase (ALK)1 is an antagonistic mediator of lateral TGFbeta/ALK5 signaling. *Molecular cell* 12(4):817–828
- Gunschmann C, Chiticariu E, Garg B, Hiz MM, Mostmans Y, Wehner M, Scharfenberger L (2014) Transgenic mouse technology in skin biology: inducible gene knockout in mice. *The Journal of investigative dermatology* 134(7):e22

## 9 References

- Haddad S, Chen CA, Santangelo SL, Seddon JM (2006) The genetics of age-related macular degeneration: a review of progress to date. *Survey of Ophthalmology* 51(4):316–363
- Hamilton RD, Leach L (2011) Isolation and properties of an in vitro human outer blood-retinal barrier model. *Methods in molecular biology* (Clifton, N.J.) 686:401–416
- Hammes H (2005) Pericytes and the pathogenesis of diabetic retinopathy. *Hormone and metabolic research = Hormon- und Stoffwechselforschung = Hormones et métabolisme* 37 Suppl 1:39–43
- Hammes H, Feng Y, Pfister F, Brownlee M (2011) Diabetic retinopathy: targeting vasoregression. *Diabetes* 60(1):9–16
- Hammes H, Lin J, Renner O, Shani M, Lundqvist A, Betsholtz C, Brownlee M, Deutsch U (2002) Pericytes and the Pathogenesis of Diabetic Retinopathy. *Diabetes* 51(10):3107–3112
- Hammes H, Lin J, Wagner P, Feng Y, Vom Hagen F, Krzizok T, Renner O, Breier G, Brownlee M, Deutsch U (2004) Angiopoietin-2 Causes Pericyte Dropout in the Normal Retina. Evidence for Involvement in Diabetic Retinopathy. *Diabetes* 53(4):1104–1110
- Hayashi S, McMahon AP (2002) Efficient recombination in diverse tissues by a tamoxifen-inducible form of Cre: a tool for temporally regulated gene activation/inactivation in the mouse. *Developmental biology* 244(2):305–318
- Heldin CH, Miyazono K, Dijke P ten (1997) TGF-beta signalling from cell membrane to nucleus through SMAD proteins. *Nature* 390(6659):465–471
- Hellström M, Gerhardt H, Kalén M, Li X, Eriksson U, Wolburg H, Betsholtz C (2001) Lack of Pericytes Leads to Endothelial Hyperplasia and Abnormal Vascular Morphogenesis. *J Cell Biol* 153(3):543–554
- Hellström M, Kalén M, Lindahl P, Abramsson A, Betsholtz C (1999) Role of PDGF-B and PDGFR-beta in recruitment of vascular smooth muscle cells and pericytes during embryonic blood vessel formation in the mouse. *Development (Cambridge, England)* 126(14):3047–3055

## 9 References

- Herrnberger L, Seitz R, Kuespert S, Bösl MR, Fuchshofer R, Tamm ER (2012) Lack of endothelial diaphragms in fenestrae and caveolae of mutant Plvap-deficient mice. *Histochem Cell Biol* 138(5):709–724
- Hirase K, Ikeda T, Sotozono C, Nishida K, Sawa H, Kinoshita S (1998) Transforming growth factor beta2 in the vitreous in proliferative diabetic retinopathy. *Archives of ophthalmology* (Chicago, Ill. : 1960) 116(6):738–741
- Hirschi KK, Rohovsky SA, D'amore PA (1998) PDGF, TGF- $\beta$ , and Heterotypic Cell–Cell Interactions Mediate Endothelial Cell–induced Recruitment of 10T1/2 Cells and Their Differentiation to a Smooth Muscle Fate. *J Cell Biol* 141(3):805–814
- Hogg RE, Chakravarthy U (2006) Visual function and dysfunction in early and late age-related maculopathy. *Progress in retinal and eye research* 25(3):249–276
- Hughes S, Chan-Ling T (2004) Characterization of smooth muscle cell and pericyte differentiation in the rat retina in vivo. *Investigative ophthalmology & visual science* 45(8):2795–2806
- Hughes S, Yang H, Chan-Ling T (2000) Vascularization of the human fetal retina: roles of vasculogenesis and angiogenesis. *Investigative ophthalmology & visual science* 41(5):1217–1228
- Hume DA, Halpin D, Charlton H, Gordon S (1984) The mononuclear phagocyte system of the mouse defined by immunohistochemical localization of antigen F4/80: macrophages of endocrine organs. *Proceedings of the National Academy of Sciences of the United States of America* 81(13):4174–4177
- Hume DA, Perry VH, Gordon S (1983) Immunohistochemical localization of a macrophage-specific antigen in developing mouse retina: phagocytosis of dying neurons and differentiation of microglial cells to form a regular array in the plexiform layers. *The Journal of Cell Biology* 97(1):253–257

## 9 References

- Indra AK, Warot X, Brocard J, Bornert JM, Xiao JH, Chambon P, Metzger D (1999) Temporally-controlled site-specific mutagenesis in the basal layer of the epidermis: comparison of the recombinase activity of the tamoxifen-inducible Cre-ER(T) and Cre-ER(T2) recombinases. *Nucleic Acids Research* 27(22):4324–4327
- Itoh F, Itoh S, Adachi T, Ichikawa K, Matsumura Y, Takagi T, Festing M, Watanabe T, Weinstein M, Karlsson S, Kato M (2012) Smad2/Smad3 in endothelium is indispensable for vascular stability via S1PR1 and N-cadherin expressions. *Blood* 119(22):5320–5328
- Jager RD, Mieler WF, Miller JW (2008) Age-related macular degeneration. *The New England journal of medicine* 358(24):2606–2617
- Jakobsson L, van Meeteren LA (2013) Transforming growth factor  $\beta$  family members in regulation of vascular function: in the light of vascular conditional knockouts. *Experimental cell research* 319(9):1264–1270
- Jeon S, Chae B, Kim H, Seo G, Seo D, Chun G, Kim N, Yie S, Byeon W, Eom S, Ha K, Kim Y, Kim P (2007) Mechanisms underlying TGF-beta1-induced expression of VEGF and Flk-1 in mouse macrophages and their implications for angiogenesis. *Journal of leukocyte biology* 81(2):557–566
- Jiang B, Bezhadian MA, Caldwell RB (1995) Astrocytes modulate retinal vasculogenesis: effects on endothelial cell differentiation. *Glia* 15(1):1–10
- Jin K, Zhu Y, Sun Y, Mao XO, Xie L, Greenberg DA (2002) Vascular endothelial growth factor (VEGF) stimulates neurogenesis in vitro and in vivo. *Proceedings of the National Academy of Sciences of the United States of America* 99(18):11946–11950
- Jordan J, Ruiz-Moreno JM (2013) Advances in the understanding of retinal drug disposition and the role of blood-ocular barrier transporters. *Expert opinion on drug metabolism & toxicology* 9(9):1181–1192
- Joussen AM, Doehmen S, Le ML, Koizumi K, Radetzky S, Krohne TU, Poulaki V, Semkova I, Kociok N (2009) TNF-alpha mediated apoptosis plays an important role in the development

## 9 References

- of early diabetic retinopathy and long-term histopathological alterations. *Molecular vision* 15:1418–1428
- Joussen AM, Murata T, Tsujikawa A, Kirchhof B, Bursell S, Adamis AP (2001) Leukocyte-Mediated Endothelial Cell Injury and Death in the Diabetic Retina. *The American journal of pathology* 158(1):147–152
- Joussen AM, Poulaki V, Le ML, Koizumi K, Esser C, Janicki H, Schraermeyer U, Kociok N, Fauser S, Kirchhof B, Kern TS, Adamis AP (2004) A central role for inflammation in the pathogenesis of diabetic retinopathy. *FASEB journal : official publication of the Federation of American Societies for Experimental Biology* 18(12):1450–1452
- Kamba T, Tam BYY, Hashizume H, Haskell A, Sennino B, Mancuso MR, Norberg SM, O'Brien SM, Davis RB, Gowen LC, Anderson KD, Thurston G, Joho S, Springer ML, Kuo CJ, McDonald DM (2006) VEGF-dependent plasticity of fenestrated capillaries in the normal adult microvasculature. *American journal of physiology. Heart and circulatory physiology* 290(2):H560-76
- Kannan R, Zhang N, Sreekumar PG, Spee CK, Rodriguez A, Barron E, Hinton DR (2006) Stimulation of apical and basolateral VEGF-A and VEGF-C secretion by oxidative stress in polarized retinal pigment epithelial cells. *Molecular vision* 12:1649–1659
- Karnovsky MJ (1965) A Formaldehyde-Glutaraldehyde Fixative of High Osmolarity for Use in Electron Microscopy. *The Journal of Cell Biology*(Vol. 27, No. 2):137–138
- Kaufman PL, Alm A, Adler FH (eds) (2003) *Adler's physiology of the eye. Clinical application*, 10th edn. Mosby, St. Louis
- Kern TS (2007) Contributions of inflammatory processes to the development of the early stages of diabetic retinopathy. *Experimental diabetes research* 2007:95103
- Kilic U, Kilic E, Jarve A, Guo Z, Spudich A, Bieber K, Barzena U, Bassetti CL, Marti HH, Hermann DM (2006) Human vascular endothelial growth factor protects axotomized retinal

## 9 References

- ganglion cells in vivo by activating ERK-1/2 and Akt pathways. *The Journal of neuroscience* : the official journal of the Society for Neuroscience 26(48):12439–12446
- Kim J, Nakashima K, Crombrughe B de (2004) Transgenic mice expressing a ligand-inducible cre recombinase in osteoblasts and odontoblasts: a new tool to examine physiology and disease of postnatal bone and tooth. *The American journal of pathology* 165(6):1875–1882
- Kim LA, Amarnani D, Gnanaguru G, Tseng WA, Vavvas DG, D'amore PA (2014) Tamoxifen toxicity in cultured retinal pigment epithelial cells is mediated by concurrent regulated cell death mechanisms. *Investigative ophthalmology & visual science* 55(8):4747–4758
- Kingsley DM (1994) The TGF-beta superfamily. New members, new receptors, and new genetic tests of function in different organisms. *Genes & Development* 8(2):133–146
- Kita T, Hata Y, Kano K, Miura M, Nakao S, Noda Y, Shimokawa H, Ishibashi T (2006) Transforming Growth Factor- 2 and Connective Tissue Growth Factor in Proliferative Vitreoretinal Diseases. Possible Involvement of Hyalocytes and Therapeutic Potential of Rho Kinase Inhibitor. *Diabetes* 56(1):231–238
- Klaassen I, Van Noorden, Cornelis J F, Schlingemann RO (2013) Molecular basis of the inner blood-retinal barrier and its breakdown in diabetic macular edema and other pathological conditions. *Progress in retinal and eye research* 34:19–48
- Klaver CC, Wolfs RC, Vingerling JR, Hofman A, Jong PT de (1998) Age-specific prevalence and causes of blindness and visual impairment in an older population: the Rotterdam Study. *Archives of ophthalmology (Chicago, Ill. : 1960)* 116(5):653–658
- Klein R, Klein BE, Cruickshanks KJ (1999) The prevalence of age-related maculopathy by geographic region and ethnicity<sup>1</sup>This paper has been edited by Neville N. Osborne, PhD, DSc, Nuffield Laboratory of Ophthalmology, University of Oxford, Walton Street, Oxford, UK; and Gerald J. Chader, The Foundation Fighting Blindness, Hunt Valley, MS.1. *Progress in retinal and eye research* 18(3):371–389

## 9 References

- Klein R, Klein BE, Linton KL (1992) Prevalence of Age-related Maculopathy. *Ophthalmology* 99(6):933–943
- Kritzenberger M, Junglas B, Framme C, Helbig H, Gabel V, Fuchshofer R, Tamm ER, Hillenkamp J (2011) Different collagen types define two types of idiopathic epiretinal membranes. *Histopathology* 58(6):953–965
- Kroeber M, Davis N, Holzmann S, Kritzenberger M, Shelah-Goraly M, Ofri R, Ashery-Padan R, Tamm ER (2010) Reduced expression of Pax6 in lens and cornea of mutant mice leads to failure of chamber angle development and juvenile glaucoma. *Human molecular genetics* 19(17):3332–3342
- Krueger M, Bechmann I (2010) CNS pericytes: concepts, misconceptions, and a way out. *Glia* 58(1):1–10
- Kugler M, Schlecht A, Fuchshofer R, Kleiter I, Aigner L, Tamm ER, Braunger BM (2015) Heterozygous modulation of TGF-beta signaling does not influence Muller glia cell reactivity or proliferation following NMDA-induced damage. *Histochemistry and cell biology* 144(5):443–455
- Kuhbandner S, Brummer S, Metzger D, Chambon P, Hofmann F, Feil R (2000) Temporally controlled somatic mutagenesis in smooth muscle. *Genesis (New York, N.Y. : 2000)* 28(1):15–22
- Kuhn R, Torres RM (2002) Cre/loxP recombination system and gene targeting. *Methods in molecular biology (Clifton, N.J.)* 180:175–204
- Kühn R, Torres RM (2002) Cre/loxP recombination system and gene targeting. *Methods in molecular biology (Clifton, N.J.)* 180:175–204
- Kumar MS, Owens GK (2003) Combinatorial control of smooth muscle-specific gene expression. *Arteriosclerosis, thrombosis, and vascular biology* 23(5):737–747

## 9 References

- Kur J, Newman EA, Chan-Ling T (2012) Cellular and physiological mechanisms underlying blood flow regulation in the retina and choroid in health and disease. *Progress in retinal and eye research* 31(5):377–406
- Kurihara T, Westenskow PD, Bravo S, Aguilar E, Friedlander M (2012) Targeted deletion of Vegfa in adult mice induces vision loss. *The Journal of clinical investigation* 122(11):4213–4217
- Kuwabara T (1963) Retinal Vascular Patterns. *Arch Ophthalmol* 69(4):492
- Lang RA, Bishop JM (1993) Macrophages are required for cell death and tissue remodeling in the developing mouse eye. *Cell* 74(3):453–462
- Langmann T (2007) Microglia activation in retinal degeneration. *Journal of leukocyte biology* 81(6):1345–1351
- Larsson J, Goumans MJ, Sjöstrand LJ, van Rooijen MA, Ward D, Levéen P, Xu X, Dijke P ten, Mummery CL, Karlsson S (2001) Abnormal angiogenesis but intact hematopoietic potential in TGF-beta type I receptor-deficient mice. *The EMBO journal* 20(7):1663–1673
- Le Y, Bai Y, Zhu M, Zheng L (2010) Temporal requirement of RPE-derived VEGF in the development of choroidal vasculature. *Journal of neurochemistry* 112(6):1584–1592
- Le Y, Zheng W, Rao P, Zheng L, Anderson RE, Esumi N, Zack DJ, Zhu M (2008) Inducible expression of cre recombinase in the retinal pigmented epithelium. *Investigative ophthalmology & visual science* 49(3):1248–1253
- Lee KS, Park SJ, Kim SR, Min KH, Lee KY, Choe YH, Hong SH, Lee YR, Kim JS, Hong SJ, Lee YC (2008) Inhibition of VEGF blocks TGF-beta1 production through a PI3K/Akt signalling pathway. *The European respiratory journal* 31(3):523–531
- Leenaars M, Hendriksen CFM (2005) Critical steps in the production of polyclonal and monoclonal antibodies: evaluation and recommendations. *ILAR journal / National Research Council, Institute of Laboratory Animal Resources* 46(3):269–279

## 9 References

- Leenaars M, Koedam MA, Hendriksen CF, Claassen E (1998) Immune responses and side effects of five different oil-based adjuvants in mice. *Veterinary immunology and immunopathology* 61(2-4):291–304
- Leone DP, Genoud S, Atanasoski S, Grausenburger R, Berger P, Metzger D, Macklin WB, Chambon P, Suter U (2003) Tamoxifen-inducible glia-specific Cre mice for somatic mutagenesis in oligodendrocytes and Schwann cells. *Molecular and cellular neurosciences* 22(4):430–440
- Li DY (1999) Defective Angiogenesis in Mice Lacking Endoglin. *Science* 284(5419):1534–1537
- Li F, Lan Y, Wang Y, Wang J, Yang G, Meng F, Han H, Meng A, Wang Y, Yang X (2011) Endothelial Smad4 maintains cerebrovascular integrity by activating N-cadherin through cooperation with Notch. *Developmental cell* 20(3):291–302
- Li Z, Bork JP, Krueger B, Patsenker E, Schulze-Krebs A, Hahn EG, Schuppan D (2005) VEGF induces proliferation, migration, and TGF-beta1 expression in mouse glomerular endothelial cells via mitogen-activated protein kinase and phosphatidylinositol 3-kinase. *Biochemical and biophysical research communications* 334(4):1049–1060
- Lim LS, Mitchell P, Seddon JM, Holz FG, Wong TY (2012) Age-related macular degeneration. *Lancet (London, England)* 379(9827):1728–1738
- Lindahl P, Johansson BR, Levéen P, Betsholtz C (1997) Pericyte loss and microaneurysm formation in PDGF-B-deficient mice. *Science (New York, N.Y.)* 277(5323):242–245
- Ling TL, Mitrofanis J, Stone J (1989) Origin of retinal astrocytes in the rat: evidence of migration from the optic nerve. *The Journal of comparative neurology* 286(3):345–352
- Livak KJ, Schmittgen TD (2001) Analysis of relative gene expression data using real-time quantitative PCR and the 2<sup>(-Delta Delta C(T))</sup> Method. *Methods (San Diego, Calif.)* 25(4):402–408

## 9 References

- Lobov IB, Rao S, Carroll TJ, Vallance JE, Ito M, Ondr JK, Kurup S, Glass DA, Patel MS, Shu W, Morrissey EE, McMahon AP, Karsenty G, Lang RA (2005) WNT7b mediates macrophage-induced programmed cell death in patterning of the vasculature. *Nature* 437(7057):417–421
- Loeffler KU, Lee WR (1992) Is basal laminar deposit unique for age-related macular degeneration? *Archives of ophthalmology (Chicago, Ill. : 1960)* 110(1):15–16
- Loffler KU, Lee WR (1986) Basal linear deposit in the human macula. *Graefe's Arch Clin Exp Ophthalmol* 224(6):493–501
- Ma M, Ma Y, Yi X, Guo R, Zhu W, Fan X, Xu G, Frey WH2, Liu X (2008) Intranasal delivery of transforming growth factor-beta1 in mice after stroke reduces infarct volume and increases neurogenesis in the subventricular zone. *BMC neuroscience* 9:117
- Ma W, Zhao L, Fontainhas AM, Fariss RN, Wong WT (2009a) Microglia in the mouse retina alter the structure and function of retinal pigmented epithelial cells: a potential cellular interaction relevant to AMD. *PLoS one* 4(11):e7945
- Ma Y, Li K, Wang J, Huang Y, Huang Y, Sun F (2009b) Vascular endothelial growth factor acutely reduces calcium influx via inhibition of the Ca<sup>2+</sup> channels in rat hippocampal neurons. *Journal of neuroscience research* 87(2):393–402
- Maddison K, Clarke AR (2005) New approaches for modelling cancer mechanisms in the mouse. *The Journal of pathology* 205(2):181–193
- Maguire P, Vine AK (1986) Geographic atrophy of the retinal pigment epithelium. *American Journal of Ophthalmology* 102(5):621–625
- Mandarino LJ, Sundarraj N, Finlayson J, Hassell JR (1993) Regulation of Fibronectin and Laminin Synthesis by Retinal Capillary Endothelial Cells and Pericytes In Vitro. *Experimental Eye Research* 57(5):609–621
- Marneros AG, Fan J, Yokoyama Y, Gerber HP, Ferrara N, Crouch RK, Olsen BR (2005) Vascular endothelial growth factor expression in the retinal pigment epithelium is essential

## 9 References

- for choriocapillaris development and visual function. *The American journal of pathology* 167(5):1451–1459
- Marshall GE, Konstas AG, Reid GG, Edwards JG, Lee WR (1992) Type IV collagen and laminin in Bruch's membrane and basal linear deposit in the human macula. *The British journal of ophthalmology* 76(10):607–614
- Massague J (2000) How cells read TGF-beta signals. *Nature reviews. Molecular cell biology* 1(3):169–178
- Massagué J (1992) Receptors for the TGF- $\beta$  family. *Cell* 69(7):1067–1070
- Massagué J (1998) TGF-beta signal transduction. *Annual review of biochemistry* 67:753–791
- Massagué J (2012) TGF $\beta$  signalling in context. *Nat Rev Mol Cell Biol* 13(10):616–630
- Massagué J, Attisano L, Wrana JL (1994) The TGF-beta family and its composite receptors. *Trends in cell biology* 4(5):172–178
- Mattapallil MJ, Wawrousek EF, Chan C, Zhao H, Roychoudhury J, Ferguson TA, Caspi RR (2012) The Rd8 mutation of the Crb1 gene is present in vendor lines of C57BL/6N mice and embryonic stem cells, and confounds ocular induced mutant phenotypes. *Investigative ophthalmology & visual science* 53(6):2921–2927
- Miller JW (2013) Age-related macular degeneration revisited--piecing the puzzle: the LXIX Edward Jackson memorial lecture. *American Journal of Ophthalmology* 155(1):1-35.e13
- Miller JW, Le Couter J, Strauss EC, Ferrara N (2013) Vascular endothelial growth factor a in intraocular vascular disease. *Ophthalmology* 120(1):106–114
- Mitchell P, Smith W, Attebo K, Wang JJ (1995) Prevalence of Age-related Maculopathy in Australia. *Ophthalmology* 102(10):1450–1460
- Mizutani M, Kern TS, Lorenzi M (1996) Accelerated death of retinal microvascular cells in human and experimental diabetic retinopathy. *The Journal of clinical investigation* 97(12):2883–2890
- Monvoisin A, Alva JA, Hofmann JJ, Zovein AC, Lane TF, Iruela-Arispe ML (2006) VE-cadherin-CreERT2 transgenic mouse: a model for inducible recombination in the endothelium.

## 9 References

- Developmental dynamics : an official publication of the American Association of Anatomists  
235(12):3413–3422
- Muzumdar MD, Tasic B, Miyamichi K, Li L, Luo L (2007) A global double-fluorescent Cre reporter mouse. *Genesis* (New York, N.Y. : 2000) 45(9):593–605
- Nakayama M, Iejima D, Akahori M, Kamei J, Goto A, Iwata T (2014) Overexpression of HtrA1 and exposure to mainstream cigarette smoke leads to choroidal neovascularization and subretinal deposits in aged mice. *Investigative ophthalmology & visual science* 55(10):6514–6523
- Nam E, Park S, Kim P (2010) TGF-beta1 induces mouse dendritic cells to express VEGF and its receptor (Flt-1) under hypoxic conditions. *Experimental & molecular medicine* 42(9):606–613
- National Research Council (U.S.), Institute for Laboratory Animal Research (U.S.) (2011) Guide for the care and use of laboratory animals, 8th edn. National Academies Press, Washington, D.C
- Nehls V (1991) Heterogeneity of microvascular pericytes for smooth muscle type alpha- actin. *The Journal of Cell Biology* 113(1):147–154
- Neubauer K, Krüger M, Quondamatteo F, Knittel T, Saile B, Ramadori G (1999) Transforming growth factor- $\beta$ 1 stimulates the synthesis of basement membrane proteins laminin, collagen type IV and entactin in rat liver sinusoidal endothelial cells. *Journal of Hepatology* 31(4):692–702
- Nguyen H, Lee YJ, Shin J, Lee E, Park SO, McCarty JH, Oh SP (2011) TGF- $\beta$  signaling in endothelial cells, but not neuroepithelial cells, is essential for cerebral vascular development. *Laboratory investigation; a journal of technical methods and pathology* 91(11):1554–1563
- Niederhorn JY (2006) See no evil, hear no evil, do no evil: the lessons of immune privilege. *Nature immunology* 7(4):354–359
- Nussenblatt RB, Ferris F (2007) Age-related macular degeneration and the immune response: implications for therapy. *American Journal of Ophthalmology* 144(4):618–626

## 9 References

- Ohlmann A, Scholz M, Koch M, Tamm ER (2016) Epithelial-mesenchymal transition of the retinal pigment epithelium causes choriocapillaris atrophy. *Histochemistry and cell biology*
- Orlidge A (1987) Inhibition of capillary endothelial cell growth by pericytes and smooth muscle cells. *The Journal of Cell Biology* 105(3):1455–1462
- Oshima M, Oshima H, Taketo MM (1996) TGF-beta receptor type II deficiency results in defects of yolk sac hematopoiesis and vasculogenesis. *Developmental biology* 179(1):297–302
- Oshima Y, Oshima S, Nambu H, Kachi S, Hackett SF, Melia M, Kaleko M, Connelly S, Esumi N, Zack DJ, Campochiaro PA (2004) Increased expression of VEGF in retinal pigmented epithelial cells is not sufficient to cause choroidal neovascularization. *Journal of cellular physiology* 201(3):393–400
- Ozerdem U, Grako KA, Dahlin-Huppe K, Monosov E, Stallcup WB (2001) NG2 proteoglycan is expressed exclusively by mural cells during vascular morphogenesis. *Developmental dynamics : an official publication of the American Association of Anatomists* 222(2):218–227
- Pardali E, Goumans M, Dijke P ten (2010) Signaling by members of the TGF-beta family in vascular morphogenesis and disease. *Trends in cell biology* 20(9):556–567
- Park HL, Kim JH, Park CK (2013) VEGF induces TGF-beta1 expression and myofibroblast transformation after glaucoma surgery. *The American journal of pathology* 182(6):2147–2154
- Park SM, Jung JS, Jang MS, Kang KS, Kang SK (2008) Transforming growth factor-beta1 regulates the fate of cultured spinal cord-derived neural progenitor cells. *Cell proliferation* 41(2):248–264
- Pascolini D, Mariotti SP, Pokharel GP, Pararajasegaram R, Etya'ale D, Negrel AD, Resnikoff S (2004) 2002 global update of available data on visual impairment: a compilation of population-based prevalence studies. *Ophthalmic epidemiology* 11(2):67–115
- Patel-Hett S, D'amore PA (2011) Signal transduction in vasculogenesis and developmental angiogenesis. *The International journal of developmental biology* 55(4-5):353–363

## 9 References

- Pauleikhoff D (2005) neovascular age-related macular degeneration: Natural History and Treatment Outcomes. *Retina* (Philadelphia, Pa.) 25(8):1065–1084
- Peyman GA, Bok D (1972) Peroxidase diffusion in the normal and laser-coagulated primate retina. *Investigative ophthalmology* 11(1):35–45
- Pfeffer BA, Flanders KC, Guerin CJ, Danielpour D, Anderson DH (1994) Transforming growth factor beta 2 is the predominant isoform in the neural retina, retinal pigment epithelium-choroid and vitreous of the monkey eye. *Experimental Eye Research* 59(3):323–333
- Phillips BE, Antonetti DA, Berkowitz BA (2007) Blood Retinal Barrier. In: *Retinal Vascular Disease Retinal Vascular Disease*. Springer-Verlag Berlin Heidelberg, Berlin, Heidelberg, pp 139–166
- Rajewsky K, Gu H, Kuhn R, Betz UA, Muller W, Roes J, Schwenk F (1996) Conditional gene targeting. *The Journal of clinical investigation* 98(3):600–603
- Richardson KC, Jarett L, Finke EH (2009) Embedding in Epoxy Resins for Ultrathin Sectioning in Electron Microscopy. *Stain technology* 35(6):313–323
- Risau W, Sariola H, Zerwes HG, Sasse J, Eklom P, Kemler R, Doetschman T (1988) Vasculogenesis and angiogenesis in embryonic-stem-cell-derived embryoid bodies. *Development* (Cambridge, England) 102(3):471–478
- Robaye B, Mosselmans R, Fiers W, Dumont JE, Galand P (1991) Tumor necrosis factor induces apoptosis (programmed cell death) in normal endothelial cells in vitro. *The American journal of pathology* 138(2):447–453
- Robinson GS, Ju M, Shih SC, Xu X, McMahon G, Caldwell RB, Smith LE (2001) Nonvascular role for VEGF: VEGFR-1, 2 activity is critical for neural retinal development. *FASEB journal : official publication of the Federation of American Societies for Experimental Biology* 15(7):1215–1217

## 9 References

- Ross RJ, Zhou M, Shen D, Fariss RN, Ding X, Bojanowski CM, Tuo J, Chan C (2008) Immunological protein expression profile in Ccl2/Cx3cr1 deficient mice with lesions similar to age-related macular degeneration. *Experimental Eye Research* 86(4):675–683
- Roussa E, von Bohlen und Halbach, Oliver, Kriegelstein K (2009) TGF-beta in dopamine neuron development, maintenance and neuroprotection. *Advances in experimental medicine and biology* 651:81–90
- Rousseau B (2003) Involvement of fibroblast growth factors in choroidal angiogenesis and retinal vascularization. *Experimental Eye Research* 77(2):147–156
- Roy S, Maiello M, Lorenzi M (1994) Increased expression of basement membrane collagen in human diabetic retinopathy. *The Journal of clinical investigation* 93(1):438–442
- Rucker HK, Wynder HJ, Thomas WE (2000) Cellular mechanisms of CNS pericytes. *Brain research bulletin* 51(5):363–369
- Ryan SJ (1982) Subretinal Neovascularization. *Arch Ophthalmol* 100(11):1804
- Saint-Geniez M, D'amore PA (2004) Development and pathology of the hyaloid, choroidal and retinal vasculature. *Int. J. Dev. Biol.* 48(8-9):1045–1058
- Saint-Geniez M, Kurihara T, Sekiyama E, Maldonado AE, D'amore PA (2009) An essential role for RPE-derived soluble VEGF in the maintenance of the choriocapillaris. *Proceedings of the National Academy of Sciences of the United States of America* 106(44):18751–18756
- Saint-Geniez M, Maldonado AE, D'amore PA (2006) VEGF expression and receptor activation in the choroid during development and in the adult. *Investigative ophthalmology & visual science* 47(7):3135–3142
- Sakurai E, Anand A, Ambati BK, van Rooijen N, Ambati J (2003) Macrophage depletion inhibits experimental choroidal neovascularization. *Investigative ophthalmology & visual science* 44(8):3578–3585

## 9 References

- Sarks SH, Arnold JJ, Killingsworth MC, Sarks JP (1999) Early drusen formation in the normal and aging eye and their relation to age related maculopathy: a clinicopathological study. *The British journal of ophthalmology* 83(3):358–368
- Sato Y (1989) Inhibition of endothelial cell movement by pericytes and smooth muscle cells. Activation of a latent transforming growth factor-beta 1-like molecule by plasmin during co-culture. *The Journal of Cell Biology* 109(1):309–315
- Sato Y (1990) Characterization of the activation of latent TGF-beta by co-cultures of endothelial cells and pericytes or smooth muscle cells. A self-regulating system. *The Journal of Cell Biology* 111(2):757–763
- Sato Y, Tsuboi R, Lyons R, Moses H, Rifkin DB (1990) Characterization of the activation of latent TGF-beta by co-cultures of endothelial cells and pericytes or smooth muscle cells: a self-regulating system. *The Journal of Cell Biology* 111(2):757–763
- Schallek J, Geng Y, Nguyen H, Williams DR (2013) Morphology and topography of retinal pericytes in the living mouse retina using in vivo adaptive optics imaging and ex vivo characterization. *Investigative ophthalmology & visual science* 54(13):8237–8250
- Schlecht A, Leimbeck SV, Tamm ER, Braunger BM (2016) Tamoxifen-Containing Eye Drops Successfully Trigger Cre-Mediated Recombination in the Entire Eye. *Advances in experimental medicine and biology* 854:495–500
- Scholl HPN, Fleckenstein M, Charbel Issa P, Keilhauer C, Holz FG, Weber BHF (2007) Genetics of Age-Related Macular Degeneration: Update. In: *Medical Retina Medical Retina*. Springer-Verlag Berlin Heidelberg, Berlin, Heidelberg, pp 35–52
- Schwesinger C, Yee C, Rohan RM, Joussen AM, Fernandez A, Meyer TN, Poulaki V, Ma JJ, Redmond TM, Liu S, Adamis AP, D'Amato RJ (2001) Intrachoroidal neovascularization in transgenic mice overexpressing vascular endothelial growth factor in the retinal pigment epithelium. *The American journal of pathology* 158(3):1161–1172

## 9 References

- Seitz R, Tamm ER (2014) Müller cells and microglia of the mouse eye react throughout the entire retina in response to the procedure of an intravitreal injection. *Advances in experimental medicine and biology* 801:347–353
- Shi X, Guo L, Seedial SM, Si Y, Wang B, Takayama T, Suwanabol PA, Ghosh S, DiRenzo D, Liu B, Kent KC (2014) TGF-beta/Smad3 inhibit vascular smooth muscle cell apoptosis through an autocrine signaling mechanism involving VEGF-A. *Cell death & disease* 5:e1317
- Sieczkiewicz GJ, Herman IM (2003) TGF- $\beta$ 1 signaling controls retinal pericyte contractile protein expression. *Microvascular Research* 66(3):190–196
- Siemerink MJ, Klaassen I, Van Noorden, Cornelis J F, Schlingemann RO (2013) Endothelial tip cells in ocular angiogenesis: potential target for anti-angiogenesis therapy. *The journal of histochemistry and cytochemistry : official journal of the Histochemistry Society* 61(2):101–115
- Sivaprasad S, Gupta B, Crosby-Nwaobi R, Evans J (2012) Prevalence of diabetic retinopathy in various ethnic groups: a worldwide perspective. *Survey of Ophthalmology* 57(4):347–370
- Sjøløe AK, Klein R, Porta M, Orchard T, Fuller J, Parving HH, Bilous R, Aldington S, Chaturvedi N (2011) Retinal microaneurysm count predicts progression and regression of diabetic retinopathy. Post-hoc results from the DIRECT Programme. *Diabetic medicine : a journal of the British Diabetic Association* 28(3):345–351
- Sone H, Kawakami Y, Okuda Y, Sekine Y, Honmura S, Matsuo K, Segawa T, Suzuki H, Yamashita K (1997) Ocular vascular endothelial growth factor levels in diabetic rats are elevated before observable retinal proliferative changes. *Diabetologia* 40(6):726–730
- Soriano P (1999) Generalized lacZ expression with the ROSA26 Cre reporter strain. *Nature genetics* 21(1):70–71
- Speiser P, Gittelsohn AM, Patz A (1968) Studies on diabetic retinopathy. 3. Influence of diabetes on intramural pericytes. *Archives of ophthalmology (Chicago, Ill. : 1960)* 80(3):332–337

## 9 References

- Stahl A, Connor KM, Sapieha P, Chen J, Dennison RJ, Krah NM, Seaward MR, Willett KL, Aderman CM, Guerin KI, Hua J, Löfqvist C, Hellström A, Smith LEH (2010) The Mouse Retina as an Angiogenesis Model. *Invest. Ophthalmol. Vis. Sci.* 51(6):2813
- Stan RV, Arden KC, Palade GE (2001) cDNA and protein sequence, genomic organization, and analysis of cis regulatory elements of mouse and human PLVAP genes. *Genomics* 72(3):304–313
- Stan RV, Kubitza M, Palade GE (1999) PV-1 is a component of the fenestral and stomatal diaphragms in fenestrated endothelia. *Proceedings of the National Academy of Sciences of the United States of America* 96(23):13203–13207
- Stan RV, Tse D, Deharvengt SJ, Smits NC, Xu Y, Luciano MR, McGarry CL, Buitendijk M, Nemani KV, Elgueta R, Kobayashi T, Shipman SL, Moodie KL, Daghljan CP, Ernst PA, Lee H, Suriawinata AA, Schned AR, Longnecker DS, Fiering SN, Noelle RJ, Gimi B, Shworak NW, Carriere C (2012) The diaphragms of fenestrated endothelia: gatekeepers of vascular permeability and blood composition. *Developmental cell* 23(6):1203–1218
- Sternberg N, Hamilton D (1981) Bacteriophage P1 site-specific recombination. I. Recombination between loxP sites. *Journal of Molecular Biology* 150(4):467–486
- Strauss O (2005) The retinal pigment epithelium in visual function. *Physiological reviews* 85(3):845–881
- Streilein JW (1999) Immunoregulatory mechanisms of the eye. *Progress in retinal and eye research* 18(3):357–370
- Sunness JS, Gonzalez-Baron J, Applegate CA, Bressler NM, Tian Y, Hawkins B, Barron Y, Bergman A (1999) Enlargement of atrophy and visual acuity loss in the geographic atrophy form of age-related macular degeneration. *Ophthalmology* 106(9):1768–1779
- Thornton J, Edwards R, Mitchell P, Harrison RA, Buchan I, Kelly SP (2005) Smoking and age-related macular degeneration: a review of association. *Eye (London, England)* 19(9):935–944

## 9 References

- Thylefors B, Negrel AD, Pararajasegaram R, Dadzie KY (1995) Global data on blindness. Bulletin of the World Health Organization 73(1):115–121
- Toussaint D, Cogan DG, Kuwabara T (1962) Extravascular Lesions of Diabetic Retinopathy. Archives of Ophthalmology 67(1):42–47
- Trost A, Schroedl F, Lange S, Rivera FJ, Tempfer H, Korntner S, Stolt CC, Wegner M, Bogner B, Kaser-Eichberger A, Krefft K, Runge C, Aigner L, Reitsamer HA (2013) Neural crest origin of retinal and choroidal pericytes. Investigative ophthalmology & visual science 54(13):7910–7921
- Urness LD, Sorensen LK, Li DY (2000) Arteriovenous malformations in mice lacking activin receptor-like kinase-1. Nature genetics 26(3):328–331
- van der Schaft, T L, Mooy CM, Bruijn WC de, Bosman FT, Jong PT de (1994) Immunohistochemical light and electron microscopy of basal laminar deposit. Graefe's archive for clinical and experimental ophthalmology = Albrecht von Graefes Archiv fur klinische und experimentelle Ophthalmologie 232(1):40–46
- van Geest RJ, Klaassen I, Vogels IMC, Van Noorden, Cornelis J F, Schlingemann RO (2010) Differential TGF- $\beta$  signaling in retinal vascular cells: a role in diabetic retinopathy? Investigative ophthalmology & visual science 51(4):1857–1865
- van Lookeren Campagne M, LeCouter J, Yaspan BL, Ye W (2014) Mechanisms of age-related macular degeneration and therapeutic opportunities. The Journal of pathology 232(2):151–164
- Vierkotten S, Muether PS, Fauser S (2011) Overexpression of HTRA1 leads to ultrastructural changes in the elastic layer of Bruch's membrane via cleavage of extracellular matrix components. PloS one 6(8):e22959
- Visser JA, Themmen AP (1998) Downstream factors in transforming growth factor- $\beta$  family signaling. Molecular and Cellular Endocrinology 146(1-2):7–17

## 9 References

- Vokes SA (2004) Hedgehog signaling is essential for endothelial tube formation during vasculogenesis. *Development* 131(17):4371–4380
- Walshe TE (2010) TGF-beta and microvessel homeostasis. *Microvascular Research* 80(1):166–173
- Walshe TE, Saint-Geniez M, Maharaj ASR, Sekiyama E, Maldonado AE, D'amore PA (2009) TGF-beta is required for vascular barrier function, endothelial survival and homeostasis of the adult microvasculature. *PloS one* 4(4):e5149
- Wickham H (2009) ggplot2. *Elegant Graphics for Data Analysis. Use R.* Springer-Verlag New York, New York, NY
- Wilkinson-Berka JL, Babic S, Gooyer T de, Stitt AW, Jaworski K, Ong LG, Kelly DJ, Gilbert RE (2004) Inhibition of Platelet-Derived Growth Factor Promotes Pericyte Loss and Angiogenesis in Ischemic Retinopathy. *The American journal of pathology* 164(4):1263–1273
- Winkler EA, Bell RD, Zlokovic BV (2010) Pericyte-specific expression of PDGF beta receptor in mouse models with normal and deficient PDGF beta receptor signaling. *Molecular neurodegeneration* 5:32
- Wrana JL, Attisano L, Cárcamo J, Zentella A, Doody J, Laiho M, Wang XF, Massagué J (1992) TGF beta signals through a heteromeric protein kinase receptor complex. *Cell* 71(6):1003–1014
- Wrana JL, Attisano L, Wieser R, Ventura F, Massagué J (1994) Mechanism of activation of the TGF-beta receptor. *Nature* 370(6488):341–347
- Wu M, Chen Y, Wilson K, Chirindel A, Ihnat MA, Yu Y, Boulton ME, Szweda LI, Ma J, Lyons TJ (2008) Intraretinal leakage and oxidation of LDL in diabetic retinopathy. *Investigative ophthalmology & visual science* 49(6):2679–2685
- Xu H, Chen M, Forrester JV (2009) Para-inflammation in the aging retina. *Progress in retinal and eye research* 28(5):348–368

## 9 References

- Yang X, Castilla LH, Xu X, Li C, Gotay J, Weinstein M, Liu PP, Deng CX (1999) Angiogenesis defects and mesenchymal apoptosis in mice lacking SMAD5. *Development (Cambridge, England)* 126(8):1571–1580
- Yang Z, Camp NJ, Sun H, Tong Z, Gibbs D, Cameron DJ, Chen H, Zhao Y, Pearson E, Li X, Chien J, Dewan A, Harmon J, Bernstein PS, Shridhar V, Zabriskie NA, Hoh J, Howes K, Zhang K (2006) A variant of the HTRA1 gene increases susceptibility to age-related macular degeneration. *Science (New York, N.Y.)* 314(5801):992–993
- Yang Z, Tong Z, Chen Y, Zeng J, Lu F, Sun X, Zhao C, Wang K, Davey L, Chen H, London N, Muramatsu D, Salazar F, Carmona R, Kasuga D, Wang X, Bedell M, Dixie M, Zhao P, Yang R, Gibbs D, Liu X, Li Y, Li C, Li Y, Campochiaro B, Constantine R, Zack DJ, Campochiaro P, Fu Y, Li DY, Katsanis N, Zhang K (2010) Genetic and functional dissection of HTRA1 and LOC387715 in age-related macular degeneration. *PLoS genetics* 6(2):e1000836
- Ye X, Wang Y, Nathans J (2010) The Norrin/Frizzled4 signaling pathway in retinal vascular development and disease. *Trends in Molecular Medicine* 16(9):417–425
- Young RW (1987) Pathophysiology of age-related macular degeneration. *Survey of Ophthalmology* 31(5):291–306
- Zeng H, Green WR, Tso MOM (2008) Microglial activation in human diabetic retinopathy. *Archives of ophthalmology (Chicago, Ill. : 1960)* 126(2):227–232
- Zhang L, Lim SL, Du H, Zhang M, Kozak I, Hannum G, Wang X, Ouyang H, Hughes G, Zhao L, Zhu X, Lee C, Su Z, Zhou X, Shaw R, Geum D, Wei X, Zhu J, Ideker T, Oka C, Wang N, Yang Z, Shaw PX, Zhang K (2012) High temperature requirement factor A1 (HTRA1) gene regulates angiogenesis through transforming growth factor-beta family member growth differentiation factor 6. *The Journal of biological chemistry* 287(2):1520–1526
- Zhu Y, Culmsee C, Klumpp S, Kriegelstein J (2004) Neuroprotection by transforming growth factor-beta1 involves activation of nuclear factor-kappaB through phosphatidylinositol-3-OH

## 9 References

kinase/Akt and mitogen-activated protein kinase-extracellular-signal regulated kinase1,2 signaling pathways. *Neuroscience* 123(4):897–906

## 10 Abbreviations

ALK	Activin receptor-like kinase
AMD	Age related macular degeneration
Ang-2	Angiopoietin-2
$\alpha$ -SMA	alpha-smooth muscle actin
AU	Arbitrary unit
BlamD	Basal laminar deposits
BlinD	Basal linear deposits
BM	Bruch's membrane
BRB	Blood-retinal barrier
C	Choroid
Casp8	Caspase 8
CB	Ciliary body
CC	Choriocapillaris
Ccl2	CC- <i>chemokine ligand 2</i>
CD31	Cluster of differentiation 31
CD68	Cluster of differentiation 68
CO	Cornea
Col	Collagen
CNV	Choroidal neovascularization
CMV	Cytomegalovirus
Cre	Causes recombination
DNA	Deoxyribonucleic acid
DR	Diabetic retinopathy
EC	Endothelial cell
Egr-1	Early growth response protein-1
Er	Erythrocyte
ERG	Electroretinogram
Fgf2	Basic fibroblast growth factor-2

## 10 Abbreviations

FITC-dextran	Fluorescein isothiocyanate-dextran
FLA	Fluorescein angiography
GAPDH	Glycerinaldehyde-3-phosphate dehydrogenase
GCL	Ganglion cell layer
GDF6	Growth differentiation factor 6
GFAP	Glial acidic fibrillary protein
Gnb2l	Guanine nucleotide binding preotein, beta polypeptide 2-like
HIF-1 $\alpha$	Hypoxia inducible factor-1 $\alpha$
Hsp90	Heat shock protein 90
HTRA1	High temperature requirement factor A1
IBA-1	Ionized calcium-binding adapter molecule-1
Igf-1	Insulin-like growth factor-1
Il6	Interleukin 6
INL	Inner nuclear layer
iNos	Inducible nitric oxide synthase
Le	Lens
NBL	Neuroblast layer
Ndp	Norrie disease protein
NG2	Neural/glial antigen 2
ON	Optic nerve
ONH	Optic nerve head
ONL	Outer nuclear layer
OPL	Outer plexiform layer
OS	Ora serrata
PB	Phosphate buffer
PBS	Phosphate buffered saline
PC	Pericyte
PCR	Polymerase chain reaction
PDGF- $\beta$	Platelet-derived growth factor-beta

## 10 Abbreviations

PDGFR- $\beta$	Platelet-derived growth factor receptor-beta
PLVAP	Plasmalemma vesicle associated protein
PFA	Paraformaldehyde
PPD	Phenylendiamine
RGC	Retinal ganglion cell
Rgs-5	Regulator of G-protein signaling-5
RNA	Ribonucleic acid
RPE	Retinal pigment epithelium
Rpl32	Ribosomal protein l32
SC	Schlemm`s canal
SEM	Standard error of the mean
TBS	Tris buffered saline
TEM	Transmission electron microscopy
TGF	Transforming growth factor
TGF- $\beta$	Transforming growth factor-beta
Tgfr1	Transforming growth factor-beta receptor type 1
Tgfr2	Transforming growth factor-beta receptor type 2
T $\beta$ RII	Transforming growth factor-beta receptor type 2
TM	Trabecular meshwork
Tnf- $\alpha$	Tumor necrosis factor- $\alpha$
TUNEL	Terminal deoxynucleotidyl transferase dUTP nick end labeling
Tx	Tamoxifen
VEGF	Vascular endothelial growth factor

## 11 Acknowledgments - Danksagung

Zu Beginn möchte ich Herrn Prof. Dr. Ernst Tamm danken, dafür dass er mir die Möglichkeit gegeben hat, meine Arbeit an seinem Lehrstuhl durchzuführen. Ich bedanke mich für Ihre Unterstützung, für die viele Zeit die Sie in mein Projekt investiert haben und für die Möglichkeit meine Arbeit auch auf Kongressen vorstellen zu dürfen. Ich habe sehr viel gelernt in den letzten Jahren.

Herrn Prof. Dr. Bernhard Weber möchte ich ganz herzlich für die Übernahme des Zweitgutachtens danken und dafür, dass Sie mich während meiner Doktorarbeit als Mentor begleitet haben.

Desweiteren möchte ich Herrn Prof. Dr. Frank Schweda meinen Dank aussprechen für die Bereitschaft mich in meinem Kolloquium zu prüfen.

Mein ganz besonderer Dank gilt Frau Dr. Dr. Barbara Braunger. Du hast mir die Möglichkeit gegeben, so viel Neues zu lernen und hast mich in die wunderbare Welt der okulären Gefäße eingeführt. Ohne dich wäre meine wissenschaftliche Laufbahn mit Sicherheit in eine ganz andere Richtung gegangen. Vielen Dank für all die Unterstützung, die Betreuung und alle Ratschläge in den letzten Jahren, du hast mich nicht nur durch meine Doktorarbeit begleitet, sondern bist mir auch eine gute Freundin geworden.

Angelika, Silvia und Margit möchte ich ganz herzlich für eure Unterstützung im Laboralltag danken, ihr hattet immer für all meine Probleme Lösungen parat. Elke, tausend Dank dir für deine tatkräftige Unterstützung in der Histo, für alle Gespräche und all die offenen Ohren. Und natürlich auch für sämtliche Tape-Verbände.

Meine lieben Labor-Mädels, es war so eine schöne Zeit mit euch, ihr wart immer für mich da, habt mich unterstützt bei jeden Report, Vortrag oder Kongress. Vielen, vielen Dank für das tolle Klima, die Freundschaften, die Zusammenarbeit und diverse außerarbeitsliche Aktivitäten. Danke

## 11 Acknowledgments - Danksagung

Lena, für viele schöne Stunden beim Bogenschießen; Andrea für diverse "Quality-times"; Silke für Spezi-Abende im Garten und danke Sabrina, mit dir macht sogar Tierstall-Arbeit Spass. Ihr seid ein wahnsinns Team!

Zu guter Letzt möchte ich mich bei meinen Eltern bedanken, ihr seid immer meine Stütze gewesen, habt meine Launen (vor allem zum Ende der Doktorarbeit) ertragen und habt mir immer den Rücken freigehalten. Ohne euch wäre mein Studium und meine Doktorarbeit nicht möglich gewesen.

## 12 Curriculum vitae

M. Sc. Anja Schlecht

Unterislinger Weg 6

93053 Regensburg

### Personal Information

Name: Anja Schlecht

Gender: Female

Date of Birth: 14. Mai 1987

Place of Birth: Roding

Nationality: German

### Education

2013 to present      Dissertation at the Institute of Human Anatomy und Embryology, University of Regensburg, Supervisors PD Dr. Dr. Barbara Braunger and Prof. Dr. Ernst Tamm, Thesis "The Role of TGF $\beta$ -Signaling in Development and Maintenance of the Ocular Vasculature"

2010 – 2012      Master of Science Biology, University of Regensburg, Thesis "Untersuchung der Induzierbarkeit sowie möglicher Kosten der chemischen Verteidigung bei *Ampulex compressa* F. (Hymenoptera, Ampulicidae)"

2006 – 2010      Bachelor of Science Biology, University of Regensburg, Thesis "Alters- und reproduktionsabhängige Veränderungen der Giftdrüse bei *Ampulex compressa* F. (Hymenoptera, Ampulicidae)"

2006      Abitur at the Joseph von Fraunhofer Gymnasium in Cham, Germany